UNIVERSITÀ
DI PAVIA

Department of Biology and Biotechnology "L. Spallanzani"

# Role of HMGB1 in vascular aging and calcification

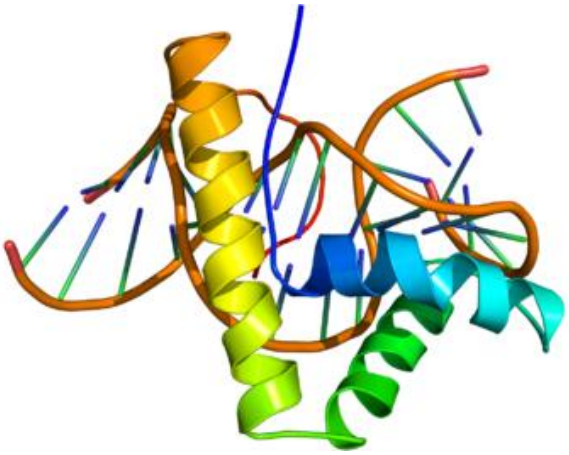

**Luigi Mancinelli**

Research Doctorate in
Genetics, Molecular and Cellular Biology
Cycle XXXII – A.A. 2016-2019

UNIVERSITÀ
DI PAVIA

Department of Biology and Biotechnology "L. Spallanzani"

# Role of HMGB1 in vascular aging and calcification

**Luigi Mancinelli**

**Supervised by Dr. Angela Raucci, Prof. Valeria Merico, Prof. Francesco Moccia**

Research Doctorate in
Genetics, Molecular and Cellular Biology
Cycle XXXII – A.A. 2016-2019

# *Abstract*

***BACKGROUND-*** Vascular calcification (VC) is an age-associated complication of cardiovascular diseases, in which the main cellular event is the trans-differentiation of vascular smooth muscle cells (VSMCs) from a contractile to an osteochondrogenic phenotype that leads to an accumulation of calcium deposits. Senescence facilitates VSMCs osteogenic transition. VC is strongly associated with inflammation, oxidative stress and high level of DNA damage. High mobility group box 1 (HMGB1) is a highly conserved non-histone chromatin binding protein involved in transcription, DNA repair, and maintenance of nucleosome structure that can be actively secreted or passively released in the extracellular space acting as an alarmin. HMGB1 is involved in age-associated nuclear defects, cellular senescence and the acquisition of senescence-associated secretory phenotype (SASP). Finally, HMGB1 is implicated in VSMCs proliferation and migration and in osteochondrogenic transformation of human dental pulp stem cells (hDPCs) and valve interstitial cells (VICs).

***OBJECTIVE-*** The role of HMGB1 in vascular aging and calcification has been only partially explored. Herein, we investigated HMGB1 behavior and function in human aortic smooth muscle cells (HASMCs) senescence and osteochondrogenic trans-differentiation associated to senescence *in vitro* and vascular aging and VC *in vivo.*

***RESULTS-*** HMGB1 protein expression decreases in aortas of old mice and during replicative senescence of HASMCs along with an increase of p16 expression. HMGB1 downregulation during senescence is mainly due to decrease of its gene expression and not relocation of the protein to the cytosol and in the extracellular space. HMGB1 declines also in the course of HASMCs calcification induced by hyperphosphatemia and in calcified aortas of a rat model of adenine-induced calcification and inversely correlates with calcium content in human abdominal aneurism of aorta (AAA). Silencing of HMGB1 in young but not in old HASMCs induces senescence-like phenotype through inhibition of cell proliferation, blocking the cell cycle in G0/G1 phase and increasing p21 and senescence-associate β-galactosidase (SA-β-gal) expressions, in respect to control cells. Notably, HMGB1 downregulation reduces HASMCs secretion of pro-inflammatory SASPs factors, DNA damage and ROS content both in young and old cells. Finally, silencing of HMGB1 in HASMCs initially impairs cell calcification and SASP factors release but eventually favours calcium deposition and IL-6, IL1-β and OPN secretion. In accordance, aortas of vitamin D-treated *Hmgb1*$^{+/-}$ mice exhibit a lower

accumulation of calcium in the early phase of calcification while a higher tissue mineralization later, in respect to *Hmgb1*$^{+/+}$ animals.

***CONCLUSION-*** Hence, during vascular aging, the reduction of HMGB1 in VSMCs induces a senescence-like phenotype that favours DNA damage repair, avoid SASP spreading and limit cell proliferation. However, this response is initially protective but becomes deleterious after a long-term period in response to pro-calcification conditions.

# *Acknowledgements*

*I would like to thank all the people who have always believed in me and helped me through difficult times. A special thanks goes to all the members of my laboratory, to my tutors Angela Raucci, Valeria Merico and Francesco Moccia and to the coordinator Antonio Torroni.*

# *Contents*

***Abstract*** ..... **3**

***Acknowledgements*** ..... **5**

***Contents*** ..... **6**

***Abbreviations*** ..... **8**

**1.Introduction** ..... **10**

*1.1 The history of aging research*
*1.2 Vascular aging*
*1.2.1. Structure and physiology of vascular smooth muscle cells (VSMCs)*
*1.2.2. Mechanisms and hallmarks of aging*
*1.2.3. The impact of aging on VSMCs*
*1.3. Vascular calcification*
*1.4. High mobility group box 1 (HMGB1)*
*1.4.1. Nuclear roles of HMGB1*
*1.4.2. Extracellular roles of HMGB1*
*1.4.3. HMGB1 and senescence*
*1.4.4. HMGB1 and calcification*

**2.Aims of the project** ..... **49**

**3. Materials and Methods** ..... **50**

*3.1. Cell culture*
*3.2. Generation of shB1/SMCs and shCTRL/SMCs*
*3.2.1. Virus production*
*3.2.2. Virus titration*
*3.2.3. Transduction of HASMCs*
*3.3. Western Blot*
*3.4. Immunofluorescence (IF)*
*3.5. ELISA assay*
*3.6. Quantitative RT-PCR (q-RT-PCR)*
*3.7. Cell proliferation assay*
*3.8. Cell cycle analysis*
*3.9. Neutral comet assay*
*3.10. Reactive oxygen species (ROS) content assay*
*3.11. Senescence-associated β-galactosidase (SA-β-gal) staining*
*3.12. Calcification assay for cells*
*3.12.1. Colorimetric Assay*
*3.12.2. Von Kossa staining on HASMCs*
*3.12.3. Alizarin red staining on HASMCs*
*3.13. Animal experiments*
*3.14. Calcium content quantification on tissue animals*
*3.14.1. Colorimetric assay*
*3.14.2. Von Kossa staining on aortic sections*
*3.15. Immunohistochemistry (IHC)*

*3.16. Human Samples*
*3.17. Statistical analysis*
**4.Results** ..... **63**
*4.1. HMGB1 protein levels decrease during vascular aging in vitro and in vivo*
*4.2. HMGB1 does not re-localize to the cytosol or the extracellular environment during HASMCs replicative senescence*
*4.3. The absence of HMGB1 promotes senescence-like alterations in HASMCs*
*4.4. HMGB1 controls the acquisition of SASP in HASMCs*
*4.5. The absence of HMGB1 diminishes basal DNA damage and oxidative stress in HASMCs*
*4.6. HMGB1 protein level declines during vascular calcification in vitro and in vivo*
*4.7. HMGB1 down-regulation is protective in the early phases of HASMCs calcification, but favours it in the late phases*
*4.8. HMGB1 affects calcification of aortas in vivo*
**5.Discussion** ..... **85**
***References*** ..... **90**
***List of original manuscripts*** ..... **102**

# *Abbreviations*

| | |
|---|---|
| **AAA** | Aortic abdominal aneurism |
| **a-EJ** | Alternative end joining |
| **ALP** | Alkaline phosphatase |
| **AMPK** | AMP-activated kinase |
| **APOE** | Apolipoprotein E |
| **APLF** | Aprataxin and PNKP-like factor |
| **ARF** | Alternate reading frame protein |
| **α-SMA** | Alpha smooth muscle actin |
| **ATM** | Ataxia telangiectasia mutated |
| **ATR** | Ataxia telangiectasia and Rad3-related |
| **BF** | Blood flow |
| **BMP2** | Bone morphogenetic protein 2 |
| **BP** | Blood pressure |
| **CCL16** | Chemokine (C-C motif) ligand 16 |
| **CDK** | Cyclin-dependent kinase |
| **CDKI** | Cyclin-dependent kinase inhibitor |
| **CKD** | Chronic kidney disease |
| **CVDs** | Cardiovascular diseases |
| **CXCL1** | Chemokine (C-X-C motif) ligand 1 |
| **CXCL2** | Chemokine (C-X-C motif) ligand 2 |
| **CXCL3** | Chemokine (C-X-C motif) ligand 3 |
| **DDR** | DNA damage response |
| **DSBs** | Double strand breaks |
| **ECM** | Extracellular matrix |
| **ECs** | Endothelial cells |
| **ELK-1** | ETS-like transfer factor 1 |
| **FEN-1** | Flap endonuclease 1 |
| **FOXO3A** | Fork head box 3A |
| **HASMCs** | Human aortic smooth muscle cells |
| **HMGB1** | High mobility group box 1 |
| **HR** | Homologous recombination |
| **IGF-1** | Insulin grow factor 1 |
| **IL-1β** | Interleukin 1β |
| **IL-6** | Interleukin 6 |
| **IL-8** | Interleukin 8 |
| **MIP-1α** | Macrophage Inflammatory Protein 1α |
| **MIP-3α** | Macrophage Inflammatory Protein 3α |
| **MCP-1** | Monocyte chemotactic protein-1 |
| **MGP** | Matrix Gla protein |
| **MMP** | Matrix metalloproteinase |
| **Msx2** | Msh homeobox 2 |
| **mTOR** | Mammalian target of rapamycin |
| **mtDNA** | Mitochondrial DNA |
| **NHEJ** | Non-homologous end joining |

| | |
|---|---|
| **NHEJ1** | Non-homologous end joining factor 1 (see XLF) |
| **OPG** | Osteoprotegerin |
| **OPN** | Osteopontin |
| **PAXX** | Paralogue of XRCC4 and XLF protein |
| **PCNA** | Proliferating cell nuclear antigen |
| **PPi** | Inorganic pyrophosphate |
| **RAGE** | Receptor for advanced glycation end products |
| **RANKL** | Receptor activator for nuclear factor kappa ligand |
| **RUNX2** | Runt-related transcription factor 2 |
| **ROS** | Reactive oxygen species |
| **SA-β-gal** | Senescence-associated β-galactosidase |
| **SAHFs** | Senescent associated heterochromatin foci |
| **SASP** | Senescent associated secretory phenotype |
| **SDFs** | Senescent associated DNA damage foci |
| **SRF** | Serum response factor |
| **SSA** | Single strand annealing |
| **SOX-9** | Sex-determining region Y-box 9 |
| **T2DM** | Type 2 diabetes mellitus |
| **TGF-β1** | Transforming grow factor β1 |
| **TLR** | Toll like receptor |
| **VC** | Vascular calcification |
| **VCi** | Intimal vascular calcification |
| **VCm** | Medial vascular calcification |
| **VSMCs** | Vascular smooth muscle cells |
| **XLF** | XRCC4-like factor |
| **XRCC4** | X-ray cross-complementing protein |

# 1. Introduction

## *1.1 The history of aging research*

Aging is defined as a gradual and time-dependent alteration of physiological functions and it has always fascinated interests of scientists during the history of humankind. Nowadays, we know that this biological phenomenon is amenable to scientific study, but just thirty years ago, it was hotly debated due to pre-existing theories based on evolutionary biology. In summary, these theories assumed that the deleterious changes observed during aging were due to lack of natural selection. So, since wild animals die relatively early because of the several risks of wildlife, there had been a little pressure to select genes that confer advantage in later life. For these reasons, evolutionary theory stated that aging was an inevitable by-product of the rules of natural selection and therefore not a regulated process [1]. Despite this cynicism, in the late twentieth century proofs began to emerge that challenged these beliefs (Table 1). At the beginning, it come out that the mortality rates for widely divergent organisms, covering from yeasts to humans, were closely similar one to another. This suggested that general features in the aging process were potentially amenable to scientific study, particularly in model organisms. Then, it was noticed that while aging itself may not be regulated, the rate of aging could be. This was greatly underlined by the disparate lifespans of closely related species; in the rodent family, for instance, common rat lives around 5 years, while the average naked-mole rat lives 30 years. The initial studies attempting to find a genetic basis for aging starts when Johnson, Klass and colleagues isolate the first long-lived strain in *Caenorhabditis elegans*. From that moment, the research to elucidate the molecular and cellular basis of aging and to develop new treatments and drugs to prevent, delay, or utopistically revert it, begin to grow amazingly. Studies on animal models such as yeasts, worms and mice have demonstrated effects on mutations in genes that can increase lifespan even by ten times[2]. They have also revealed the existence of many specific genes that regulate lifespan such as the insulin/insulin-like grow factor 1 (IGF-1), mammalian target of rapamycin (mTOR), AMP-activated kinase (AMPK) and nicotinamide adenine dinucleotide (NAD)-dependent deacetylase or sirtuins (Table 1).

| Year | Finding | Reference |
|---|---|---|
| 1935 | Report of lifespan extension in rodents with calorie restriction | McCay et al., 1935 |
| 1950 | Report of a premature aging syndrome in humans (Hutchinson-Gilford) | Thomson and Forfar, 1950 |
| 1977 | Finding that worm lifespan could be modulated with environmental interventions | Klass, 1977 |
| 1980 | Report that Snell dwarf mice may live longer than wildtype counterparts | Eicher and Beamer, 1980 |
| 1982 | Finding that inbred strains of worms can have significantly different lifespans, indicating possible genetic regulation of aging | Johnson and Wood, 1982 |
| 1983 | First creation of genetic mutants (in worms) that display increased lifespan | Klass, 1983 |
| 1988 | Identification of the first gene mutation (age-1) that increases lifespan (in worms) | Friedman and Johnson, 1988 |
| 1993, 1995 | Demonstration that DAF-16 is required for longevity phenotypes of insulin signaling mutant worms, defining the first regulatory network for aging | Kenyon et al., 1993; Larsen et al., 1995 |
| 1995 | First evidence implicating Sirtuins in aging (in yeast) | Kennedy et al., 1995 |
| 1996 | First definitive description of a long-lived mouse strain (Ames dwarf mice), indicating genetic regulation of aging in mammals | Brown-Borg et al., 1996 |
| 1997 | Extrachromosomal rDNA circles identified as a cause of aging in yeast | Sinclair and Guarente, 1997 |
| 1999 | Identification of SIR2 as the key Sirtuin mediating longevity in yeast | Kaeberlein et al., 1999 |
| 1999 | Discovery of a non-deacetylase activity (ADP-ribosyltransferase) for Sirtuins, hinting at broader enzymatic functions | Frye, 1999 |
| 2000 | Discovery of a $NAD^+$ dependent deacetylase activity for SIR2 | Imai et al., 2000 |
| 2001 | Description of a second long-lived mouse strain (Snell dwarf mice) | Flurkey et al., 2001 |
| 2001 | Evidence of SIR2 regulation of lifespan in multicellular organisms (worms) | Tissenbaum and Guarente, 2001 |
| 2002 | Discovery that increased respiration during CR is required for lifespan extension in yeast | Lin et al., 2000 |
| 2003 | Extension of mouse lifespan via heterozygous deletion of IGF1 receptor or deletion of insulin receptor in white adipose tissue | Holzenberger et al., 2003; Blüher et al., 2003 |
| 2003 | First evidence indicating a role of TOR in aging (in worms) | Vellai et al., 2003 |
| 2003, 2004 | The first SIR2 agonist, resveratrol, discovered and shown to extend the lifespan of yeast and later, worms | Howitz et al., 2003; Wood et al., 2004 |
| 2004 | First evidence that AMP-Kinase regulates aging (in worms) | Apfeld et al., 2004 |
| 2007 | Two neurons found to be required for lifespan extension via calorie restriction in worms, highlighting the importance of neuronal regulation of aging | Bishop and Guarente, 2007 |
| 2007 | Extension of mouse lifespan via deletion of insulin receptor in the brain | Taguchi et al., 2007 |
| 2008 | First evidence that a pharmacological agent (metformin) can extend the lifespan of mice | Anisimov et al., 2008 |
| 2009 | Association of genetic variants in insulin-IGF1 signaling with human longevity | Pawlikowska et al., 2009 |
| 2009 | A second pharmacological agent (rapamycin) found to extend the lifespan of mice | Harrison et al., 2009 |
| 2010 | Association of SIRT1 variants with aging in a Han Chinese Population | Zhang et al., 2010 |
| 2011 | Discovery of a more general deacylase enzymatic function for mammalian Sirtuins | Du et al., 2011 |
| 2012 | Mammalian SIRT6 shown to regulate the lifespan of male mice | Kanfi et al., 2012 |
| 2013 | Brain-specific overexpression of SIRT1 shown to extend lifespan of mice | Satoh et al., 2013 |
| 2014 | Pharmacological inhibition of glucose digestion and release into the blood (with Acarbose) shown to extend lifespan of mice | Harrison et al., 2014 |
| 2014 | First evidence that pharmacological activation of SIRT1 extends lifespan in mice | Mitchell et al., 2014; Mercken et al., 2014 |
| 2016 | Evidence that repletion of $NAD^+$ levels with use of precursors extends lifespan of mice | Zhang et al., 2016 |
| 2016 | Demonstration that combination of longevity associated drugs (metformin and rapamycin) can additively extend lifespan in mice | Strong et al., 2016 |
| 2017 | Association of a variant in human growth hormone receptor with longevity in males | Ben-Avraham et al., 2017 |

IGF1, insulin-like growth factor 1; rDNA, ribosomal DNA; TOR, target of rapamycin; ADP, adenosine diphosphate; NAD+, nicotinamide adenine dinucleotide; CR, calorie restriction

**Table 1. List of key findings in aging research.** ***(Adapted from Zainabadi K., et al Exp Geront. 2018)***

Regarding humans, besides initially several candidate gene associations were discovered, only two of them, APOE and FOXO3A, were successively recognised to be consistently associated with aging in different populations [3] (Table 2). APOE was identified through one of the largest linkage studies of exceptionally long-lived individuals (2118 over 90 years old Europeans) that was done in the European Genetics of Healthy Aging Study (GEHA)[3]. APOE possesses three main isoforms: APOE2, APOE3, and APOE4. APOE4 is well known to increase risk of Alzheimer's disease and cardiovascular diseases (CVDs) and is found in significantly lower proportions of nonagenarians and centenarians, which suggests that individuals with high expression of APOE4 do not live as long as those with lower expression[4]. By contrast, APOE2 is enriched in long-lived individuals and may offer a protective effect for Alzheimer's disease and CVDs[5]. FOXO3A is the homologue transcription factor of the C. *elegans* Daf-16 gene, which is important in control of lifespan in the worm[6]; it is part of the insulin/IGF1 signalling, which negatively regulates it[7]. When insulin or insulin-like growth factor signalling is low, FOXO3A is activated and lifespan extension occurs. Moreover, genetic variation of this transcription factor has been associated with longevity in multiple Asian and European populations[8].

One possible explanation for this minority of longevity genes in mammals could be that healthy aging is a variegated phenotype that include not only preservation of long-term functions but also absence of diseases or other disorders [9]. In other words, the extension of lifespan is not always accompanied by an extension of healthy lifespan. It will be important to understand the effect of the environment and the genetic as well as how they interact to influence health and lifespan or in a world "healthspan".

| Gene | Initial populations | Number of LLI | Polimorphism | p-value | Replication population? |
|---|---|---|---|---|---|
| **APOE** | **French, Caucasian** | **325** | **2 SNP haplotype** | **0.001** | **many** |
| MTP | US, Caucasian | 653 | 2 SNP haplotype | 0.0005 | none |
| APOC3 | Ashkenazi | 213 | SNP rs2542052 | 0.0001 | none |
| IGFIR | Ashkenazi | 384 | 2 rare SNPs | 0.02 | none |
| **FOXO3A** | **Japanese** | **213** | **SNP rs2802292** | **0.00009** | **many** |
| hTERT | Ashkenazi | 74 | 4 SNP haplotype | 0.007 | none |

**Table 2. Candidate gene association studies in long lived individuals (LLI).** The genes in **bold** are genes in which the association has been found many times. ***(Adapted from Wheeler H, et al. Phil Trans 2011).***

## *1.2 Vascular aging*

Nowadays the average of human lifespan is increasing, and it is estimated that by 2030 about 20% of the population will be aged 65 or older[10]. If we describe aging depending on the cellular component in which is developing, we can distinguish cardiac, brain, skin aging, etc. Among all of these, vascular aging is extremely significant as sir William Osler said in 1891: *"Longevity is a vascular question, which has been well expressed in the axiom that man is only as old as his arteries"* [11]. Indeed, by delivering oxygenated blood to all tissues in the body, vasculature together with heart are indispensable for the healthfulness of the whole organism. During aging, blood vessels undergo to different structural and molecular modifications that predispose or exacerbate CVDs. Moreover, the health of the vascular system is not mutually exclusive, as each system greatly affects the other. A more stiffen arterial wall, for instance, leads to compensatory consequences by the myocardium, such as left ventricular (LV) hypertrophy and fibroblast proliferation ending with reduced cardiac functionality and extension in fibrotic tissue. In order to better understand the pathogenic changes involving vessels during aging, we will describe their structure and physiology in healthy conditions. Then, since the blood vessels are composed mainly by vascular smooth muscle cells (VSMCs), we will also describe in detail their structure and physiology alterations during the process of aging.

### *1.2.1. Structure and physiology of vascular smooth muscle cells (VSMCs)*

The heterogeneous structure of blood vessels reflects their function that consists in delivering oxygen and nutrients to the whole body with a minimal energy dissipation within the vascular wall. Three layers compose the arteries and veins (Fig. 1). The inner layer or *tunica intima* is made of a single layer of flat cells surrounded by a thin layer of sub endothelial connective tissue combined with a number of circularly arranged elastic bands called the elastic lamina. The middle layer or *tunica media* consists of circularly arranged elastic fibre, connective tissue and polysaccharide substances. Especially in arteries, the tunica media is rich in vascular smooth muscle cells (VSMCs) arranged in a helical pattern around the vessel lumen that control the calibre of the vessel. Finally, the outer layer is the *tunica adventitia* and

it is mainly made of connective tissue but it also contains nerves that supply the vessel as well as nutrient capillaries, called *vasa vasorum* (Fig.1).

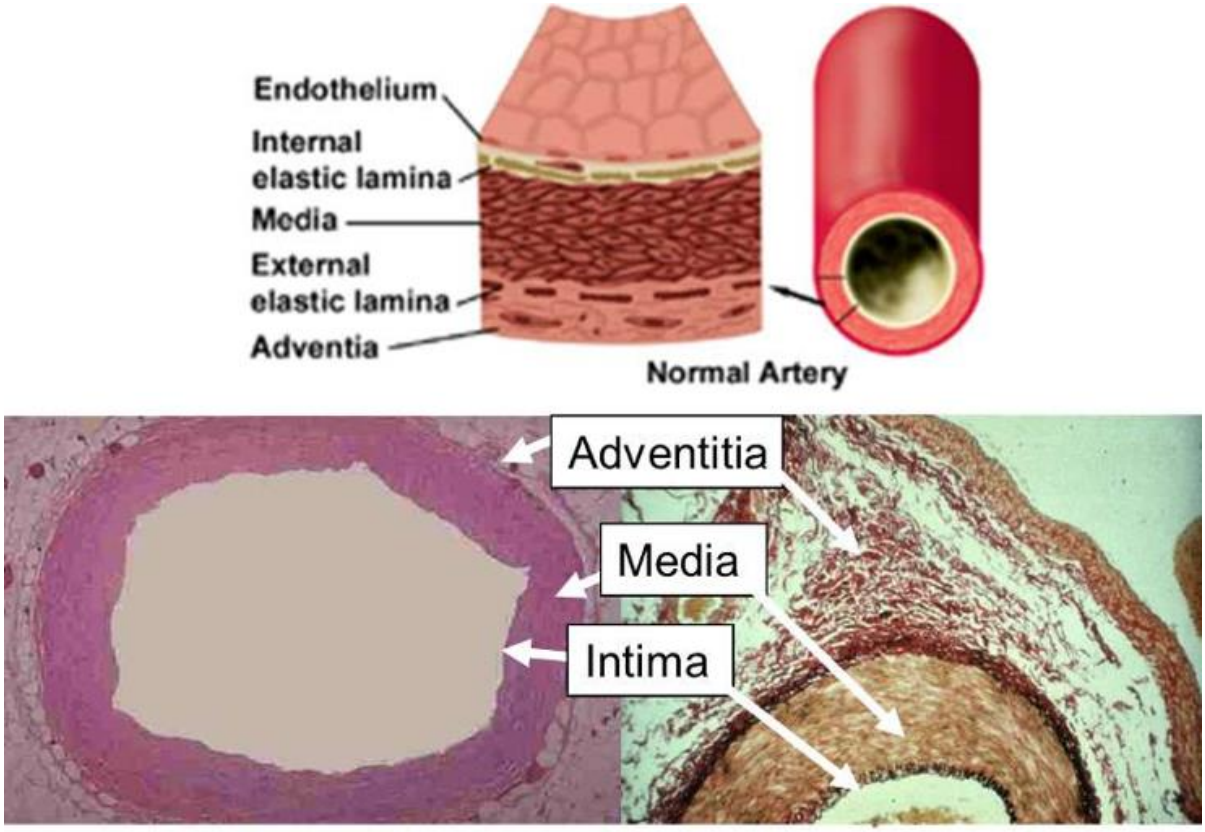


**Figure 1. Histological structure of blood vessels.** Three layers compose the blood vessel: tunica intima, media and adventitia. The tunica intima is the inner layer and it contains a number of circularly arranged elastic bands called the internal elastic lamina. The middle layer or tunica media consists of elastic fibre, connective tissue and is rich of VSMCs. The tunica adventitia is the outer layer and it is entirely made of connective tissue.

VSMCs are the most numerous cell type in blood vessels and are necessary for their physiological functioning, particularly for vasoconstriction, vasodilatation and synthesis of vascular extracellular matrix[12]. Over the last three decades, several studies have identified at least eight independent origins for VSMCs progenitors with a distinct different lineage history. How such dissimilar progenitor cells differentiate into a common VSMCs fate is still unclear, but it plays an important role in VSMCs physiology and response to stimuli[13]. In the course of their development, VSMCs undergo ultrastructural changes and exhibit separate phenotypic states related to expression of an increasing number of cytoskeletal and extracellular

molecules[14]. Initially, they manifest a proliferative and migratory phenotype, they synthetize ECM proteins (elastin and collagen) and express α-smooth muscle actin (α-SMA) and thrombospondin; at the middle stage of differentiation, they express transgelin, SM-actinin and metavinculin. Mature and totally differentiate VSMCs display a quiescent and contractile phenotype and express smoothelin, desmin and a series of contractile proteins involved in the regulation of hemodynamic resistance. All these phenotypes are present in the media of all arteries along the arterial tree with a majority being contractile cells. In adult vessels, VSMCs progenitors are still present in the adventitia layer and the transcription of VSMC marker genes is inhibited to sustain the progenitor phenotype. From a morphological point of view, we can identify two main types of VMSCs: spindle-shaped, that possess contractile phenotype, and epithelioid cells that exhibit a synthetic phenotype[15]. Moreover, thin elongated and senescent VSMCs have been described as well[15]. The heterogeneity of VSMCs can influence vascular tree properties and predispose to vascular diseases (Fig. 2). More importantly, VSMCs could revert from the quiescent contractile phenotype to the former migratory, secretory and proliferating phenotype, accompanied by ECM remodelling, leading to arterial stiffness (Fig. 2). This VSMCs ability is called "plasticity" and it is controlled by several factors such as blood flow (BF), blood pressure (BP), ligand-receptor interactions, reactive oxygen species (ROS), grow factors and regulatory transcriptional pathways (Fig. 2). BF and BP can modify mechanical forces within the vessel to which VSMCs response reprogramming their expression patterns to organize the ECM network in one way or another; growth factors and ROS have been reported to trigger autophagic programs that can degrade contractile proteins and favourite the conversion to the synthetic phenotype. Regarding regulatory transcriptional pathways, the most relevant is serum response factor (SRF) that controls two well-defined VSMCs gene programs depending on its interaction with specific cofactors, myocardin and ETS-like transcription factor 1 (Elk-1). The binding with myocardin promotes the expression of contractile genes while the binding with Elk-1 activates the migratory and secretory pattern genes (Fig. 2). Myocardin and Elk-1 competition for SRF common binding site is regulates VSMCs phenotypic switching [12] VSMCs phenotypic modulation is a field of intense research, mostly because it is altered during vascular aging and is involved in the onset of vascular calcification (VC).

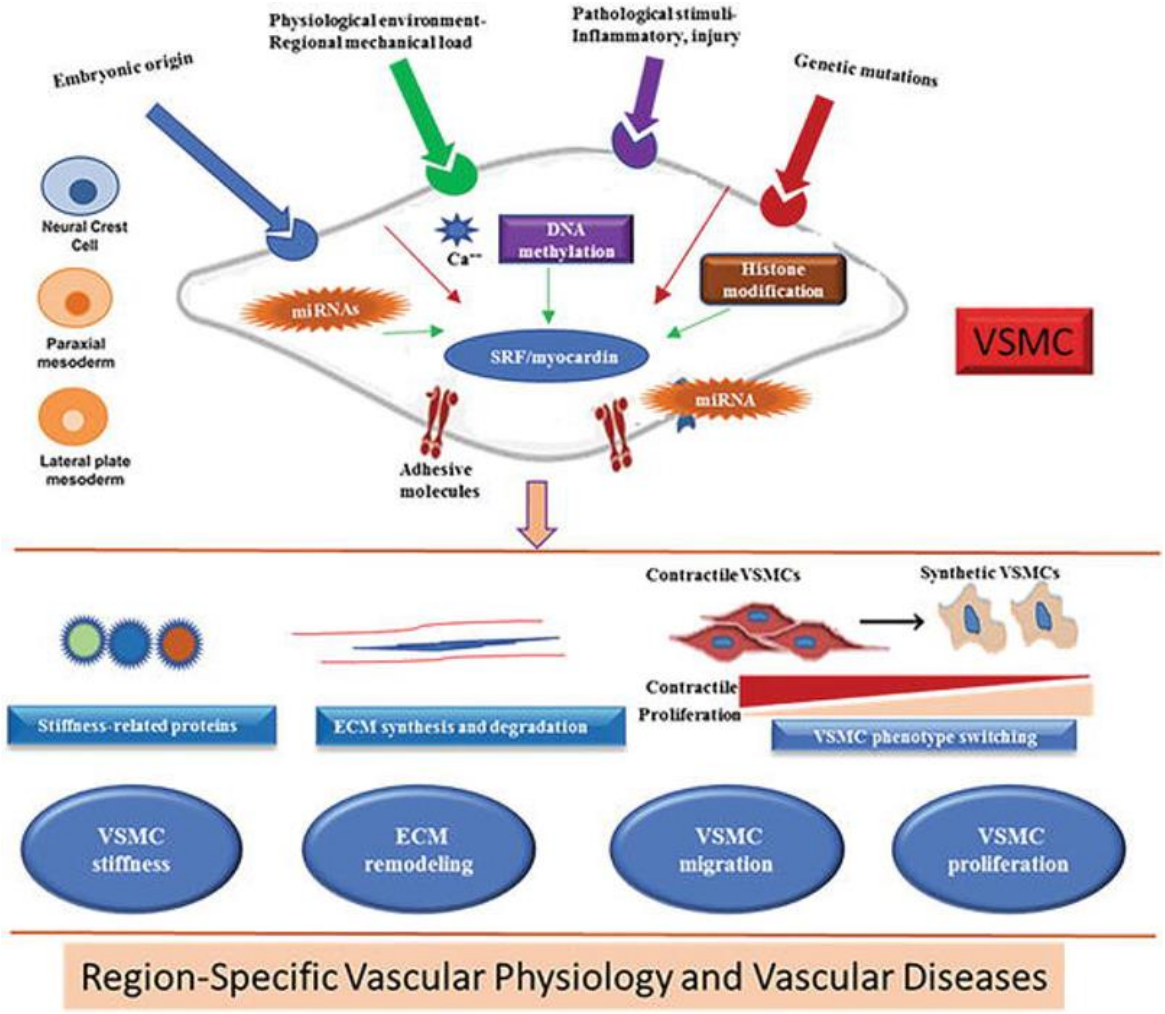


**Figure 2. VSMCs roles in vascular physiology and development of diseases.** Multiple factors including embryonic origin, regional mechanical load, pathological stimuli and genetic mutations mediate the gene expression of VSMCs through different signaling pathways which involves the VSMC membrane receptors, calcium channels, miRNAs, DNA methylation, and histone modification. This results in the regulation of VSMC phenotypes, the expression of stiffness-related proteins, and ECM production. These changes subsequently affect VSMCs stiffness, migration, and proliferation, as well as ECM remodeling, thus, playing a role in vascular normal physiology and diseases. ***(Zhou N. et al., Intechopen 2018)***

## *1.2.2. Mechanisms and hallmarks of aging*

Aging is multifactorial process driven by lot of mechanisms, probably not all known yet and therefore not so easy to define. Hallmark of aging are genomic instability, telomere attrition,

epigenetic alteration, loss of proteostasis, mitochondrial dysfunction, stem cell exhaustion, inflammation and cellular senescence (Fig. 3).

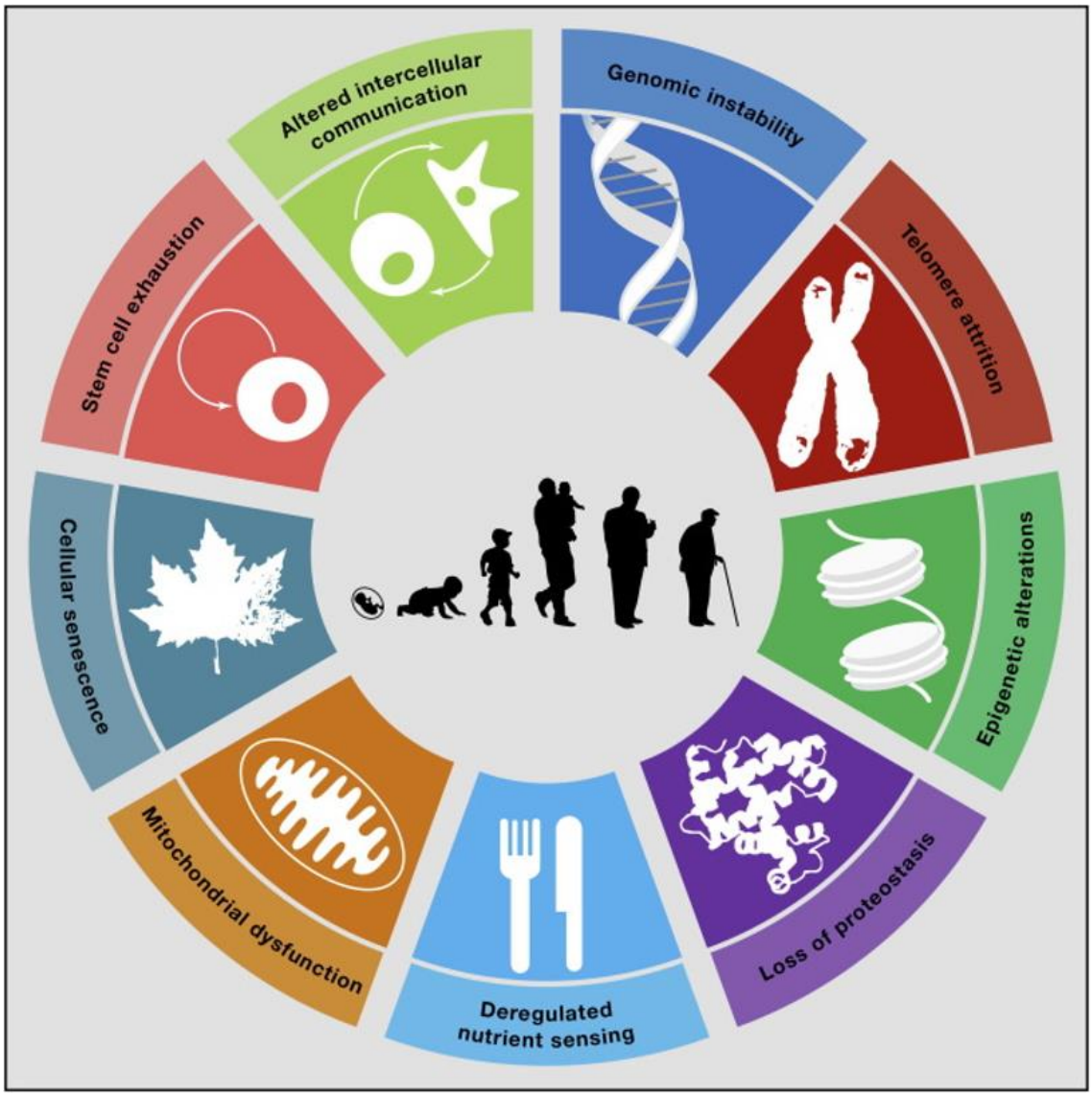


**Figure 3. Hallmarks of aging.** The nine accepted hallmarks that represent common denominators of aging in different organisms. (***Lopez-Otin et al Cell 2013)***

## *-Genomic instability*

The accumulation of DNA damage is known as genomic instability and it is an inducer of aging[16]. The integrity of the whole genome is continuously exposed to both, exogenous (chemical, physical and biological agents) and endogenous stressors (replication errors, oxidative stress coupled with normal cell metabolism, spontaneous hydrolytic reactions, defects

in nuclear structure…etc.) (Fig. 4). The resulting genetic scars can be highly different and embrace point mutations, translocation, single and double strand breaks of DNA, telomere shortening and chromosomal gain or loss. All these forms of DNA alterations may modify the expression or the functionality of essential genes and related pathways resulting in dysfunctional cells that, if not erase by apoptosis or senescence, may compromise tissue or organismal homeostasis (Fig. 4). Therefore, organisms have evolved a refined and composite system of DNA surveillance and repair to counteract the majority of nuclear DNA damage. The most dangerous type of DNA damage are the double-strand breaks (DSBs) and it has been estimated that there are ten DSBs per day per cell [17]. Apart from DSBs that occur during certain physiological processes like V (D) J recombination and immunoglobulin heavy chain class switch recombination, DSBs are predominantly repaired through the non-homologous end-joining pathway (NHEJ)[18]. However, there are also minor DSBs repair pathways that are engaged when NHEJ is somehow compromised (due to the lack of key protein components, for example) or when a substantial DNA end resection is needed. These mechanisms include the alternative end joining (a-EJ), the single strand annealing (SSA) and the homologous recombination (HR). Which pathway is adopted depends on the organism and on the range of micro homology, which is the number of the complementary base pairs at the two ends of the break after DNA resection. The a-EJ requires a micro homology range between 2bp and 20bp, the SSA more than 20bp and the HR more than 100bp. DNA resection generating micro homology regions is necessary because DSBs rarely have compatible DNA ends to permit direct ligation but it is still a damage, so bigger the resection, more serious is the damage. Indeed, since NHEJ requires less than 4bp of micro homology it can repair DSBs with minimal DNA resection. The inconvenience is represented by mutations that often accompany repaired DNA junctions after NHEJ, which does not occur in HR. Moreover, extensive resection also depends on the action of CDKs during the cell cycle and on the abundance of the Ku complex (see below) which is capable to prevent it. Indeed, CDKs target the checkpoint proteins of DNA damage response ATM and ATR as well as enzyme promoting resection and activate them. Usually, factors that elicit extensive end resection are more active during S and G2 phases. Therefore, NHEJ is dominant during the whole cycle whereas HR and SSA became favoured in S and G2 phases.

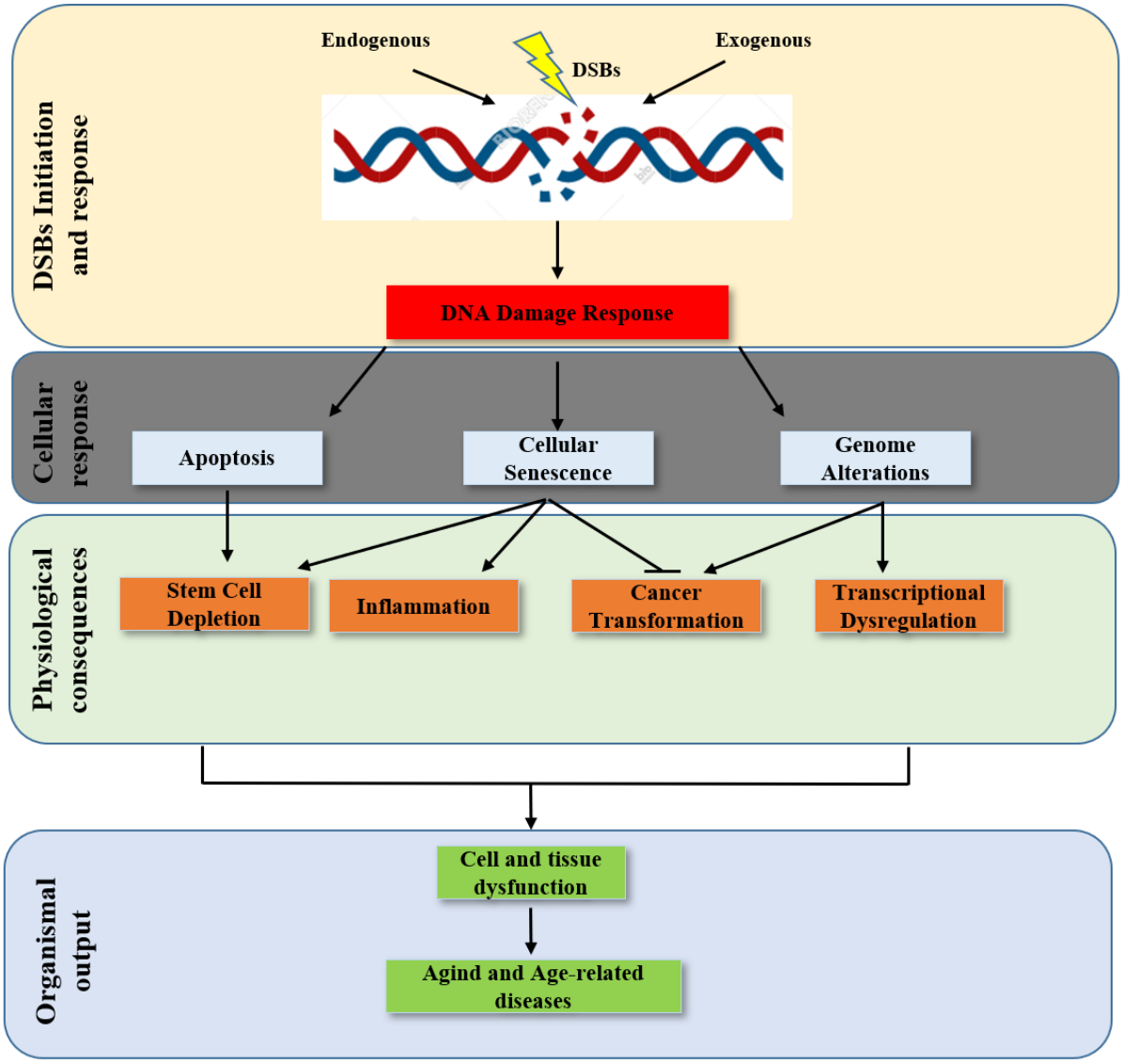


**Figure 4. DNA double strand breaks (DSBs) and triggered pathways in the way of aging.** Endogenous and exogenous stimuli can trigger DNA DSBs inducing DNA damage response that can lead to cellular apoptosis, senescence and genome alterations. These responses can drive trancriptional dysregulation, inflammation, cancer transformation and stem cell depletion that can culminate in cell and tissue dysfuncion causing premature aging and age-related diseases.

The first step in NHEJ (Fig. 5) is the recognition of DSBs by the Ku70-Ku80 heterodimer (known as Ku complex), which allow other NHEJ components to be recruited [19]. Once Ku complex binds DSBs the repair is carried out through NHEJ. A DNA-dependent protein kinase (DNA-PKcs) binds the Ku heterodimer forming the DNA-PK complex. After DSBs identification, DNA is resected if necessary. This process is performed by several nucleases in relation to their concentration and localization at DSBs sites, though the complex between endonuclease Artemis and DNA-PKcs, which is usually referred as the primary nuclease. Other nucleases involved especially in ionizing radiation-induced DSBs are aprataxin

and PNKP-like factor (APLF), the MRN-complex, exonuclease 1 and flap endonuclease 1 (FEN1). Once DNA resection is completed, few gaps within the strands can be generated, so DNA polymerases are needed to fill them. In human NHEJ, two polymerases are engaged: Pol μ and Pol λ[20]. These polymerases interact with the N-terminal domain of Ku complex and both can incorporate either dNTPs or rNTPs. If ribonucleotides are introduced, they are removed by BER. The processes of DNA resection, addition of nucleotides or a phosphate group or other modifications are collectively called *end processing*. The final step in NHEJ is the ligation of the strands performed by a ligase complex, which consist of four different proteins: DNA ligase IV, X-ray cross-complementing protein 4 (XCCR4), XRCC4-like factor (XLF, also known as NHEJ factor 1) and Paralogue of XRCC4 and XLF protein (PAXX).

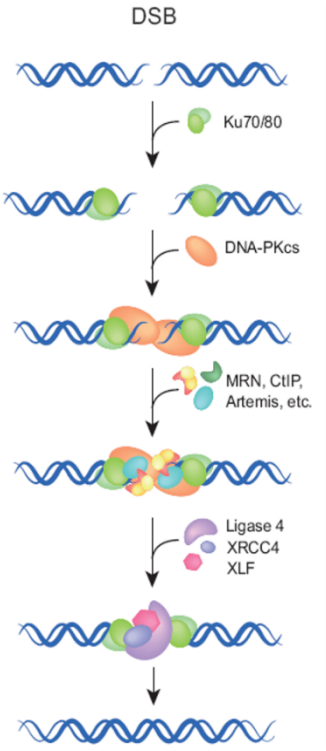


**Figure 5. Non-homologous end joining (NHEJ) pathway.** NHEJ depends on Ku heterodimer and DNA-PK catalytic subunit (DNA-PKcs), which together form the DNA-PK holoenzyme. The DNA ends are processed by additional enzymes and rejoined by the LIG4/XRCC4/XLF complex. ***(Dueva R. et al. TCR 2013)***

DNA ligase IV, XRCC4 and XLF are the most fundamental elements of eukaryotic NHEJ [21]. DNA ligase IV is an ATP-dependent DNA ligase encoded by the LIG4 gene whether XRCC4 is a tetrameric 38 kDa protein composed by two dimers, each of made up of two similar subunits. XRCC4 accelerates DNA ligase IV activity and interacts with the N-terminal head domain of XLF creating the XRCC4-XLF complex that forms a sleeve-like structure around

the DNA duplex. The created sleeve stabilizes the positioning of the two ends before covalent ligation by DNA ligase IV. XLF and PAXX are a 33kDa and 22kDa respectively proteins structurally like XRCC4. Other additional proteins can be engaged in NHEJ if the DNA ends requires modifications. For instance, a 5' end without phosphate commission a polynucleotide kinase (PNK). Depending on the micro homology between the ends, DNA joining can require nucleases and polymerases or only the ligase complex[18]. Each different case results in a different NHEJ sub-pathway. Blunt ends are usually repaired without *end processing* and promptly ligated while incompatible 5' ends are processed resecting the 5' overhang by Artemis-DNA-PKcs complex, followed by ligation. Compatible ends that have a short stretch of micro homology along with a non-base paired flap necessitate only the cleavage of the flap by Artemis-DNA-PKcs complex to start ligation. If the ends are incompatible at 3', they are treated by repetitive processes of end resection and nucleotide synthesis to generate short regions of base pairing before the ligation. Other cases may appear in which DNA ends present additional alterations but, after being somehow modified, they are processed in one of NHEJ sub-pathway discussed above.

A case apart is represented by mitochondrial DNA damage, because is known to be repaired with less efficiency [22]. Indeed, mtDNA has always been considered a major target for aging-associated mutations due to the high amount of ROS in the microenvironment of the mitochondria, the limited effectiveness of mtDNA repair machinery and the lack of protective histones in mtDNA [23]. Interestingly, several studies observed that replication errors instead of oxidative lesions cause most of mtDNA mutations in aged cells. In addition to genomic damage, accumulation observed in nuclear and mtDNA during aging, alterations in the structure of nuclear lamina can also generate genome instability[24]. The nuclear laminas participate in genome maintenance by suppling a scaffold for anchoring chromatin and other protein complexes involved in genome stability. The importance of nuclear laminas in genome instability and aging raised after finding that mutations in genes coding for their components or factors altering their maturation and function, provoke premature aging syndromes like the Hutchinson-Gilford and the Nestor-Guillermo progeria syndromes.

## -*Telomere attrition*

It might appear that the increase of DNA damage during aging can affect the genome randomly, but at each end of chromosome there are regions composed by repetitive nucleotide

sequences that are more vulnerable to age-related deterioration and they are called telomeres[25]. Since replicative DNA polymerases cannot replicate completely the terminal ends of DNA, after each replication the resulting chromosome is shortened. This phenomenon, known as telomere exhaustion or telomere shortening, occurs with aging and reflects the capacity *in vitro* of primary cells to divide in a limited number of times until they reach the so-called replicative senescence or Hayflick limit [26]. However, there is a specialized DNA polymerase, known as telomerase, which can restore telomere length. Most of mammalian somatic cells do not express telomerase, but other types of cells like germ and stem cells do, and several studies demonstrate that the only ectopic expression of telomerase is enough to confer immortality to otherwise mortal cells without causing oncogenic transformation, confirming telomere undeniable involvement in aging[27]. Moreover, mice lacking telomerase expression display premature aging that can be reverted when telomerase is genetically reactivated [28]; also, normal physiological aging in mice can be retarded without augment in cancer predisposition by pharmacological activation or viral transduction of telomerase [29]. Telomeres have also another peculiarity: they are invisible to the DNA repair machinery. Indeed, at the very end of telomeres a 300 pairs base single stranded portion forms a T-loop where a specialized protein complex called shelterin binds to telomeres and prevent their recognition as break point in DNA by repair machinery [30]. This can appear self-defeating because a damage at telomere level is permanent and leads cellular detrimental effects such as senescence and/or apoptosis, but it also precludes chromosomal fusion as a result of the non-homologous end-joining pathway of DNA repair.

## *-Epigenetic alterations*

A multiplicity of epigenetic modifications influence all cells in our body in the course of life[31]. They involve changing in DNA methylation pattern, post-translational modifications of histones and chromatin remodeling and they are controlled by the multiple enzymatic systems (DNA methyltransferases, histones methylases, demethylases, acetylases, deacetylases and protein complexes involved in chromatin remodeling) which are genetically inherited assuring the preservation of the epigenetic patterns [32]. Age-associated epigenetic marks are represented by increase in histone H4K16 acetylation and H3K4 trimethylation accompanied by decrease in H3K9 methylation [32]. Furthermore, aging take place with a global reduction in DNA methylation, apart from various tumor suppressor genes that became hyper-methylated [33], and heterochromatin formation at DNA repeated domains that affect chromosomal stability

[34]. It is good to note that epigenetic alterations can alter DNA also at telomeric repeats level and so attend on the regulation of telomeric length, underling that different hallmarks of aging can influence each other. Finally, epigenetic modifications are, at least theoretically, reversible offering researchers the occasions for the design of novel anti-aging treatments [35].

## -*Loss of proteostasis*

Since everything in our body works through the action of thousands of proteins, from enzymes to receptors, it is not surprising that the loss of proteostasis during aging is a hallmark of considerable relevance[36]. Proteostasis include all the mechanisms for the correct folding of proteins by chaperons, as well as all the mechanisms for their degradation by proteasomes or lysosomes [37]. Besides, all cells benefit of various quality control systems to safeguard the stability and functionality of their proteins and all these mechanisms work together to reestablish the correct structure of misfolding proteins or to degrade them completely, preventing the augment of damaged and non-functional components and providing constant replenishment of intracellular proteins [38]. Indeed, chronic presence of misfolded or agglomerated proteins is associated with the development of age-related pathologies like Parkinson and Alzheimer's diseases[36]. Regarding correct folding and protein stability, many evidences sustain the idea of chaperone decline during aging. Accordingly, overexpression of chaperones increases transgenic worms and lies lifespan and the activation of the transcription factor HSF-1, that is a master regulator in the heat-shock response, confers longevity in nematodes[39].

## -*Mitochondrial dysfunction*

Another important hallmark of aging is mitochondrial dysfunction. As mentioned earlier, mitochondria microenvironment is rich of ROS resulting from oxidative phosphorylation in the course of normal glucose metabolism and usually, an increase of ROS content accompanies aging. Therefore, mtDNA and all mitochondrial components are highly exposed to oxidative stress that can arise mischief and compromise global mitochondrial functionality. This theory, known as "mitochondrial free radical theory", has been accepted for many years and supported by multiple data[40]. However, recently studies have reported

contradictory results that have required an intense re-evaluation of the theory in question and they have boosted the investigation in ROS intracellular signaling discovering a role for ROS in triggering proliferative and survival signals[40]. Consequently, we can speculate that ROS are stress-induced molecules acting to promote survival during the progressive deterioration associated with aging. Then, as age increases, ROS levels reach such values that they deceive their original purpose and start to originate and elicit age-related damages. Among these studies, are of considerable impact the observation that 1. replication error instead of oxidative lesions causes most of mtDNA mutations in aged cells; 2.augmented ROS content can prolong *C.elegans* and yeast lifespan [41]; 3.genetic manipulations inducing mitochondrial dysfunction without increasing ROS accelerate aging [42]. Hence, the contribute of mitochondrial deficiencies, in the context of aging, must be consider also regardless of ROS actions; the mechanisms figured until today are numerous and sustain the idea that sirtuins act as metabolic sensors to check mitochondrial functionality in order to prevent age-related diseases. In particular, SIRT3, that is the main mitochondrial deacetylase, targets different components of energy metabolism and regulate the amount of ROS production by deacetylating manganese superoxide dismutase[43]. Other mechanisms include reduced biogenesis of mitochondria, defects in respiratory chain complexes and accumulation of mtDNA mutations along with oxidation in mitochondrial proteins[44].

## *-Stem cells exhaustion, inflammation and SASP factors*

The deterioration of the regenerative potential of tissues is one of the clearest feature occurring during aging and studies on aged mice, showing decrease proliferation in hematopoietic stem cell (HSCs), corroborate this phenomenon[45]. Nevertheless, also an exorbitant proliferation of stem cells can be identically detrimental for organisms by depleting stem cells niches. Aging affects also stem cell function and pharmacological approaches are tested to ameliorate it[46]. An example is represented by mTOR inhibition with rapamycin, which improve stem cell performance and enhance proteostasis[46].

One of the most common observation by scientists is that low chronic inflammation always accompanies the process of aging, so that they coined the term “inflammaging” to describe such process[47]. Inflammaging is a consequence of accumulation of pro-inflammatory tissue damage and the active secretion of cytokines and growth factors by senescent cells. Moreover, during inflammaging occurs a decline of the immune system that became less

capable to recognize and clear damaged, infected and senescent cells that consequently accumulate in aged tissues facilitating the onset of age-related pathologies[48].

The active production and release of pro-inflammatory molecules by senescent cells constitute the so-called senescence associated secretory phenotype (SASP) and the molecules, that include cytokine, growth factors, angiogenic factors, interleukins and matrix metalloproteases, are usually referred as SASP factors. Current evidence suggests that senescent cells and the SASP might participate to or be major drivers in chronic inflammation, the loss of tissue function, and age-related diseases [49]. Most of senescent cells typically overexpress chemokines like IL-6, IL-8 (CXCL8), GROα (CXCL1), GROβ (CXCL2), GROγ (CXCL3), MCP-1 (CCL2), MCP-2 (CCL8), MCP-4 (CCL13), MIP-1α (CCL3), MIP-3α (CCL20) and HCC-4 (CCL16) and others depending on cell type, cellular context and senescence stimuli [49]. The two most relevant factors among the list of SASP factors are interleukin 6 and 1.

Interleukin 6 (IL-6) is a pro-inflammatory cytokine that has been related with DNA damage and oncogenic-induced senescence in different cell types like human and mouse fibroblasts, monocytes and melanocytes[50 51]. Furthermore, increased DNA damage signalling enhances IL-6 extracellular secretion, amplifying its effects through the binding with the interleukin 6 receptor (IL-6R), which is present at the surface of nearby cells[52].

Interleukin 1 (IL-1) is another pro-inflammatory cytokine, which has been showed increased in senescent cells. There are two types of IL-1, encoded by two different genes: IL-1α and IL-1β. Both are overexpressed in fibroblasts, epithelial and endothelial cells and both act primarily triggering the nuclear factor kappa B (NF-κB), which is the key transcriptional regulator of SASP.

Despite generally there is an increase in the secretion of several SASP factors, it is important to note that the level of expression of many others do not change when cells senesce or it is down regulated like IL-2, 11 and Fractalkine[51]. Moreover, also the time to develop SASP is another considerable feature to consider, as not all SASP factors begin to be secreted at the same time[51]. It has been verified that mRNA expression profile of SASP factors in senescent cells follows the same behaviour in terms of protein expression, meaning that generally SASP factor secretion is regulated at the transcriptional level. However, since during senescence it is known to occur chromatin alterations, which change gene expression, the transcriptional control could be more probably at the level of chromatin organization.

The SASP may be a key target of anti-ageing therapies. Several treatments such as the inhibition of NF-κB pathway with metformin or the use of senolytics drugs or SASP suppressor are promising, but further studies are needed to avoid their negative side-effects and also to calculate the right time of intervention since senescence exerts also some beneficial effects like tumour suppression.

## - *Cellular senescence*

Senescence derives from the Latin word "*senex*" that means old man. In biology, Hayflick and colleagues firstly used the term senescence to identify cells that stop to divide during culture, despite the presence of space, nutrients and growth factors, demonstrating that normal cells have a limited capacity to proliferate [53]. This discovery raised two assumptions about senescence: the first one suggests cellular senescence as a benefit tumour-suppressive mechanism, to avoid the indefinitely proliferation characterizing cancer cells; the second one, instead, proposes cellular senescence as a deleterious age-related mechanism due to decline of tissue renewal and function observed during aging. Both hypotheses seem to contradict the other, but today recent progress in understanding the causes of senescence underlines that both are true. Indeed, we can consider cellular senescence as a mechanism of defence against cancer [54], as it stops nascent cancer cells from dividing. However, at the same time, it can generate deleterious effects [55], for example due to the accumulation of senescent cells accompanied by the release of SASP factors that spread inflammation, tissue dysfunction and age-related diseases. This, in biology, is called *"antagonistic pleiotropy"* [56]. There are different types of senescence. The senescence recognized by Hayflick and colleagues is named replicative senescence because arise during normal cellular replication and looks like an aging process but at cellular level instead of the whole organism [57]. When senescence is due to a telomeric dysfunction that activate the p53 pathway is termed telomere-initiated cellular senescence, whether if it is telomere independent, it stimulates p16 expression and trigger the p16-retinoblastoma protein (pRB) pathway and is called premature senescence [57]. Finally, senescence caused by oncogenes or by the loss of onco-suppressor genes is known as oncogene-induced senescence [57]. Senescence can also be induced exposing the cells to chemical or physical treatment that caused somehow DNA damage (hydrogen peroxide, X-irradiation, γ-irradiation, etc…). Anyway, this classification did not encase all the possible types of senescence because the phenotype can be even more variegated presenting mixed features.

Nevertheless, senescence possesses certain common peculiarities. First, it is restricted to proliferative cells, so non-dividing cells owing to differentiation cannot became senescent, like neuron or cells that compose brain, heart and skeletal muscle. Moreover, it is usually accompanied by cell cycle arrest, apoptosis resistance and gene expression alterations.

The cell cycle is the series of events that happen in a cell from its birth to its division into two daughter cells (Fig.6). It consists of four phases: the gap 1 (G1) phase, the S (synthesis) phase, the gap 2 (G2) phase and the M (mitosis) phase. The first three phases collectively constitute the interphase while the M phase include the mitosis and the cytokinesis. There is also another phase called G0 or quiescent phase, typical of non-proliferative fully differentiate cells in which they remain for all their life. It can also be detected in proliferating cells under certain stress conditions (often lack of nutrients and growth factors) by which they exit and resume to proliferate in response to positive stimuli. To proceed from a phase of the cycle to another, a cell must pass successfully through different cell cycle checkpoints, which are controlled by cyclin and cyclin-dependent kinases (CDKs). Therefore, the irreversible growth arrest induced by senescence is usually established through expression of cyclin and CDK inhibitors[58]. The features and severity of the growth arrest are different depending on the species and the genetic background of the cell[59]. It is interestingly to note that tumour cells can senesce too, often in response to anti-cancer treatments [60].

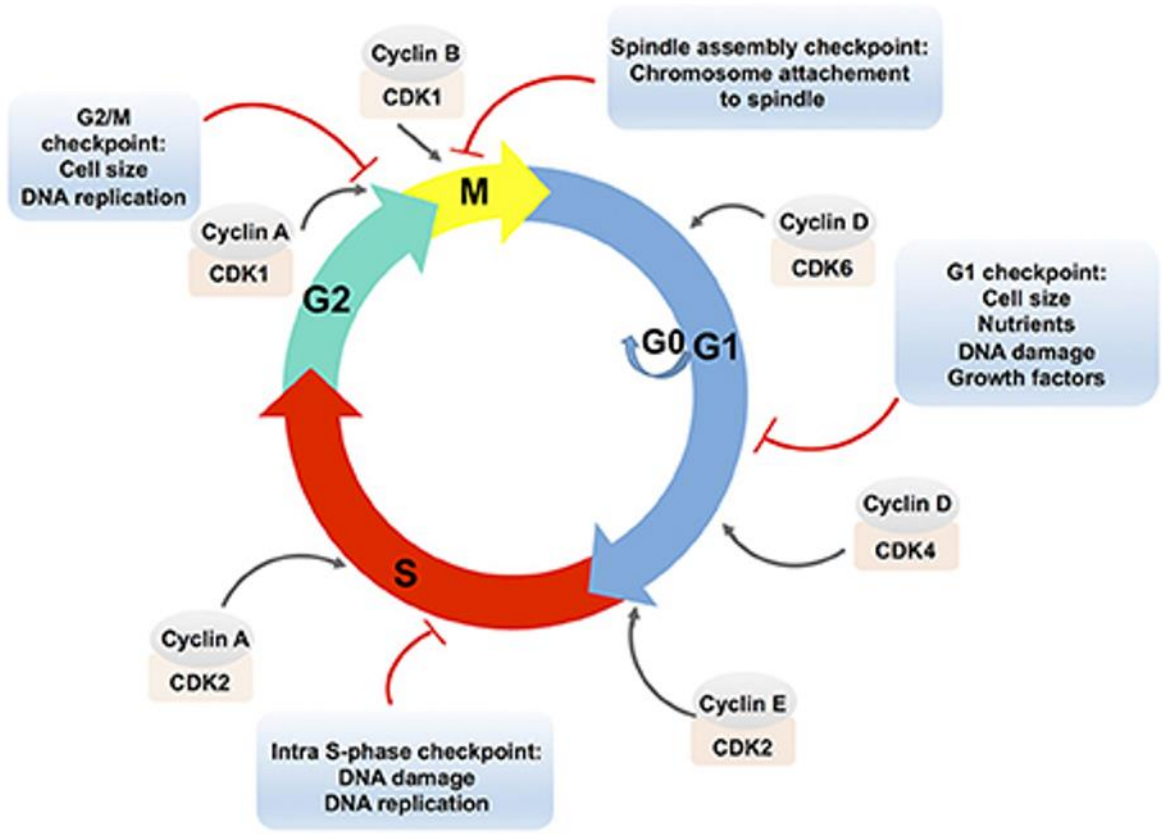


**Figure 6. The cell cycle.** The cell cycle consists of four phases: the gap 1 (G1) phase, the S (synthesis) phase, the gap 2 (G2) phase and the M (mitosis) phase. The first three phases collectively constitute the interphase while the M phase include the mitosis and the cytokinesis. There is also another phase called G0 in which the cell can enter transiently in case of lack of nutrients or permanently in case of non-proliferating cells. To successfully progress through the cell cycle phases a cell must pass three different checkpoints controlled by cyclin-dependent kinases (CDKs).

Apoptosis is a highly programmed form of cell death that can be caused by disparate stimuli and, like senescence, is an important tumour suppressive mechanism [61]. However, while apoptosis rapidly eliminates cancer cells, senescence only prevents the growth of stressed or damaged cells, which are more prone to transform in a cancer one. Moreover, senescence can induce apoptosis resistance[62]. This explains how senescent cells are so stable in culture and more important why their number increases during aging. Senescence-induced apoptosis resistance depends on the nature of senescence-induced stimulus and cell type[63]. Experiments performed manipulating pro- and anti-apoptotic genes show that a cell designed to die by apoptosis can be shifted to senesce and, inversely, a cell designed to senesce can be shifted to die by apoptosis[63]. This means that apoptosis and senescence regulatory systems are in deep

contact, presumably through the p53 protein, but how senescent cells became resistant to apoptosis is poorly understood.

Several markers identify senescent cells *in vivo* and *in vitro*. A clear marker of senescence is the lack of DNA replication, which can be detected by checking proliferating cell nuclear antigen (PCNA) protein expression or by incorporating fluorescent dyes in DNA. Unfortunately, these markers are just proliferation markers so they cannot discern a senescent cell from a quiescent or a differentiated cell. The senescence-associated β-galactosidase (SA-β-gal), which is detectable simply by histochemical staining, is very specific [64] and it results from the increased lysosomal biogenesis that commonly happen in senescent cells [65], but for the same reason it can results also by other cellular stressors not necessarily related with senescence, like metabolic stress or nutrient deficiency. There are also cytological markers that are useful to recognize senescent cells like the senescence-associated heterochromatin foci (SAHFs) and the senescence-associated DNA damage foci (SDFs)[66]. The first are due to a pRB-dependent chromatin rearrangement while the second result from dysfunctional telomeres or other sources of DNA damage. The two most common senescent markers are the CDK inhibitors (CDKIs) protein p21 and p16. These CDKIs are components of tumour-suppressor pathways directed by the p53 and pRB proteins and they can induce growth arrest that is typical of senescence. The p53 pathway usually is activated when stimuli trigger a DNA-damage response (DDR) (Fig. 7); this stimulates the alternate-reading-frame protein (ARF) that negatively controls the E3 ubiquitin-protein ligase HDM2 [67]. This protein recognizes the N-terminal trans-activation domain (TAD) of p53 and add an ubiquitin residue to it, promoting its degradation by proteasome. Finally, p53 degradation increases the expression of its transcriptional target p21 that provokes cell cycle arrest. The pRB pathway can be also recruited after DDR, but this usually occurs secondary to the involvement of p53 pathway[68]. In this case, senescence-inducing signals cause a direct augment of p16 protein, which inhibits cell cycle progression and prevents pRB phosphorylation and inactivation[69]. Afterwards, pRB stops cell proliferation by repressing E2F, a transcription factor required for the expression of genes that are involved in cell cycle progression and it increases ARF content engaging the p53 pathway[69]. Therefore, both pathways regulate each other (Fig. 7).

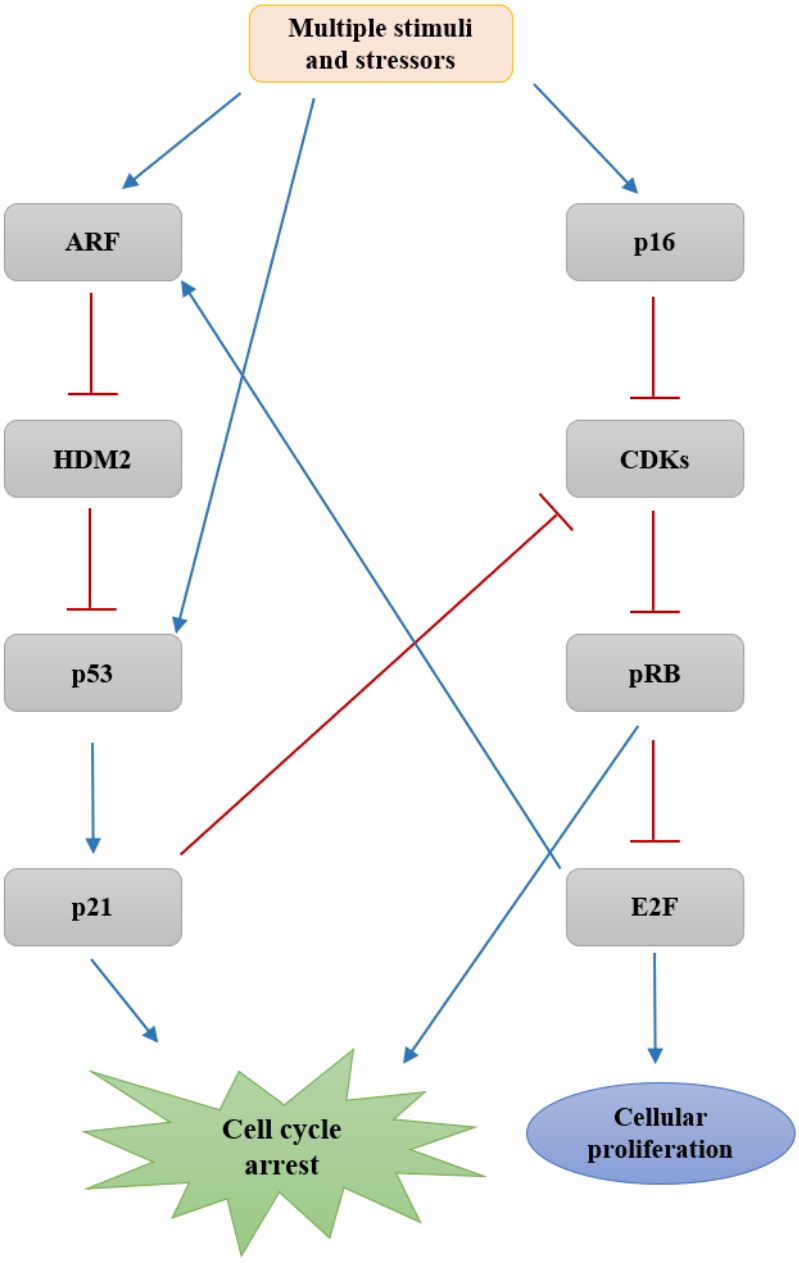


**Figure 7. The p53 and p16-pRB pathways.** The p53 pathway usually activates when stimuli trigger a DNA-damage response (DDR); this stimulate the alternate-reading-frame protein (ARF) that negatively control the E3 ubiquitin-protein ligase HDM2, which promote p53 degradation by proteasome. p53 degradation increase the expression of its transcriptional target p21 provoking cell cycle arrest. The p16-pRB pathway activation causes a direct augment of p16 protein, which inhibit cell cycle progression and prevents pRB phosphorylation and inactivation. pRB also stops cell proliferation by repressing E2F, a transcription factor required for the expression of genes that are involved in cell cycle progression and it increase ARF content engaging the p53 pathway.

It is not so clear how senescent is totally established or what determines whether cells senesce or arrest their growth transiently. There are evidences that reduction in p21, p53 or DDR proteins prevents senescence [70, 71], but once the cell is harmed, the proliferation, even in absence of p53 function, cannot be sustained because telomeres became critically damaged leading to cell death [71]. Since senescence markers are not so unique and precise to define senescence, researchers are always looking for new molecules available as better senescence markers.

As described earlier, a familiar characteristic of senescent cells is the active production and secretion of SASP factors. Studies using animal and cellular models have demonstrated that SASP factors can massively affect the function of nearby cells, upregulating inflammasome components and increasing the metabolic burden of senescent cells [49]. Therefore, the SASP is not only the result of senescence but also its promoter, creating a vicious circle in aging and age-related diseases. This primary-senescent-cell-induced cellular senescence has another name referred to as paracrine senescence [49]. Senescence and aging are closely interconnected and often they are unconsciously used as synonyms. As noted earlier, senescent cell accumulates with age and they are found at sites of age-related pathologies like atherosclerosis and diabetes type II [72]. Moreover, p16 expression increases with aging in many cell types and aged animal models [73, 74] and, as said earlier, the factors secreted by senescent cells can influence the behaviour of surrounding or even distant cells within tissues inciting their senescence and stimulating the growth and angiogenic activity of premalignant cells [49].

## *1.2.3. The impact of aging on VSMCs*

The effects of age on VSMCs behaviour have been widely studied and various VSMCs processes are recognized to be altered during aging, such as VSMCs proliferation, migration, apoptosis, inflammation, calcification and extracellular matrix (ECM) secretion (Fig. 8). Concerning proliferation, literature is still controversial: many studies indicate an increase of VSMCs proliferation rate during aging[75], while others report a reduction[76]. In the vascular wall of aged vessels, the intima is rich of VSMCs infiltrated from the underlying media, producing collagen and elastin that composed ECM. Since VSMCs are not capable to migrate *per sé*, it is necessary that, in the course of aging, they undergo a phenotypic change from their classical quiescent contractile behaviour that they possess in the media to a synthetic one [77]. Indeed, during aging, decreased levels of contractile proteins and increased expression of migratory

factors like monocyte chemotactic protein-1 (MCP-1) and matrix-degrading metalloproteinase (MMPs) have been described in different studies[78]. Moreover, enhanced MCP-1 expression by aged VSMCs boosts MMPs levels and activity, which promote migration of VSMCs *via* digestion of ECM and activates transforming growth factor-β1 (TGF- β1) that, in turn, positively regulates MCP-1 and MMPs[79]. Furthermore, degradation of ECM in the media, along with calcification and increase ratio of collagen to elastin, are responsible for aged-induced modifications resulting in an augmented stiffness and reduced elasticity of blood vessels. Moreover, MCP-1 together with interleukin-6 (IL-6) and reactive oxygen species (ROS) are the most inflammatory molecules elevated in aged vessels (Fig. 8). Evidences suggest that increased ROS levels are in part due to augmented nicotinamide adenine dinucleotide phosphate (NADPH) oxidase and impaired antioxidant enzymes expression during aging[80].

Finally, aging changes intercellular communications between vascular cells, immune cells, platelets and stem cells modifying their respective usual and functional locations (Fig. 8). For instance, alterations in the interaction between platelets and the vessel wall together with vascular leucocytes migration contribute to thrombin generation at the level of endothelium that stimulate VSMCs proliferation and migration via activation of focal adhesion (FA)-stress fibre complex [81]. In addition, infiltrated leucocytes released extracellular vesicles carry integrins on the surface of VSMCs that activate the AKT and ERK pathways[81]. Another example of aging-related intercellular alteration is represented by the increase in Notch signalling in VSMCs encouraged by endothelial cells (ECs). As a result, apolipoprotein D decreases attenuating the formation and stabilization of FAs and reducing stress resistance[81].

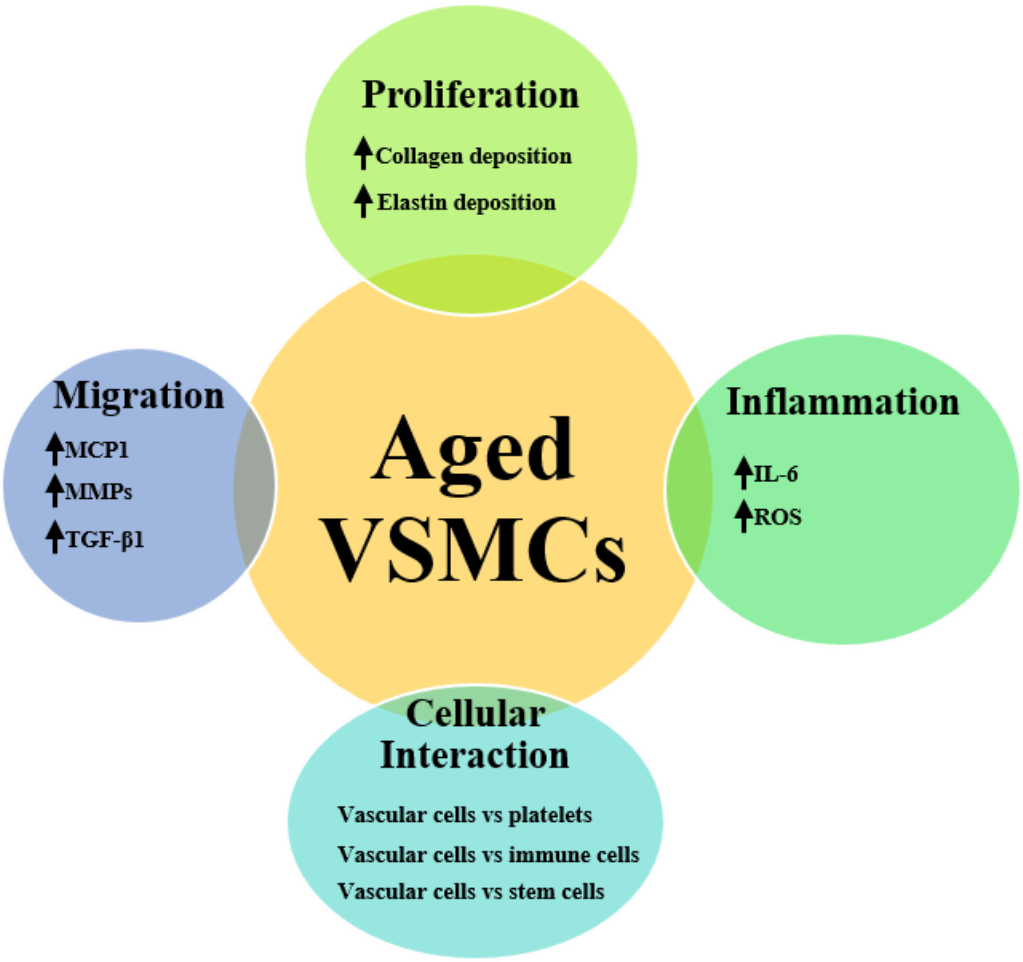


**Figure 8. VSMCs alteration during aging.** Aging influences several VSMCs propierties such as proliferation, migration, inflammation and cellular interactions compromising their function and resulting, terminally, with the onset of tissue dysfunction and age-associated pathologies.

## *1.3. Vascular calcification*

Vascular calcification (VC) is a biological process that involves crystallization of hydroxyapatite in the extracellular matrix and in the cells of the arterial wall[82]. Initially, VC was thought to be the outcome of a passive degenerative process, but recent findings show that VC is active and well-orchestrated by several signalling pathways[83]. There are many kinds of VC that can be variously classified (Fig. 10). From an anatomical point of view, two main types of VC have been described: vascular calcification of the intima (VCi) and vascular calcification of the media (VCm) (Fig. 9, 10). Both processes are more prevalent in men than in women,

they are associated with aging, they are equally relevant from a clinical point of view and they share several overlapping mechanisms.

VCi involves the cells of the intimal layer of blood vessels and it is commonly associated with atherosclerosis and aging (Fig. 9). Indeed, atherosclerotic plaques display classical signs of cellular senescence (reduced cell proliferation, DNA damage, telomere shortening, etc…), and there are growing evidences that senescence can also promote it[84]. VCi occurs in the presence of risk factors, especially hyperlipidaemia, and manifests locally at branch points as a chronic inflammatory process induced by lipid accumulation in the arterial wall. Then, principally in the middle age and older people, calcification of the atherosclerotic plaque arises leading to clinical manifestations like myocardial infarction and angina (if the plaque develops in the coronaries), stroke and ischemic attack (if the carotid is interested), and claudication and critical limb ischemia (if the plaque interests the peripheral artery) [85].

VCm includes a group of distinct pathological conditions that have different aetiology, but a common result, that is the calcification of the medial layer of arteries (Fig. 9, 10). Monckeberg medial sclerosis is the most frequent VCm and it is commonly associated with type 2 diabetes mellitus (T2DM) and chronic kidney diseases (CKD)[86]. Indeed, aging has an enormous impact on kidneys, and the onset of CKD is much higher in elderly patients. In fact, aged kidneys are characterized by a loss in renal mass that begin between the ages of 30 and 80 years with a more severe decline after 50 years [87] and a series of anatomical and morphological changes (glomerular sclerosis, tubular atrophy, interstitial fibrosis), which weaken its functionalities. Moreover, aging predisposes to several other diseases that can contribute to an easier and faster development of CDK [88].

Four stages have been described in order to distinguish the severity and the extent of VCm[86]. In the first stage, intra- and extra-cellular calcification deposits, consisting of fine granulations, appear; intracellular deposits are located in VSMCs, while the extracellular are largely associated with damaged elastic fibres insert within the ECM. Other inflammatory components like foam cells, lymphocytes and mast cells can be present. The granular calcifications develop alongside the internal elastic membrane and nearby VSMCs, where they can extend deep into the inner layer of the media. With further progression we enter in the second stage, where calcifications may deform the junction of the innermost and outermost layers of the media until, in the third stage, they involve the entire circumference. In the fourth stage, foci of bone formation within the arterial media are found and calcifications undergoing osseous metaplasia, which arises true bony trabeculae.

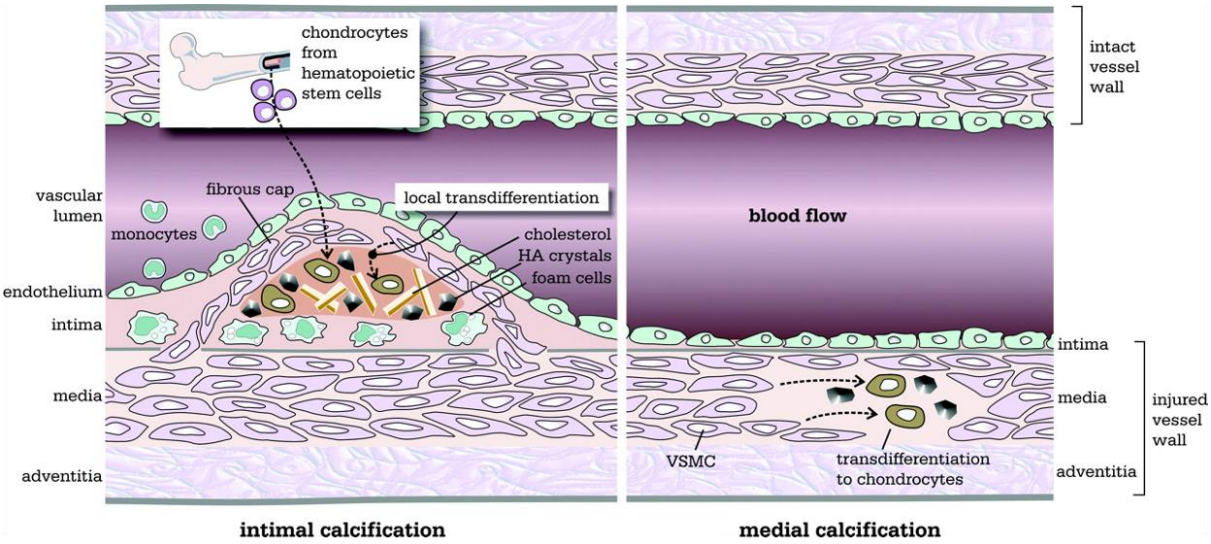


**Figure 9. The two-principal type of vascular calcification (VC)**. Anatomically there are two type of VC: the intimal calcification (VCi), which is associated with atherosclerosis and the medial calcification (VCm), which is frequently associated with T2DM and CKD. ***(Neven and D'Haese et al. Circ Res. 2011).***

The onset of VC has been associated to several mechanisms (Fig. 11). Firstly, VC can reminisce osteogenesis due to the discovery of osteoblast-like bone morphogenic protein (BMP-2) expression in calcified human atherosclerotic lesions[83]. The observation of bone-forming events like the production of matrix vesicles and apoptotic bodies in VC supports this idea[89]. Extracellular vesicles (e.g., microparticles, exosomes, matrix vesicles, apoptotic bodies) are membrane vesicles that are secreted by many cell types during both physiological and pathological conditions and emerging evidences suggest that they are involved in the initiation of calcification. Moreover, several results from different groups suggest that VC is a consequence of the loss of calcification inhibitors like vitamin-K-dependent matrix-Gla protein (MGP) [90], fetuin A [91], extracellular inorganic pyrophosphate (PPi), osteopontin (OPN) and osteoprotegerin (OPG) [92].

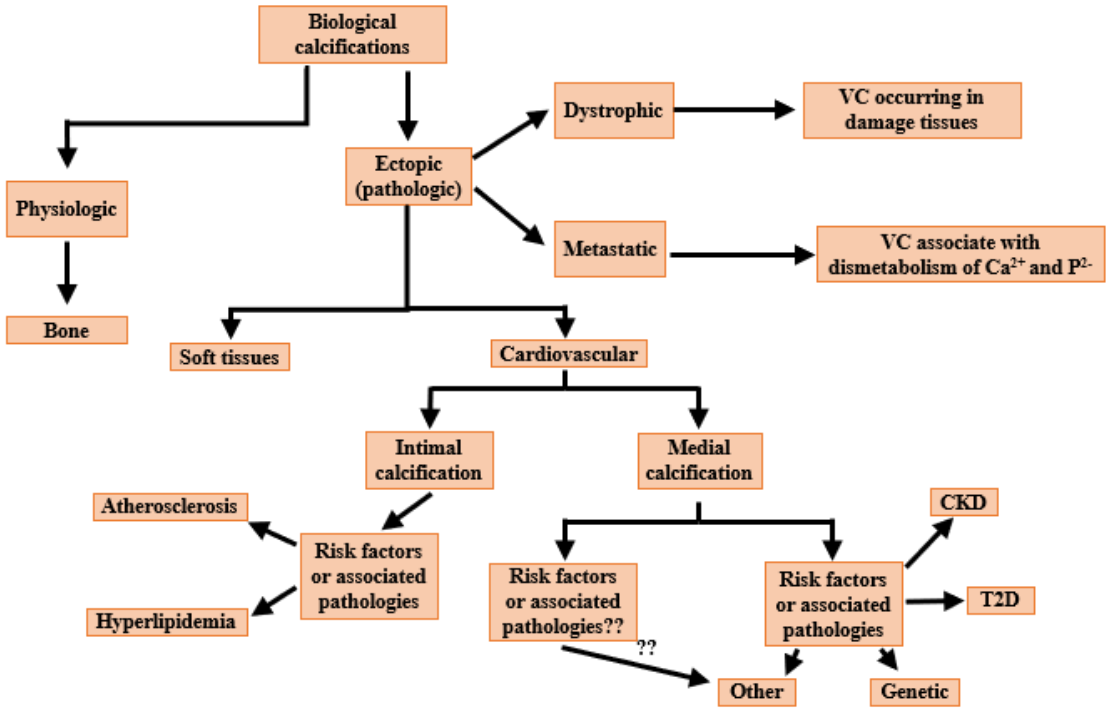


**Figure 10. Types and nomenclature of calcifications.** Calcifications that take place in bones are physiologic while outside (ectopic) became deleterious. From a pathological point of view ectopic calcifications are classified in dystrophic (occurring in damage tissues) and metastatic (associating with systemic disorders of calcium and phosphate metabolism) and they can involve both soft tissues and cardiovascular system, in which vascular calcification (VC) are the most frequent. Anatomically VC are distinguished in intimal and medial calcification and both are associated with risk factors and diseases.

MGP was originally isolated from bones and the development of VCm of the aorta in MGP deficient mice implied its engagement in VCm *in vivo*; MGP requires vitamin K-dependent γ-carboxylation to be functional and it reduces VCm through the binding of calcium ions and the inhibition of BMP-2 action in promoting VSMCs osteoblastic differentiation[90]. Fetuin A, a circulating inhibitor of VCm, is a $Ca^{2+}$-binding protein produced by the liver and it is found in serum whereas MGP and OPG are local factors implicate in VCm at the site of calcification. VSMCs uptake serum fetuin A and store it in intracellular matrix vesicles that become the nidus for mineral nucleation. When they are released from VSMCs, fetuin A binds calcium and prevents its accumulation. It has been also demonstrated that fetuin A localizes and inhibits calcification in forming apoptotic bodies[93].

OPN is an acidic phosphoprotein expressed in mineralised tissues able to block hydroxyapatite formation and activates osteoclast function[94]. Normally OPN is not present in vessels but it is largely detected in calcified arteries, suggesting that it is a regulator of VCm.

Studies of OPN deficient mice indicate that OPN has an inhibitory effect on VCm *in vivo*[95]. However, phosphorylation of OPN is necessary to block its effect on VSMCs calcification and to counteract the progression of VCm[96]. Moreover, OPN has recently emerged as a pro-inflammatory cytokine promoting vascular remodelling through the activation of MMPs that can eventually enhance VCm (Wada T et al 1999). Hence, it is evident that OPN has multifunctional and contrasting roles on VCm pathogenesis[94].

OPG is a soluble cytokine belong to the tumour necrosis factor (TNF) receptor superfamily and it is a crucial modulator of bone density and an inhibitor of VCm through its action as a decoy receptor for the Receptor Activator of Nuclear Factor kappa-B ligand (RANKL)[97]. OPG can be found as either a 60-kDa monomer or a 120-kDa dimer; the dimerization of OPG is necessary for RANK-RANKL inhibition as it increases the affinity of OPG for RANKL[98]. OPG deficient mice experience large VCm suggesting its role as a calcification repressor also *in vivo*[99]. Moreover, OPG expression in osteoblasts is highly regulated by estrogens such as estradiol that upregulate OPG mRNA transcription [100], which could explain in part why VCm occurs less in women than in men.

PPi is generated from the hydrolysis of nucleotide triphosphates by the nucleotide pyro-phosphatase phosphodiesterase family (NPP) and is the major VCm inhibitor because it attenuates the formation of hydroxyapatite crystals[101]. Moreover, PPi can also stabilize VSMCs phenotype, via inhibition of VSMCs cartilaginous metaplasia and their trans-differentiation into chondrocytes or osteoblast-like cells[102].

VC can also be promoted by an augment of calcium and phosphate concentrations and other stressors, typical of patients affected by CKD, or by particular genetic conditions such as "arterial calcification due to the deficiency of CD73" that is a monogenetic autosomal recessive disease, characterized by tortuous arteries and massive medial calcification [103].

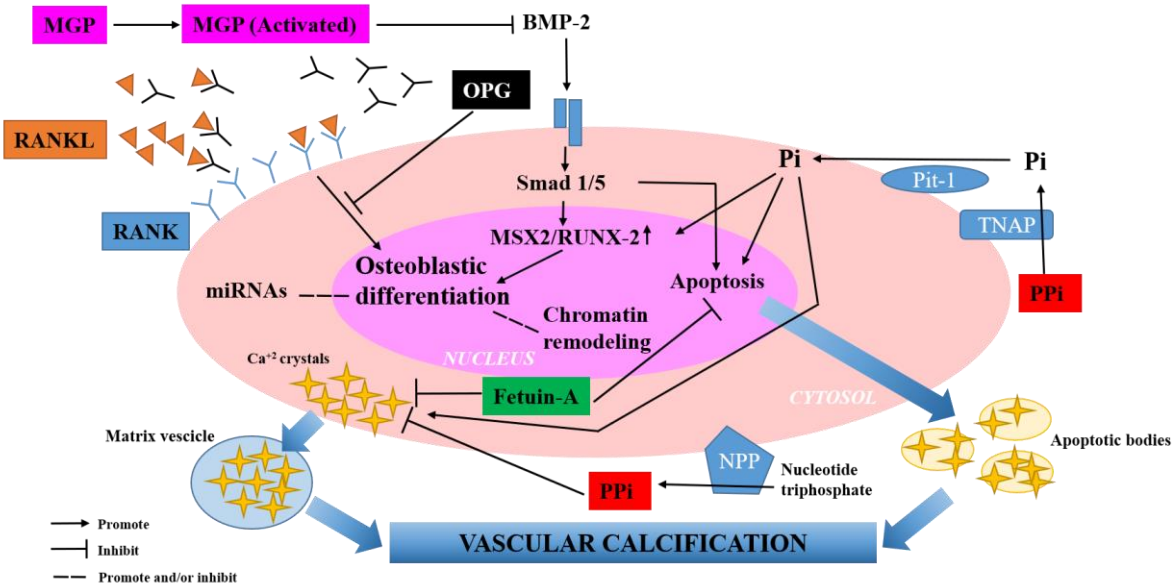


**Figure 11. Mechanisms of medial vascular calcification (VC) in vascular smooth muscle cells (VSMCs).** Multiple overlapping mechanisms are involved in VC. The main event is the osteoblastic differentiation of VSMCs which can be promoted by the MSX2/RUNX-2 axis through the activation of BMP-2. Moreover the unbalancing between calcification inhibitors (MGP, OPG, Fetuin-A and extracellular PPi) and promoters (Pi) can encourage VC development.

The main cellular event responsible for VC is the trans-differentiation of VSMCs to an osteoblast-like phenotype (Fig. 11). VSMCs are plastic cells and so are able to regulate their phenotype in response of both endogenous and exogenous stimuli; moreover, it has been demonstrated that they can differentiate to osteoblast-like cells and enact a cellular program mediating accumulation of bone matrix in blood vessels[104]. Indeed, VSMCs of calcified blood vessels express various bone-related transcription factors like msh homeobox 2 (Msx2), SRY [sex-determining region Y]-box 9 (Sox-9), Runt-related transcription factor 2 (Runx-2) and Osterix that are bone and chondrocyte proteins and regulate important processes essential for the acquisition of osteoblastic phenotype [105]. Pro-osteogenic factors can activate Msx2 and Wnt signalling, which result in increasing expression of Runx-2 and Osterix[104]. Runx-2, in turn, augment the expression of bone-related protein like osteocalcin and RANKL [106], while Osterix, which is downstream to Runx-2, increases other bone-related proteins content including alkaline phosphatase (ALP) and bone sialoprotein [107]. It is important to note that *in vivo* experiments determine that Runx-2 enhancement occur prior to the deposition of calcium in the vasculature and that only its increase, and not downregulation of VSMCs contractile proteins, is relevant for VSMCs trans-differentiation and eventually calcification [108]. Moreover, the same

studies confirmed that VSMCs, and not bone marrow-derived progenitor cells, were responsible for VCm[108].

How VSMCs reprogram their genetic code to osteoblast-like cells is an area of intense investigation. ERK pathway activation seems to be determinant and it has been shown to take place before the decreasing of VSMCs contractile protein as well as Runx-2[108]. More recently, microRNAs have been emerged as powerful regulators of VC. MicroRNAs (miRNAs) are ~22 nucleotide small non-coding RNAs that bind to complementary seed sequences in the 3'-UTR of an mRNA target to promote its degradation in order to regulate its expression. Our group have recently published that miR-34a promotes VCm via VSMCs mineralization by inhibiting cell proliferation and inducing senescence through direct downregulation of two of its known targets, Axl and SIRT1 [74]. We found also that mir34a deficient mice display reduced soft tissues and aorta medial calcification, Sox-9 and Runx-2 expression as well as the senescence markers p16 and p21[74]. Hence, inducers of VSMCs senescence facilitate osteogenic transition of these cells (Fig. 12). Furthermore, it has been demonstrated that senescent VSMCs present consistent DNA damage and a specific "pro-calcific" phenotype, which is further reinforced by a major production and secretion of inflammatory and pro-calcification SASP factors [109] (Fig. 12).

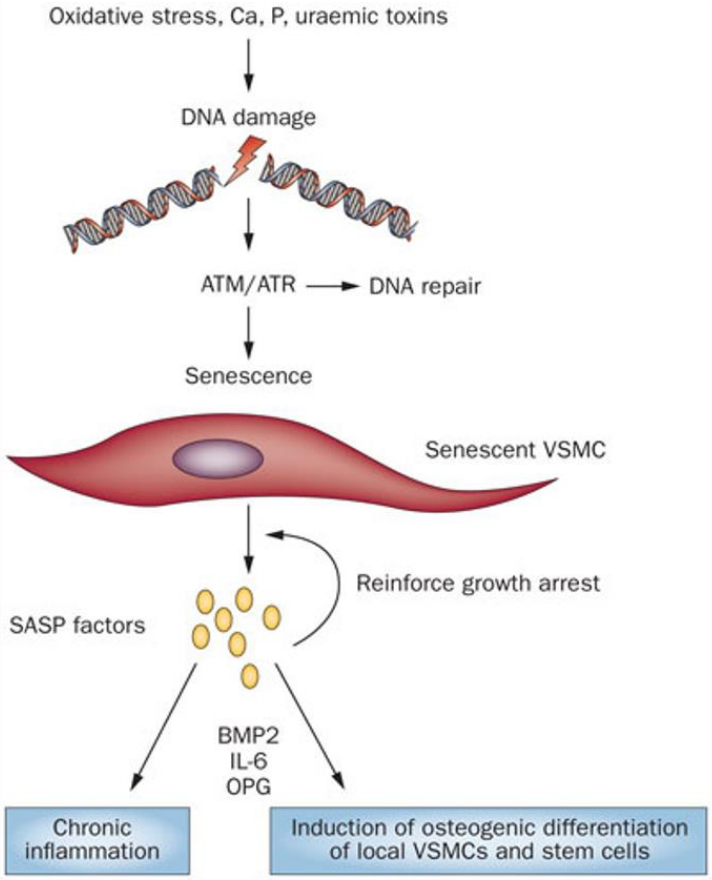


**Figure 12. Senescent VSMCs present a «pro-calcific» phenotype.** Uraemic toxins induce VSMCs DNA damage. If DNA damage cannot be repaired, cells can undergo senescence and secrete cytokines and growth factors that can act to induce osteogenic differentiation of VSMCs as well as of local and circulating stem cells ***(Shanahan CM, Nat Rev Nephrol, 2013)***

.

## *1.4. High mobility group box 1 (HMGB1)*

HMGB1 is a highly conserved non-histone chromatin binding protein present in the nucleus of almost every cell type [110]. It belongs to the superfamily of HMG proteins, consisting of HMGA, HMGB and HMGN families that share an acidic tail essential for DNA binding, but maintain a unique functional motif and participate in distinct cellular functions[111]. In mammals, there are three members of the HMGB family: HMGB1, HMGB2, and HMGB3. Evolutionary studies suggest that the organization of genes coding for the HMGB proteins is conserved among multicellular animals (99% homology between mammals) and is unknown outside Metazoans. These studies also suggest that HMG-box derives from an ancestral single HMG-box that generated in the first multicellular animal by the union of two genes, each encoding a single box. During evolution, this ancestor gene duplicates in two early "ProtoBoxA" and

"ProtoBoxB", precursors of HMG Box A and Box B [112]. Indeed structurally, human HMGB1 is a 25 kDa protein composed of 215 amino acids organized in two positively charged DNA-binding structures, named A and B boxes and a negatively charged C-tail, composed of 30 glutamic and aspartic acids (Fig. 13). The A and B boxes have helical structure, partly covered by the tail, which is folded over the protein. HMGB1 mainly resides in the nucleus where it binds to the minor groove of DNA and it is involved in transcription, replication, DNA repair, and maintenance of nucleosome structure and number [113]. Since it has two nuclear localization signals (NLS1 and NLS2) and two unusual nuclear export signals (NESs) (Fig. 13), HMGB1 can translocate from nucleus to the cytosol, even if the concentration in the first compartment is much higher (in the range of micro-molar) than in the second. Cytosolic HMGB1 has been showing to regulate cellular autophagy and apoptosis during inflammation and to participate in mitochondrial activity and functions[114]. Moreover, HMGB1 can also be present in the extracellular milieu operating as an extracellular "alarmin" and it has been proposed as the archetype of endogenous danger signals also called DAMPs (Damage-Associated Molecular Patterns) [115]. HMGB1 can be actively secreted by cells of the immune system stimulated with pro-inflammatory molecules, or passively released by necrotic cells after trauma or infection. Extracellular HMGB1 acts as signal of danger to the surrounding cells, it triggers inflammation, it activates innate and adaptive immunity and finally it promotes tissue repair[116]. Box A has anti-inflammatory properties, since it is an antagonist for HMGB1 binding to its most known receptor RAGE and it inhibits HMGB1 cytokine effects *in vivo*. On the contrary, box B has pro-inflammatory effect and contains the binding sites for different receptors, including TLR4 and RAGE [117]. HMGB1 has three conserved cysteines (Fig.13) in position 23, 45 (Box A) and 106 (Box B) that are susceptible to reduction or oxidation depending on the redox conditions of the compartment in which HMGB1 is localized and that influence the extracellular functions of the protein [118]. Studies with HMGB1-deficient mice demonstrated the vital importance of HMGB1 during embryonic development. Indeed, mice die 24 hours after birth for hypoglycaemia, also proving the involvement of HMGB1 in the expression of the glucocorticoid receptor encoded by the gene Glr1[119].

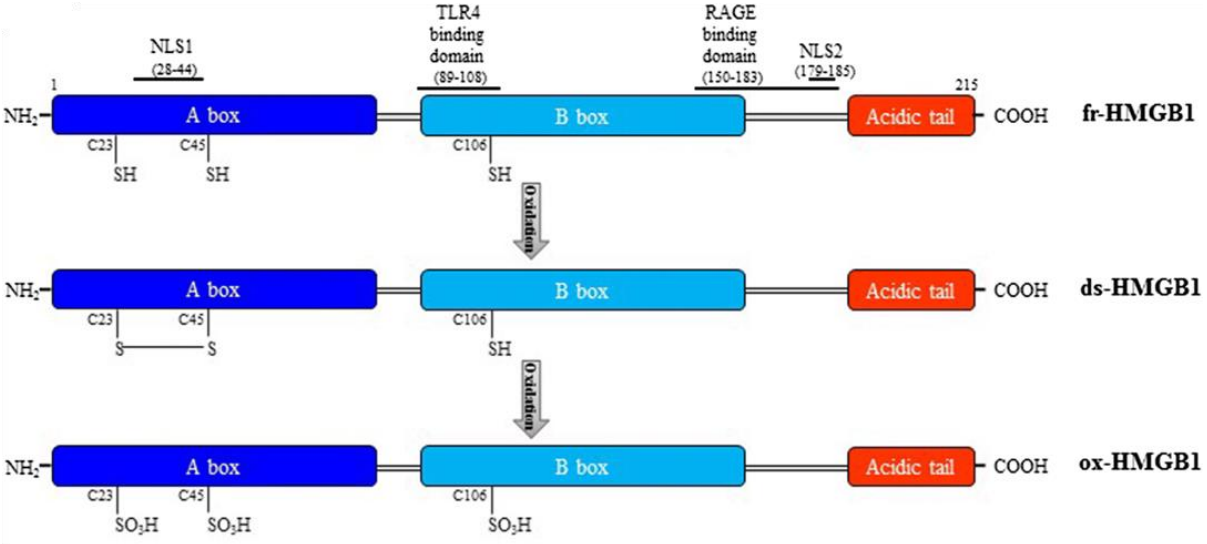


**Figure 13. Structure and redox forms of HMGB1.** HMGB is a 25 kDa protein composed of 215 amino acids organized in two positively charged DNA-binding structures, named A and B boxes and a negatively charged C-tail, composed of 30 glutamic and aspartic acids. Box A has anti-inflammatory properties, since it is an antagonist for HMGB1 binding to its receptor RAGE, while box B has pro-inflammatory effect and contains the binding sites for different receptors, including TLR4 and RAGE. In the extracellular space HMGB1 can exist in three redox forms depending on the relatively redox state of its cysteines: fully reduced HMGB1 (fr-HMGB1), disulphide HMGB1 (ds-HMGB1) and oxidized HMGB1 (ox-HMGB1).

## *1.4.1. Nuclear roles of HMGB1*

In the nucleus, HMGB1 binds to the minor groove of DNA in a no sequence-specific manner, regulating chromatin structure, gene expression and gene transcription (Fig. 14) [120]. It has been demonstrated that HMGB1 also binds with greater affinity to kinked and unwound non-B-type DNA structure[121]. An interesting peculiarity of HMGB1 is its high dynamism, being able to interact with a new nucleosome every second scanning the DNA in search for the right binding site [122]. Additional interactors might affect HMGB1-DNA association. This is the case of nuclear aggregates of polyamines (NAPs). NAPs naturally form complexes with DNA to assist the conformational changes of the double helix and to protect DNA integrity and modulate DNA-protein interaction; in this way, they actively contribute to the dynamic modelling of chromatin[121]. It has been proposed that NAPs interposition between DNA and HMGB1 is important for DNA packaging into chromatin[121]. HMGB1 is crucial for nucleosomes assembly, accelerating this process onto naked DNA, acting like a "chaperon"[123]. Mammalian cells lacking HMGB1 have a lower number of nucleosomes because of lower number of histones. *Hmgb1*$^{-/-}$ mouse embryonic fibroblasts (MEFs) have about 20% less amount of all histones[123]. Nucleosomes and histones loss can result in an increased genomic

instability and hypersensitivity to DNA-damaging agents because of the increased exposition of DNA to injurious agents, such as hydroxyl radicals[124]. Hence, loss of HMGB1 is involved in age-associated nuclear defects. Moreover, nucleosomes reduction does not alter spacing and location but reduces occupancy that correlates with an augmentation of transcript abundance, supporting the fact that transcription is due to the accessibility of DNA, which is dependent by nucleosomes[123]. The release of HMGB1 after exposure to an inflammatory stimulus reduce the histones content in macrophages [125]. In activated macrophages, HMGB1 can be removed from the nuclear pool [126] and the depletion of HMGB1 increases macrophages response to inflammation [125]. Indeed, in *Hmgb1*$^{-/-}$ fetal liver-derived monocytes (FLDMs), many chemokine transcripts involved in chemotaxis, motility, cell adhesion and response to stress stimuli were upregulated, demonstrating that the release of HMGB1 from activated macrophages leads to chromatin rearrangements caused by nucleosomes and histones loss that contribute and regulate the inflammatory response [125].

As a nuclear factor, HMGB1 has many other roles. It helps the enhanceosome formation, stabilizes nucleoprotein complexes and is involved in chromatin remodelling and gene transcription by regulating the activity of several DNA-binding factors[127]. During the process of V (D) J recombination, recombination-activating gene (RAG) 1 and RAG2 in concert with HMGB1 generate double-strand DNA breaks in recombination signal sequences (RSSs), necessary to finally generate functional antigen receptors on developing lymphocytes[128]. Thus, HMGB1 is an important component of the V (D) J recombinase complex and stabilizes RAG binding to RSS[128]. HMGB1 is also able to bind different members of the onco-suppressor gene p53 family, including the two splicing variants of the tumour suppressor factor p73 α and β. Both box A and box B can interact with p73 and the formation of a p53/p73-HMGB1 complex enhances the recruitment of both p53 and p73 to the Bax and Mdm2 promoters further facilitated by the DNA bending activity of HMGB1 [129]. Some of the functions carried out by HMGB1 are specifically related to its affinity for histone H1. These two factors share some similarities: in fact, both proteins are non-sequence specific, binds preferentially to alternative DNA structure (bent DNA, supercoiled DNA) and seem to compete for same binding sites on DNA, exerting opposite effects [130]. The ability of HMGB1 to displace histone H1 is modulated by its redox state: while reduced HMGB1 easily displaced H1 from DNA, oxidized HMGB1 had limited ability to replace it [130]. The displacement of histone H1 can have important biological effects, including destabilization of chromatin, recruitment of other factors and transcriptional activation[131].

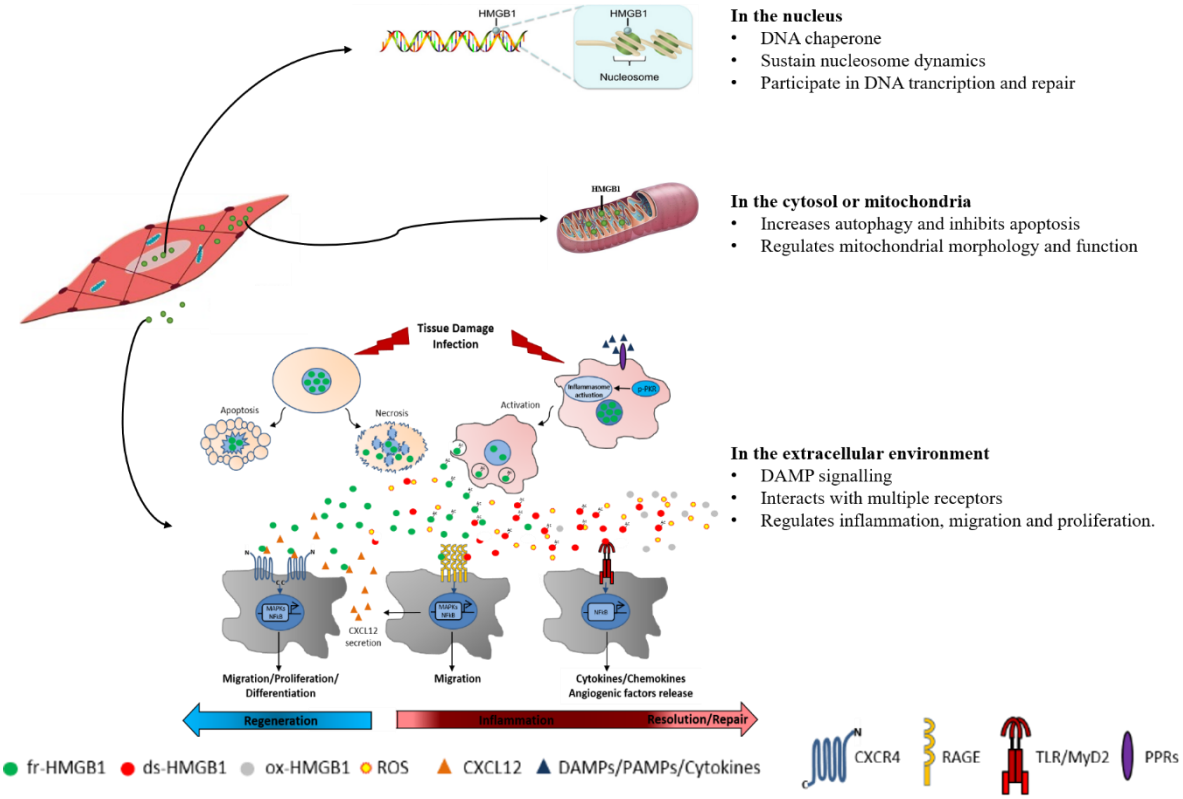


**Figure 14. Functions of HMGB1.** HMGB1 has many roles depending on its cellular localization. In the nucleus, HMGB1 binds to the minor groove of DNA in a no sequence-specific manner, regulating chromatin structure, gene expression and gene transcription; in the cytosol HMGB1 has been showing to regulate cellular autophagy and apoptosis during inflammation and also it participates in mitochondrial functions. In the extracellular space HMGB1 function as a DAMP and, regulates tissue inflammation and regeneration during an injury depending on its redox state.

## *1.4.2. Extracellular roles of HMGB1*

The first evidence of an extracellular function for HMGB1 dates to 1999 when Wang et al. described for the first time HMGB1, released by murine macrophage-like RAW 263.7 cells stimulated for 18 hours with LPS, as a late mediator of endotoxemia [122, 132]. Notably, HMGB1 neutralization with an anti-HMG-1 antibody increased the survival rate of LPS-treated mice from 30 to 70%[132]. As mentioned earlier, in the extracellular space HMGB1 function as a DAMP (Fig. 14) and, like all the alarmins, has a main role in the nucleus but it can become a danger signal when released in the extracellular environment by cells under stress or danger situations [115]. Indeed, extracellular HMGB1 can activate innate and acquired immunity, it can

promote tissue repair, and regeneration [133], but it can also directly affect fibroblasts, monocytes/macrophages, dendritic and endothelial cells activation and migration [134]. Inhibition of extracellular HMGB1 has been observed to attenuate inflammation and confer protection in several animal models of experimental diseases including cardiac and liver ischemia/reperfusion injury [135], diabetes [136], autoimmune diseases [137] and epilepsy [138].

This pleiotropic activity depends on HMGB1 sensitivity to the environmental oxidizing conditions that induce redox post-translation modifications. Based on the redox state of the cysteines, three redox forms of HMGB1 have been identified. Fully reduced HMGB1 (fr-HMGB1) in which all cysteines are reduced, disulphide HMGB1 (ds-HMGB1) in which C23 and C45 are partially oxidized forming a disulphide bond, while the unpaired C106 is reduced and sulfonyl HMGB1 (ox-HMGB1) in which all cysteines are oxidized [118] (Fig. 13). Fr-HMGB1 exerts chemotactic action and skews polarization of macrophages toward a regenerative phenotype[118]. Ds-HMGB1 stimulates pro-inflammatory cytokine/chemokine production in immune cells and is pro-angiogenic in endothelial cells[118]. Ox-HMGB1 can be found in the late stage of the inflammatory process and is associated with the resolution/regenerative phase[139].

The multifunctional activities of HMGB1 rely on the ability of the redox forms to bind different receptors, alone or in heterocomplex with other ligands [140]. The receptors most widely studied are RAGE, TLR2-4 and CXCR4 [140].

RAGE is a transmembrane receptor with structural features of adhesion molecules that recognizes several other proteins, like advanced glycation end products (AGEs), S100/calgranulin proteins, amyloid β-peptides and extracellular matrix components [141]. It has been shown that RAGE is involved in a variety of pathologies mediated by HMGB1 and this axis represents an important potential target[142]. Although all redox forms of HMGB1 interact with RAGE, ds-HMGB1 binds with higher affinity[143].

TLRs constitute a family of transmembrane molecules involved in host defence that have similar structure but differ in their subcellular localization and ligands [144]. TLR2 and TLR4 interact with HMGB1 leading to nuclear translocation of NF-κB and expression of pro-inflammatory cytokines in neutrophils and macrophages[145]. The TLR2/HMGB1 axis are known to promote natural killer (NK) and cancer stem cell activation[146].

CXCR4 is a receptor for SDF-1/CXCL12, an important chemotactic stimulus for leukocytes [147]. It has been published that fr-HMGB1 forms a heterocomplex with CXCL12 that protects CXCL12 from degradation and is responsible for CXCR4-mediated migration in mouse

embryonic fibroblasts (MEFs), human cardiac fibroblasts (hcFbs), macrophages, dendritic cells and myoblasts[118]. Moreover, fr-HMGB1 promotes muscle, skeletal, hematopoietic and liver regeneration through CXCR4, at least in part by recruiting tissue healing macrophages and promoting the transition of resident stem cells from the G0 to the G alert phase, thereby accelerating their proliferation, migration and differentiation[118].

Hence, extracellular HMGB1 undergoes progressive redox modifications necessary to start, regulate and resolve the inflammatory response, but also to coordinate tissue repair and regeneration through the recognition of different receptors and interactors.

## *1.4.3. HMGB1 and senescence*

Senescence is associated with a deep chromatin reorganization, which is essential for fine-tuning gene expression, and with inflammation promoting particularly by the secretion of SASP factors[109]. HMGB1 plays a role in both inflammation and DNA maintenance, so it is not surprising that it can influence cellular senescence.

Nuclear HMGB1 has been shown to delocalize to the cytosol and eventually to the extracellular milieu in senescent human and mouse fibroblasts[148]. Moreover, altered HMGB1 expression induces a p53-dependent growth arrest and senescence[148].

A common characteristic of senescent cells is apoptosis resistance, thus, the choice of cells to undergo apoptosis or became senescent is crucial to determine their fate. Lee and colleagues analysed HMGB1 content in highly and poorly metastatic mouse cancer cells in response to genotoxic stress after treatment with doxorubicin and camptothecin. Interestingly, they observed that highly metastatic mouse melanoma cells show a senescent phenotype and persistent HMGB1 expression, while poorly metastatic cells, with low HMGB1 levels, enter apoptosis suggesting that HMGB1 can modulate the balance between senescence and apoptosis[149]. Mesenchymal stem cells (MSCs) isolated from systemic lupus erythematosus patients, which are characterized by impaired growth and senescence, contain remarkably higher content of extracellular HMGB1 in respect to normal MSCs in their supernatants [150]. Moreover, the stimulation of normal MSCs with exogenous HMGB1 increases the ratio of SA-β-gal positive, disrupts the organization of cytoskeleton and activates the TLR4-NF-κB signalling, while treatment with ethyl pyruvate, known inhibitor of nuclear HMGB1 translocation, reverses the senescent phenotype of MSCs and alleviates inflammation [150].

HMGB1 has been shown to influence SASP acquisition. HMGB1 depletion or the use of a specific antibody anti-HMGB1 attenuates senescence-associated IL-6 secretion in human fibroblasts, while administration of exogenous HMGB1 stimulated NF-κB activity and restored IL-6 secretion in cells unable to express HMGB1[148]. Moreover, HMGB1 has been demonstrated to counteract IL-1α induced-senescence in human umbilical vein endothelial cells (HUVEC) via p53-p21 pathway[151].

Very recently, Zirkel A. and colleagues have demonstrated that HMGB2 genome positioning is cell specific[152]. Moreover, they also map topological associated domains (TADs) boundaries on the genome of different type of cells and they discovered that HMGB2 binds to a considerable and specific fraction of TADs and that this topological contribution is lost upon senescence entry[152]. Thus, is reasonable that also HMGB1 can promote similar outcomes. HMGB1 has been also proposed to bind mRNA exons, 5' and 3'UTR and a substantial number of non-coding RNAs[153]. In this way, it can influence RNA splicing and hence, control gene expression and senescence[152].

Finally, increased ROS content and oxidative stress are known to induce senescence via DNA damage as well as to participate in the pathogenesis of VC. Notably, HMGB1 has been shown to enhance ROS *via* positive feedback loop in the apoptotic process of diabetic retinopathy [154] and that oxidative stress is able to regulate HMGB1 release in various cell types [155].

## *1.4.4. HMGB1 and calcification*

Several types of cells that can undergo osteogenic trans-differentiation have been identified in the vascular wall including VSMCs, pericytes, interstitial valve cells (VIC), adventitial myofibroblasts and circulating or local progenitor cells [156]. Different studies have described that HMGB1 participates in osteogenic transformation of cells. Qi et colleagues showed that HMGB1 translocates from the nucleus to the cytosol during human dental pulp stem cells (hDPCs) odontoblastic differentiation and its release in the extracellular environment promotes hDPCs proliferation and the development of mineralized nodules [157]. HMGB1 has been reported also to be involved in VSMCs proliferation and migration [158] and it has been found elevated in a model of Angiotensin II-induced VSMCs phenotypic transformation, which was blocked after HMGB1 knockdown [159]. Jin X et colleagues have published that serum levels of HMGB1 in CKD patients were significantly higher respect to healthy controls [160]. Moreover,

aortic calcification with high concentration of phosphate promoted the translocation of HMGB1 from the nucleus to the cytosol in CKD mice aortas; on the other hand, HMGB1 knockdown in CDK mice ameliorated part of renal and vascular function, suggesting a role of the protein in VCm associated with CKD [160].

HMGB1 is also known as a bone-active cytokine that participates in both bone remodelling and ectopic calcification pathogenesis[161]. There are evidences showing that HMGB1 accumulates extracellularly in areas associated with macrophage infiltration and calcification in calcific aortic valve stenosis[162]. Wang et al. reported increased tissue and plasma levels of HMGB1 in patients with calcific aortic valve disease[163]. In addition, extracellular HMGB1 was noted to promote osteoblastic differentiation and calcification of VICs through TLR-JNK-NF-κB signalling [163]and to mediate directly VSMCs osteoblastic differentiation in patients with diabetes[164]. There are several indications that HMGB1 promotes vascular calcification by controlling the release of extracellular vesicles that are responsible for the initiation of VC. Indeed, HMGB1 has been demonstrated to induce matrix vesicle secretion by macrophages, which leads to subsequent ectopic mineralization both *in vitro* and *in vivo*[165]. Moreover, it was found to control cellular apoptosis checkpoint during inflammation[166], and hyperglycaemia-induced apoptosis[136], which may be accompanied by release of apoptotic bodies.

HMGB1 is a target of several miRNA, which can regulate its content and therefore its effects like senescence, vascular calcification and remodelling. Accordingly, it has been disclosed that the downregulation of miR-181b-5p leads to the elevation of HMGB1 levels in hypertensive patients, which accounts for VSMCs phenotypic transformation and vascular remodelling [159].

# 2. Aims of the project

Aging is a prominent risk factor for cardiovascular diseases (CVDs) and all-cause mortality. During aging, the vasculature undergoes several structural and molecular alterations, which predispose and exacerbate CVDs. Particularly, vascular smooth muscle cells (VSMCs) are also exposed to additional stresses, such as high blood pressure, turbulent flow, etc. that contribute to increase vascular complications. Vascular calcification (VC) is a common age-associated vascular complication, which pathogenesis mechanisms are still unclear. The trans-differentiation of VSMCs from a contractile to an osteogenic phenotype is one of the most prominent cellular mechanism leading to VC. Of note, senescent VSMCs have higher tendency to undergo calcification.

High mobility group box 1 (HMGB1) is a nuclear and highly conserved non-histone chromatin binding protein that binds to the minor groove of DNA and is involved in the maintenance of DNA and histones structures. HMGB1 delocalizes from the nucleus to the cytosol and the extracellular environment, leaving the nuclei partially devoid of the protein, after pro-inflammatory or stress stimuli such as senescence. Moreover, HMGB1 has been shown to be involved in osteogenic transformation of several cell types, like human dental pulp stem cells and valvular interstitial cells.

However, the involvement of HMGB1 in VSMCs senescence and osteogenic transition and eventually VC has never been explored. Thus, the aims of this project are to:

1. Investigate the role of HMGB1 in vascular aging and VSMCs senescence using cellular and animal models for *in vitro* and *in vivo* studies;
2. Investigate the role of HMGB1 in the VSMCs osteogenic trans-differentiation associated to senescence and VC *in vitro* and *in vivo*.

# 3. Materials and methods

## *3.1. Cell culture*

Human aortic smooth muscle cells (HASMCs) were purchased from Lonza (Basel, Switzerland) and cultured in SmGM-2 complete medium (Lonza). The donors were Caucasian males of 22, 30, 43 and 81 years. Replicative senescence was induced by keeping cells in culture and splitting them after reaching 90% of confluence repeatedly until they stop proliferate. Depending on the age of the donor, cells at low passages (P5-P8) with normal growth rate were defined as "young", while low-proliferative/senescent cells (P10-15) as "old". Similarly, to generate P15 *shB1/SMCs* and *shCTRL/SMCs*, P8 *shB1/SMCs* and *shCTRL/SMCs* were cultured until reaching passage P15.

## *3.2. Generation of shB1/SMCs and shCTRL/SMCs*

### *3.2.1. Virus production*

Human embryonic kidney HEK293T cells were cultured in DMEM 10% fetal bovine serum, penicillin 100U/mL, streptomycin 100U/mL, glutamine and sodium pyruvate. Two hours before transfection, medium was changed to IMDM 10% FBS, penicillin 100U/mL, streptomycin 100U/mL, and glutamine. $9x10^6$ HEK293T cells were transfected with the packaging plasmids pDM2-VSVG and pCMV-ΔR8.91 and two lentivirus vectors carrying short hairpin for human HMGB1(*shB1* Dharmacon™ GIPZ™ Lentiviral shRNA cat n° RHS4531-GE Healthcare) or for control (*shCTRL* Dharmacon™ GIPZ™ Lentiviral shRNA cat n° FE6RHS4351-GE Healthcare) along with Green Fluorescence Protein (GFP) using calcium/phosphate method. In detail, a plasmid solution containing 7μg pDM2-VSVG, 28μg pCMV-ΔR8.91, 32μg pGIPZ-*shB1* or pGIPZ-*shCTRL* was added with 0.125M $CaCl_2$ in a final volume of 1250μL and incubated at room temperature for 5 minutes; the CaPi-DNA precipitate was formed by addition of 1250μL of 2X HBS (NaCl 140.5mM; HEPES 50mM; $Na_2HPO_4$ 0.75mM pH 7.12). The precipitated complexes were immediately added drop by drop into the

cell media. Virus-containing media was collected 36 hours after transfection, centrifuged 5 minutes at 200 g, filtered through 0.22μm membrane and concentrated by ultracentrifugation (20000 g for 2 hours). The pellet was dissolved in low volume of cold PBS.

### *3.2.2. Virus titration*

Viral preparations were titrated transducing serial dilutions of the viral preparation in HEK293T. Briefly, HEK293T cells were seeded in a 12-well plate ($1.3x10^4$ cells/$cm^2$) and cultured in complete DMEM medium for 24 hours. Then, the media was changed with 500μL of fresh DMEM and 10μL of serial 1:10 diluted virus solutions were added. After 24 hours, additional 500μL of fresh DMEM were added to the wells. Forty-eight hours later, cells were collected and the percentage of GFP expression was measured using BD FACSCalibur cytometer (BD Biosciences). The number of Transducing Units (TU) of the viral preparation was determined using the following formula:
[(Number of cells at day of transduction) x (percentage of GFP + cells/100)]/ (μL of viral preparation used for transduction) = TU/μL

### *3.2.3. Transduction of HASMCs*

Twenty-two years-old donor P3-P4 HASMCs were seeded in a 6-well plate ($2.1x10^4$ cells/$cm^2$) and transduced in SmGM-2 complete medium (Lonza) with lentivirus carrying pGIPZ-*shB1* (*shB1/SMCs*) or pGIPZ-*shCTRL* (*shCTRL/SMCs*) using a multiplicity of infection (MOI) = 20. After 24 hours, the media was replaced with complete SmGM-2 plus puromycin (1μg/mL) for at least 4 days to select infected cells.

## *3.3. Western Blot*

HASMCs ($1x10^5$) were harvested by scraping in 40μL of RIPA buffer (10 mM Tris pH 7.4, 100 mM NaCl, 1 mM EDTA, 1 mM EGTA, 1% Triton X-100, 10% glycerol, 0.1% SDS, 0.5% deoxycholate) in the presence of proteases inhibitors (P8849, Sigma-Aldrich). Aortas isolated from mice or human abdominal aneurisms (AAA) were immediately frozen and then

homogenized with the TissueLyser (Qiagen, Hilden, Germany) in RIPA buffer in the presence of proteases inhibitors (Sigma-Aldrich). Following incubation at 4°C for 30 min and centrifugation at 12000 g for 15 minutes at 4°C, supernatants were collected. Protein concentration was determined with the Bio-Rad protein assay and total protein extracts (20µg) were separated by SDS-PAGE and transferred with Trans-Blot®Turbo™ Transfer System (Bio-Rad). Membranes were incubated with antibodies against GAPDH (0.2 µg/mL, sc-25778, Santa Cruz Biotechnology), HMGB1 (1.0 µg/mL, ab18256, Abcam), α-Tubulin (1.0 µg/mL, T6199, Sigma-Aldrich), β-actin (1.0 µg/mL, T5441, Sigma-Aldrich), murine p16 (0.2 µg/mL, sc-1207, Santa Cruz Biotechnology), human p16 (0.2 µg/mL, sc-468, Santa Cruz Biotechnology and 1.0 µg/mL, ab189034, Abcam) and p21 (1.0 µg/mL, ab109199, Abcam). Proteins were visualized by means of the ECL Western Blotting Detection Reagents (GE Healthcare) and protein bands on films (Amesham Hyperfilm™ ECL, cat n° 28906837, GE Healthcare) were quantified by densitometric analysis using ImageJ (rsb.info.nih.gov/ij). Alternatively, images were acquired with UVITEC Alliance MINI 2M (Cleaver Scientific Ltd, Rugby, United Kingdom) or ChemiDoc™ MP Imaging System (Bio-Rad) and densitometric analysis was performed using the UVITEC Alliance Mini 4 16.07 software (Cleaver Scientific Ltd) or ImageJ, respectively.

## *3.4. Immunofluorescence (IF)*

HASMCs were seeded ($5x10^3$ cells/$cm^2$) on microscope slides in a 24 well plate and after 48 hours were washed and fixed in 4% formalin for 10 minutes at room temperature. After washing twice in PBS, cells were incubated in HEPES-T buffer (20mM HEPES pH 7.4, 200mM sucrose, 50mM NaCl, 3mM $MgCl_2$, 0.2% TRITON X100) for 3 min, to permeabilize cells, and then blocked in 5% BSA PBS-TRITON 0.1% (PBS-T) for 1 hour at room temperature. Primary antibody against HMGB1 (1µg/mL, ab18256, Abcam, Cambridge, United Kingdom), was dissolved in 1% BSA PBS-T and incubated overnight at 4°C in a humidified chamber. After three 5 minutes-washing with PBS-T, cells were incubated in the dark for 1 hour at room temperature with secondary antibody anti-rabbit IgG coupled to Alexafluor 594 diluted in 1% BSA PBS-T (1:400, cat N° DI-1794, Vector Laboratories, Burlingame, CA, USA) and counterstained with 4,6-diamidino-2-phenylindole (DAPI) for 10 minutes, to visualize nuclei. Images were acquired with an Apotome microscope (Zeiss, Germany) with 40X objective and

analyzed with Axiovision Software Rel 4.7 (Zeiss). Nuclear or cytosolic HMGB1 staining intensity was divided by nucleus or cytosol area, respectively.

## *3.5. ELISA assay*

Supernatant from $1x10^5$ HASMCs was collected, centrifuged (12000 g for 10 minutes), transferred as aliquots into a clean polypropylene tubes and stored at -80°C. ELISA kits specific for HMGB1 (ST51011, IBL International-Tecan, Switzerland), IL-6, (DuoSet® cat n°DY206-05, R&D Systems®, Minneapolis, USA), IL-1β (DuoSet® cat n°DY201-05, R&D Systems®, Minneapolis, USA), OPG, (DuoSet® cat n°DY805, R&D Systems®, Minneapolis, USA) and OPN (DuoSet® cat n°DY1433, R&D Systems®, Minneapolis, USA), were used to test the extracellular levels of these proteins following manufacturer's instruction. Briefly, for HMGB1, seven serial 1:2 dilution (10 ng/mL to 0.313 ng/mL) of a HMGB1 standard solution were made. After adding 50µl of diluent buffer into respective wells of the microtiter plate, 50µl of standards, negative control (growth medium) and samples were added, mixed for 30 seconds and incubated at 37°C for 24 hours. After washing 5 times by adding 400 µL of washing buffer, wells were incubated with 100µL of a solution containing the secondary antibody anti-HMGB1 conjugated with a peroxidase for 2 hours at 25°C. Then, subsequent to washing, 100 µL of a color solution made of 0.005M of hydrogen peroxide and 3,3′,5,5′-Tetramethylbenzidine (TMB) were added and incubated 30 minutes at room temperature. After adding 100µL of a stop solution containing 0.35M of sulfuric acid, the absorbance at 450nm was read by using a spectrophotometer (Infinite® M200 PRO- TECAN). HMGB1 amount was expressed as pg/mL/number of cells.

For IL-6, IL-1β, OPG and OPN, a 96 well plate was coated with 100µL of diluted capture antibody in PBS, and incubated overnight at room temperature. Then each well was washed 3 times with 400 µL of wash buffer saturated with 300µL of blocking solution and incubated for 1 hour at room temperature. Meanwhile, seven dilution using 2-fold serial dilutions of relative standard solutions were made (from 4000 to 62,5pg/ml). After additional three washes, 100µL of each standard dilutions, negative control (growth medium) and samples were added and incubated at room temperature for 2 hours. Following three washes, 100µL of the Detection antibody solution were added and incubated at 37°C for 2 hours. Then, streptavidin-HRP solution (100µL) was added and incubated at room temperature for 20 minutes in the dark. After last washes, 100µL of the Substrate solution were added and incubated at room

temperature for 20 minutes in the dark. Then, 50µL of Stop solution and the absorbance at 450 nm was revealed by using a spectrophotometer (Infinite® M200 PRO- TECAN). Finally, cytokines concentration was normalized to the number of cells (pg/mL/number of cells) or to the protein concentration when cells were cultured in normal growth media for 24, 48 and 72h or in osteogenic media respectively.

## *3.6. Quantitative RT-PCR (q-RT-PCR)*

For HASMCs, the total RNA was extracted from $1x10^5$ cells using illustra RNAspin Mini RNA Isolation Kit reagent (cat n°25-0500-72, GE Healthcare) following the manufacturer's protocol. Briefly, after washing cells twice with PBS, 350µL of lysis buffer and 3.5µL of β-mercaptoethanol were added and the lysates were filtered by centrifuge 1 minute at 11000 g. Then, 350µL of 70% ethanol were added and, after mixing, the entire volume was loaded onto the column and centrifuged at 8000 g for 30 seconds. After adding 350µL of desalting buffer and centrifuge at 1100g for 30 seconds, DNA was digested by incubating with a DNase solution for 15 minutes at room temperature. Finally, after three washings, RNA was eluted from the column by adding 30µL of RNase-free water and centrifuging at 11000 g for 1 minute. cDNA was synthesized with iScript™ Reverse Transcription Supermix for RT-qPCR (Bio-Rad).
For aortic abdominal aneurism (AAA) tissues, the total RNA was extracted using miRNeasy® Mini kit (cat n°217004, Qiagen) following the manufacturer's protocol. Briefly, tissues were disrupted in presence of beads and 700µL of QIAzol® Lysis Reagent using Tissuelyser II (Qiagen, Hilden, Germany). After incubating 5 minutes at room temperature, 140µL of chloroform were added and mixed with vigorous shaking for 15 seconds. After incubating 2 minutes at room temperature, samples were centrifuged at 12000 g for 15 minutes. Then, the aqueous phase was mixed with 1.5 volumes of 100% ethanol, loaded onto the column and centrifuged 8000 g for 15 seconds. After washing, DNA was digested by incubating with a DNase solution for 15 minutes at room temperature. Finally, following three washing, RNA was eluted from the column by adding 30µL of RNase-free water and centrifuging at 8000g for 1 minute. cDNA was synthesized with the SuperScript III First-Strand Synthesis SuperMix for qRT-PCR (Invitrogen). For both cells and tissues, qRT-PCR was performed on a Bio-Rad C1000 Touch™ Thermal Cycler with CFX 96™ Real-Time PCR Detection System using the iTaq Universal SYBR® Green Supermix (cat n°1725124, Bio-Rad) and the following oligos:

| Gene | Sequence Forward (5' → 3') | Sequence Reverse (5' → 3') |
|---|---|---|
| **h_HMGB1** | GCATTTTTTGTGCAAACTTGTC | CGAGCTAAAGGAAAGCCTGAT |
| **h_IL-6** | ACAAAAGTCCTGATCCAGTTC | GACTGCAGGAACTCCTTAAAGC |
| **h_IL-1β** | CAAAATACCTGTGGCCTTGG | ACTGGGCAGACTCAAATTCC |
| **h_IL-8** | TGCCAAGGAGTGCTAAAG | CTCCACAACCCTCTGCAC |
| **h_IL-10** | TGCCTTCAGCAGAGTGAAGA | GGTCTTGGTTCTCAGCTTGG |
| **h_MCP-1** | CCCAAAGAAGCTGTGATCTTC | CCCAAAGAAGCTGTGATCTTC |
| **h_OPG** | CAACACAGCTCACAAGAACAG | GAAGGTGAGGTTAGCATGTCC |
| **h_OPN** | GAGGGCTTGGTTGTCAGC | CAATTCTCATGGTAGTGAGTTTTC |
| **h_BMP-2** | TGTATCGCAGGCACTCAGGTC | TTCCCACTCGTTTCTGGTAGTTCT |
| **h_GAPDH** | AATCCCATCACCATCTTCCAG | AAATGAGCCCCAGCCTTC |
| **h_XRCC4** | AAACTGATCTCTCTGGGTTGG | AGCCATTTTAGGTTCTGTCCC |
| **h_NHEJ1** | AGTGGGACAGAAGCATCAAG | CGTGGACTCTTTCTCAGGTG |
| **h_MSX-2** | CGGTCAAGTCGGAAAATTCAG | GGATGTGGTAAAGGGCGTG |
| **h_RUNX-2** | TCTGGCCTTCCACTCTCAGT | GACTGGCGGGGTGTAAGTAA |
| **h_ALP** | TCACTCTCCGAGATGGTGGT | GTGCCCGTGGTCAATTCT |

Relative gene expression levels were determined using the $2^{-\Delta\Delta CT}$ method and GAPDH as reference genes.

## *3.7. Cell proliferation assay*

HASMCs were seeded in a 96-well plate ($7x10^3$ cells/$cm^2$) and cultured in SmGM-2 complete medium (Lonza), added of IncuCyte® NucLight Rapid Red Reagent for Cell Labeling (cat n°4717, Essen BioScience). The growth was evaluated for 102 hours and the images were acquired every 2 hours with IncuCyte®S3 System (Essen Instruments, Ann Arbor, MI, USA). Growth curves were extrapolated automatically from data points acquired during round-the-clock kinetic imaging considering cell confluence obtained by red nuclei object count/image normalized to h "0". Slope measurements were determined with Origin 7.0 (Origin 7, Version 2002; OriginLab Corporation, Northampton, MA, USA). The slope value is the constant m expressed in the slope-intercept form of a line, y = mx + b, designed as linear regression on the growth curve between 82 and 102 hours.

## *3.8. Cell cycle analysis*

HASMCs cell cycle distribution was carry out using propidium iodide (PI) incorporation to check DNA content and flow cytometer analysis. Briefly, $3.0x10^5$ cells were seeded in 100 mm petri dish and cultured in SmGM-2 complete medium (Lonza) for 48 hours. After collecting, the cells were resuspended in 1 mL of PBS, fixed with dropwise addition of 3 mL of cold ethanol 96% (final concentration 70%) during vortex agitation and stored at 4°C for at least 24 hours. Then, cells were centrifuged 1200 rpm for 10 minutes at 4°C to remove the ethanol, washed with a solution of PBS-FBS 5% and incubated for 2 hours in the dark with a solution ($10^6$ cells/mL) of PI (25µg/mL) and RNAse (Ribonuclease A, Protease-Free, High Purity, Bovine, 10KU, Cat #556746, Calbiochem 1 mg/mL in $H_2O$). Finally, the PI incorporation was measured using BD FACSCalibur cytometer and the percentage of cells in G1, S and G2 phases was determined with ModFit software (BD Biosciences). For each analysis, at least 10000 events were recorded.

## *3.9. Neutral comet assay*

HASMCs DNA damage was detected using Comet Assay® Reagent Kit for Single Cell Gel Electrophoresis Assay (Cat. no. 4250-050 K, Trevigen®) according to the manufacturer's protocol. Briefly, $3.0x10^5$ cells were seeded in 100 mm petri dish and cultured in SmGM-2 complete medium (Lonza) for 48 hours. Cells were collected and washed once in cold PBS, then resuspended at density of $1x10^5$ cells/mL in PBS and combined with molten low melting agarose at a ratio of 1:10 (v/v). 50µl of the cellular solution were immediately pipetted onto slide and placed at 4°C in the dark. After 10 minutes, the slides were immersed in lysis solution overnight at 4°C. Then, slides were removed from lysis solution, incubated in 50 ml neutral electrophoresis buffer. After 30 minutes, the slides were placed in electrophoresis slide tray and cover. Electrophoresis was carried out at 21 volts for 45 minutes at 4°C. Slides were dipped first in DNA precipitation solution for 30 minutes at room temperature and then in 70% ethanol for 30 minutes and dried at 37°C for 10 minutes. Finally, samples were stained with 100µl of SYBR®Gold for 30 minutes and images were taking with Apotome microscope (Zeiss) and analyzed with ImageJ plugin OpenComet v1.3.1. Tail moment was calculated as the ratio of

comet tail length to comet DNA content multiply by one hundred. At least 50 randomly selected cells per sample were analyzed.

## *3.10. Reactive oxygen species (ROS) content assay*

ROS content was detected using CellROX® ROS orange Flow cytometer assay Kit (Cat. no. C10493 Life technologies) according to the manufacturer's protocol. Briefly, $3.0x10^5$ cells were seeded in 100 mm petri dish and cultured in SmGM-2 complete medium (Lonza) for 48 hours. After, cells were incubated in SmGM-2 complete medium (Lonza) containing CellROX® ROS detection reagent (500nM) for 30 minutes under normal growth conditions at a density of $5x10^5$ cells/mL. During the final 15 minutes of staining, 1µL per 1 mL of the sample of SYTOX® Red Dead Cell (5 nM) was added and cells were immediately analyzed with GALLIOS flow cytometer. For positive and negative control, 200µM tert-butil hydroperoxide (THBP) and N-acetylcysteine (NAC), respectively, were added before incubation with CellROX® ROS detection reagent. ROS content was measured using GALLIOS flow cytometer (Beckman Coulter Life Sciences) at two different wavelengths (565nm to detect oxidized products and 658nm to detect dead cells) and was determined with Kaluza analysis software (ver 1.5). For each analysis, at least 10000 events were recorded.

## *3.11. Senescence-associated β-galactosidase (SA-β-gal) staining*

Senescence was assessed with the SA-β-gal staining kit (Cell Signaling Technology, Danvers, MA, USA) following the manufacturer's protocol. Briefly, $5x10^3$ cells were seeded in a 24 well plate and cultured for 48 hours. After washing in PBS, cells were fixed for 10 minutes at room temperature and washed again in PBS. Then, a staining solution containing the substrate X-gal was added and incubated overnight at 37°C in a dry incubator. In the presence of β-galactosidase, the substrate X-gal is hydrolyzed in a blue visible compound. Finally, images of ten random fields were acquired using a Zeiss Axiovert 200M microscope equipped with a HITACHI HV-D30 Compact 3-CCD Camera (Zeiss). Percentage of SA-β-gal-positive cells

was calculated as the fraction of SA-β-gal-positive staining to the total number of cells multiply by one hundred.

## *3.12. Calcification assay for cells*

### *3.12.1. Colorimetric Assay*

HASMCs ($5x10^4$) were seeded in a 24 well-plate and after 8 hours growth medium was replaced with osteogenic medium (DMEM supplemented with 15% FBS, 5 mM phosphate, 10 mM sodium pyruvate and 50ug/mL ascorbic acid) and further cultured for 3, 5, 7 and 11 days. The osteogenic medium was replaced every 2 days. Calcium was quantified by colorimetric analysis with the QuantiChrom™ Calcium Assay Kit. Briefly, cells grown in 24-well plates were quickly washed twice with 500µL of PBS and incubated overnight with 250 µL of 0.6 N HCl at 4°C; supernatants were collected. 5µL of each sample and eight serial standard dilutions (from 20 mg/dL to 2 mg/dL) were put in a clear 96-well plate plus 200µL of the Colorimetric solution. After incubating 3 minutes at room temperature, the absorbance at 620 nm were determined with the spectrophotometer Infinite® M200 PRO- TECAN.
In order to extract protein for normalization, cells were washed twice with 500µL of PBS and incubated overnight at 4°C with 250µL of 0.1% SDS-0.1 N NaOH lysis buffer. Protein concentration was determined with the Bio-Rad protein assay (Bio-Rad Laboratories, Hercules, CA, USA). Finally, calcium content was expressed as µg of calcium/µg of protein.

### *3.12.2. Von Kossa staining on HASMCs*

HASMCs cultured in osteogenic media were washed twice with PBS and fixed with 4% paraformaldehyde (PFA) for 15 minutes at room temperature. After washing, cells were incubated with 1% silver nitrate solution under ultraviolet light for 40 minutes. The unreacted silver was removed with 5% sodium thiosulfate for 5 minutes. After rinsing cells with several changes of distilled $H_2O$, pictures were taken with a Zeiss Axiovert 200M microscope equipped with a HITACHI HV-D30 Compact 3-CCD Camera (Zeiss).

### *3.12.3. Alizarin red staining on HASMCs*

The alizarin red staining was performed with Alizarin Red S Staining Quantification Assay (ARed-Q cat n°8678, ScienCell) according to the manufacturer's protocol. Briefly, HASMCs cultured in osteogenic media were washed three times with PBS and fixed with 4% PFA for 15 minutes at room temperature. After washing with $H_2O$, Alizarin red S (40mM) was added and incubated for 30 minutes at room temperature with gentle shaking. Then, cells were washed 5 times with $H_2O$ and images were acquired with a Zeiss Axiovert 200M microscope equipped with a HITACHI HV-D30 Compact 3-CCD Camera (Zeiss).

## *3.13. Animal experiments*

Animal work was performed in conformity with the guidelines from Directive 2010/63/EU of the European Parliament on the protection of animals used for scientific purposes and in accordance with experimental protocols approved by the University Committee on Animal Resources at the University of Milan (#734-2015 or #12/12-30012012). Mice were housed in standard cages on a 12:12 h light-dark cycle and fed a normal chow diet ad libitum.

Sixteen-week-old male *Hmgb1*$^{+/+}$ and *Hmgb1*$^{+/-}$ mice were treated with either 500000 IU/kg/day vitamin D (Cholecalciferol, C1357, Sigma-Aldrich, St. Louis, MO, USA) or a mock solution (1% (v/v) Ethanol, 7% (v/v) Kolliphor® EL, 3.75% (w/v) Dextrose (all from Sigma-Aldrich)) administrated subcutaneously for three consecutive days. Five and seven days after the first injection, animals were anesthetized with an intraperitoneal injection of ketamine:medetomidine cocktail (100mg/Kg:10mg/Kg) and perfused with phosphate-buffered saline (PBS) from the apex of the heart. Aortas were dissected out and processed as describes below. For the weight analysis, mice were weighted on the first day (Day 1) and on the sacrifice day (Day 5, 7) and the ratio between the weights of these two days was calculated.

For the aging experiments, aortas were isolated from male C57BL/6J young (2.5 months-old) and old (21 months-old) mice, immediately frozen for RNA and protein extraction or fixed in 10% formalin for immunohistochemistry analysis as described before.

For rat experiments, 12 weeks old male Wistar rats were divided into two groups. The first group was fed for 2 weeks with Diet 1 (1.03% P, 1.06% Ca, 19% protein), followed by 4 weeks

of Diet 2 (0.75% Adenine, 0.92% P, 1.0% Ca, 2.5% protein) following 4 weeks of Diet 1. The second group (Control, CNTRL) was fed for 2 weeks with Diet 1 (1.03% P, 1.06% Ca, 19% protein), followed by 4 weeks of Diet 3 (0.92% P, 1.0% Ca, 2.5% protein) and then 4 weeks of Diet 1.

After two, three and four weeks of Diet 2, animals from both groups were anesthetized with an intraperitoneal injection of chloral hydrate (400mg/Kg) and perfused with PBS from the apex of the heart. Aortas were dissected out and processed as described below.

## *3.14. Calcium content quantification on tissue animals*

### *3.14.1. Colorimetric assay*

Dissected organs from rats were washed in PBS, carefully blotted dry, weighted and incubated at 4°C for 24 hours in 20 µL/mg dry weight of 0.6 N HCl. The amount of calcium in aortas was quantified by a colorimetric analysis with QuantiChrom™ Calcium Assay Kit (DICA-500, Gentaur, Kampenhout, Belgium) following the manufacturer's protocol. Briefly, 5µL of samples and eight serial standards dilution (from 20 mg/dL to 2 mg/dL) were added in a clear 96-well plate along with 200µL of the Colorimetric solution. After incubating 3 minutes at room temperature, the absorbance at 620 nm were determined with the spectrophotometer Infinite® M200 PRO- TECAN. Finally, calcium amount from the organs was normalized to the tissue dry weight (µg Calcium/mg tissue).

### *3.14.2. Von Kossa staining on aortic sections*

Mice and rats distal thoracic aortas were fixed in 10% formalin and paraffin embedded. Six µm sections were de-paraffinized as follow: 2 times in xylene for 6 minutes, 1 time in ethanol 100% for 3 minutes, 1 time in ethanol 75% for 3 minutes, 1 time in ethanol 50% for 3 minutes and then in water for 3 minutes. After washing, sections were incubated with 1% silver nitrate solution under ultraviolet light for 20 minutes. After rinsing the specimens with several changes of distilled $H_2O$, the unreacted silver was removed with 5% sodium thiosulfate for 5 minutes at

room temperature. Then, the sections were rinsed in distilled $H_2O$ and counterstained with hematossilin and eosin (H&E).

The quantification of Von Kossa positive area was made by taking images with an Axioskop II microscope (Zeiss) using a digital camera (AxioCam Color, Zeiss). The entire aorta cross section was analyzed with Axiovision Software Rel 4.7 (Zeiss) and calcium content was defined as Von Kossa staining positive area divided to the total area ($\mu m^2$) multiplied by one hundred.

## *3.15. Immunohistochemistry (IHC)*

Mouse distal thoracic aortas were fixed in 10% formalin and paraffin embedded. Six μm sections were de-paraffinized as follow: 2 times in xylene for 6 minutes, 1 time in ethanol 100% for 3 minutes, 1 time in ethanol 75% for 3 minutes, 1 time in ethanol 50% for 3 minutes and then in $H_2O$ for 3 minutes. After washing, sections were boiled for 20 minutes in Dako Target Retrieval Solution Citrate pH 6 (cat n°S2369). After washing in PBS-0.1% Triton X-100 (PBS-T) slides were incubated in 3% $H_2O_2$ (Sigma-Aldrich) for 10 min, to inactivate endogenous peroxidases, and then blocked in 5% goat serum in PBS-T for 45 minutes at room temperature. Primary antibody against HMGB1 (1μg/mL, ab18256, Abcam, Cambridge, United Kingdom), was dissolved in 1% goat serum PBS-T and incubated overnight at 4°C in a humidified chamber. After three washes of 5 minutes in PBS-T, sections were incubated with biotin-conjugated goat anti-rabbit antibody (1:200, cat number Vector Laboratories, Burlingame, CA, USA) and then with horseradish peroxidase (HRP)-conjugated streptavidin (ABC kit; PK-6100, Vector Laboratories) for 30 min at room temperature. Immunoreactions were revealed using 3.3'-Diaminobenzidine (ImmPACT DAB substrate, SK-4105, Vector Laboratories) as chromogen and slides were counterstained with hematoxylin. Images were acquired with an Axioskop II microscope (Zeiss) using a digital camera (AxioCam Color, Zeiss). HMGB1 signal was calculated as HMGB1 positive area divided to the total and multiplied by one hundred.

## *3.16. Human Samples*

Twenty-seven samples of abdominal aneurism of aorta (AAA) from different male patients with an average age of 71±8 years subjected to surgery were collected at Centro Cardiologico

Monzino after signing the consensus format approved by the Ethical Committee of Centro Cardiologico Monzino (Milano, Italy) on 4th November 2013. Protein and RNA extracts were analyzed by Western Blot and qRT-PCR as described in paragraph 3.3 and 3.6.

## *3.17. Statistical analysis*

In vitro experiments were performed at least three times. Data were analyzed with GraphPad Prism software version 5 (GraphPad Software, Inc, La Jolla, CA, USA). D'Agostino or Shapiro-Wilk test was used to assess the normality of distribution of investigated parameters. Student's t-test was used for comparison between two groups as indicated in the legends. Statistical analysis between more than two groups was conducted by 1-way or 2-way ANOVA with Bonferroni or Kruskal-Wallis post-hoc test for parametric and non-parametric distribution, respectively, as reported in the figure legends. The crude relation between two variables with normal and skewed distribution was evaluated by Pearson or Spearman test, respectively, as indicated in the figure legends. A value of $p < 0.05$ was considered statistically significant; values are presented as mean ± SE.

# 4. Results

## *4.1. HMGB1 protein levels decrease during vascular aging in vitro and in vivo*

In order to investigate HMGB1 expression changes during vascular senescence, we isolated aortas from young (2.5 months old) and old (21 months old) C57BLJ6 male mice and examined HMGB1 protein content by WB. Aortas isolated from old mice displayed a significant reduction in HMGB1 protein levels in comparison with the young ones, accompanied also with an increase of p16 protein expression, known marker of senescence (Fig.1 A, B, C). Furthermore, IHC show that HMGB1 downregulation occurs in VSMCs of intima, media and adventitia layers and endothelial cells (Fig.1 D).

In order to specifically investigate the role of HMGB1 in VSMCs, we used human aortic smooth muscle cells (HASMCs) isolated from donors of different ages (22yo, 30yo, 43yo and 81yo), and cultured them until they reached replicative senescence. Cells are senescent when they became bigger and stop to divide and proliferate. This happened for HASMCs around passage P10-P15, depending on the age of the donor. We firstly performed WB and qRT-PCR analysis on young (P5) and old (P15) HASMCs from 22, 30, 43 years old donors to check changes in HMGB1 expression during replicative senescence and we noted a significant reduction at both protein and mRNA levels (Fig.2 A-C). Then, to assess the kinetic of HMGB1 decline during the senescence arise, we performed WB analysis on HASMCs isolated from the 30-year-old donor, at different passages. The analysis revealed that HMGB1 decreased gradually with passages, whereas p16 incremented its expression (Fig. 2 D-F). Similar results were obtained with other donors (data not shown). Interestingly, we further observed that HMGB1 content decreased with the age of the donor (Fig.2 G, H).

Hence, these data demonstrate that HMGB1 levels diminish during vascular aging *in vivo* and during VSMCs replicative senescence *in vitro*.

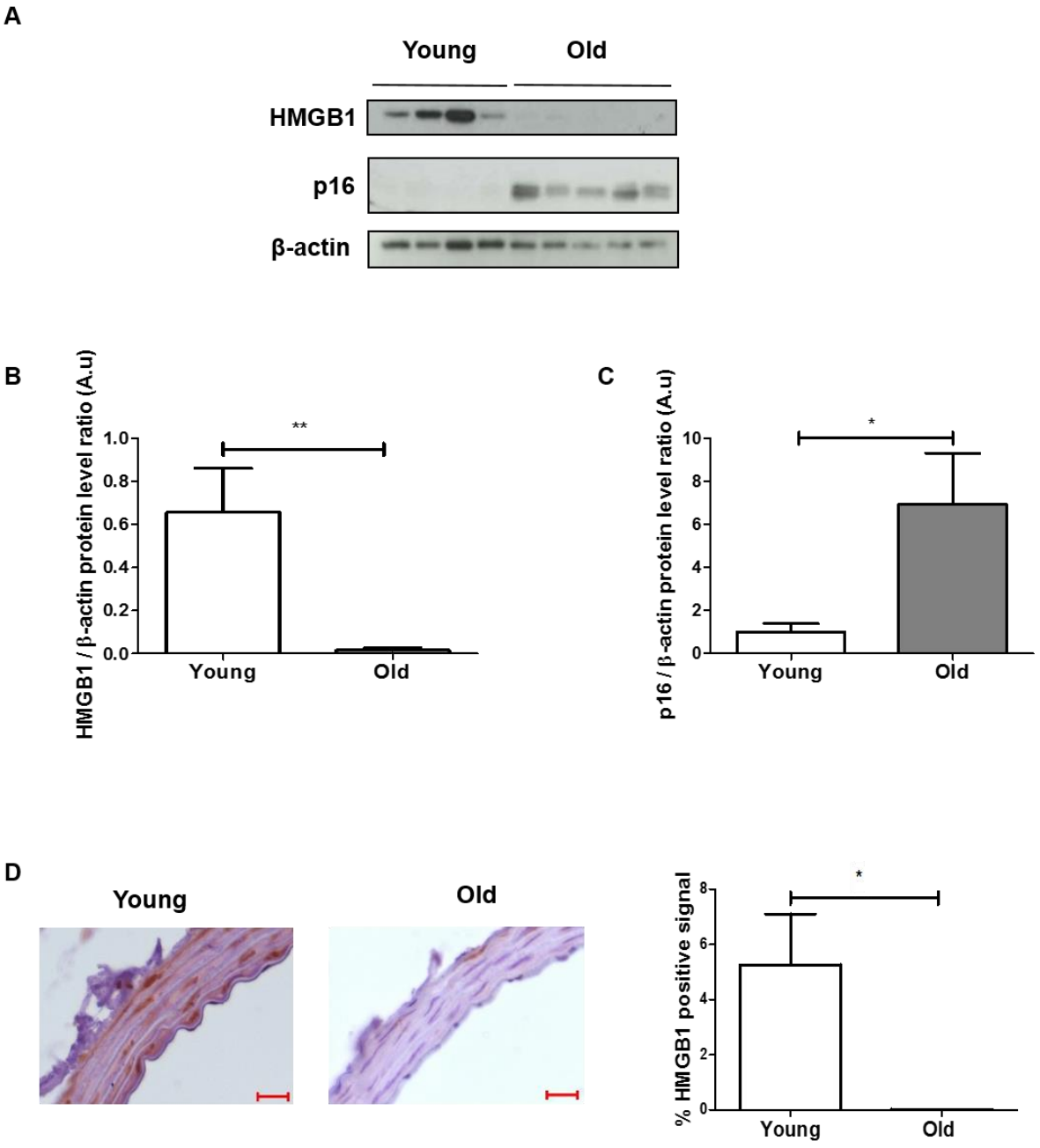


**Figure 1. HMGB1 decreases during aging *in vivo*.** **(A)** Western blot showing HMGB1 and p16 protein levels on Young (2.5 months old) and Old (21 months old) male mice aortas. β-actin was used as loading control. **(B, C)** Quantification of HMGB1 (B) or p16 (C) expression relative to panel A; (Young n=4; Old n=5). **(D)** Left panel: representative images of aortas of Young (2.5 months old) and Old (21 months old) male mice subjected to immunohistochemistry with anti-HMGB1 antibody; scale bar: 20µm. Right panel: Quantification of HMGB1 expression; (Young n=4; Old n=3). Bars show values as mean ± SE,*p<0.05 **p<0.01; Student's t-test.

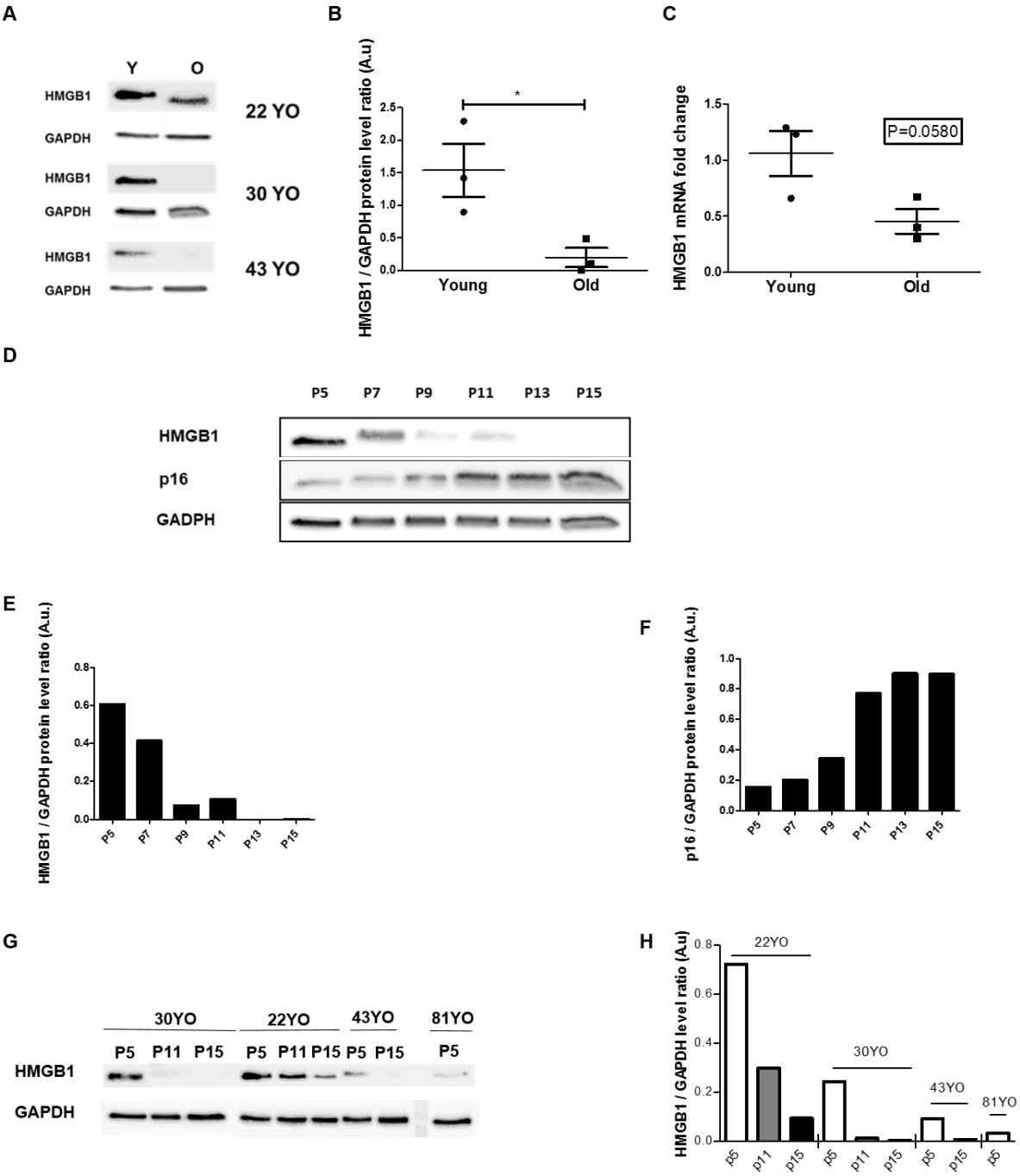


**Figure 2. HMGB1 decreases during aging *in vitro*.** **(A)** Western blot showing HMGB1 protein levels in Young (Y=P5) and Old (O=P15) HASMCs isolated from donors at different ages. GAPDH was used as loading control. **(B)** Quantification of HMGB1 expression relative to A; (Young n=3; Old n=3). **(C)** HMGB1 mRNA expression in Young (Y=P5) and Old (O=P15) HASMCs isolated from donors at different ages by qRT-PCR normalized to corresponding GAPDH levels.**(D)** Western blot showing HMGB1 and p16 protein levels in HASMCs isolated from 30 years old donor at the indicated passages. **(E-F)** Analysis of HMGB1 (E) or p16 (F) expression relative to D. **(G)** Western blot showing HMGB1 protein levels in HASMCs isolated from donors of different ages (YO) at the indicated passages. GAPDH was used as loading control. **(H)** Analysis of HMGB1 expression relative to G. Bars show values as mean ± SE,*p<0.05 **p<0.01; Student's t-test.

## *4.2. HMGB1 does not re-localize to the cytosol or the extracellular environment during HASMCs replicative senescence*

To assess the consequences of HMGB1 decline during VSMCs senescence, we silenced HMGB1 protein expression in HASMCs using lentiviral vector carrying specific shRNAs. We named HASMCs lacking HMGB1 expression as *shB1/SMCs* and HASMCs infected with a lentivirus carrying a control shRNAs as *shCTRL/SMCs*. We cultured both clones to obtain young (P8) and old (P15) cell populations and checked HMGB1 protein levels by WB, confirming HMGB1 reduction after silencing in P8 and P15 *shB1/SMCs* (Fig. 3A).

Then, we cultured cells in normal growth media for 48 hours and performed immunofluorescence (IF) to investigate HMGB1 localization during replicative senescence. The analysis revealed that HMGB1 was present at significant higher levels in the nucleus of P8 *shCTRL/SMCs* compared to P15 *shCTRL/SMCs* (Fig. 3B, C, and E). Similar behaviour was observed in the cytosol of cells that, as expected, contained very low amount of the protein (Fig. 3D, F). IF on P8 and P15 *shB1/SMCs* confirmed silencing of HMGB1 observed by WB analysis and revealed no significant differences between *shCTRL/SMCs* and *shB1/SMCs* at P15 in the cytosol (Fig. 3B-F).

Next, we examined extracellular levels of HMGB1 with ELISA assay after culturing cells for 48 hours in a medium poor of serum to exclude the detection of serum HMGB1. Likely, extracellular HMGB1 was significantly lower in *shB1/SMCs* respect to *shCTRL/SMCs* at both passages (Fig. 3G). Remarkably, ELISA assays also disclosed that extracellular HMGB1 values were extremely low, with P15 *shB1/SMCs* showing the lowest amount (Fig. 3G).

As expected [57]senescent P15 cells appeared significantly bigger in both nuclear and cytosol sizes respect to young P8 cells (Fig. 3B-D) with an inverse correlation between HMGB1 expression and the nuclear area (Fig. 4A, B). Interestingly, we noticed that both P8 and P15 *shB1/SMCs* exhibited a bigger nuclear and cytosol size in comparison with corresponding *shCTRL/SMCs*, suggesting a major disposition to senesce (Fig. 4C).

Together, these data indicate that replicative senescence in HASMCs is accompanied by a decrease in HMGB1 content that is not due to re-localization of the protein from the nucleus to the cytosol and eventually the extracellular environment.

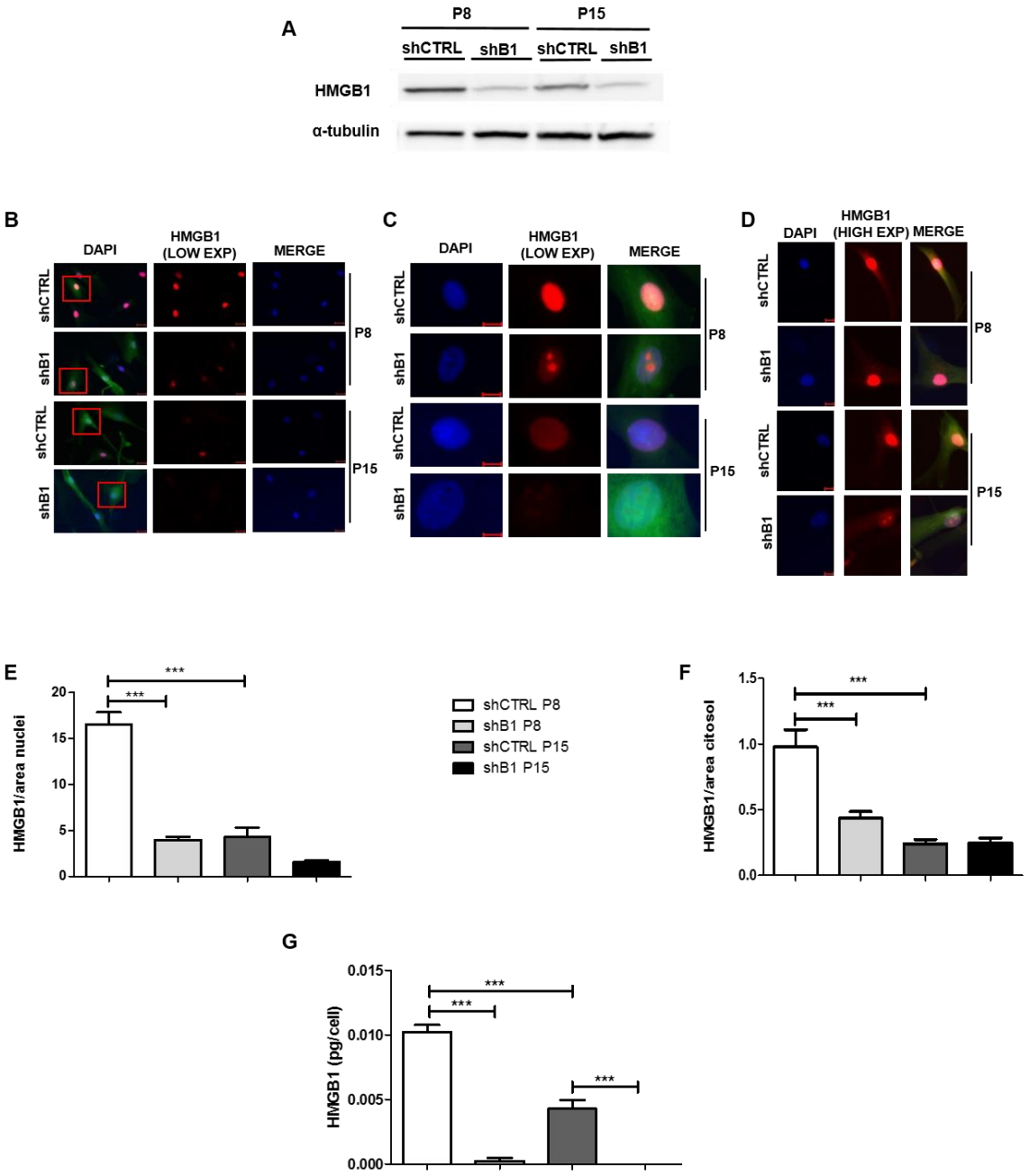


**Figure 3. HMGB1 does not delocalize to the cytosol or extracellular environment during HASMCs replicative senescence. (A)** Western blot for HMGB1 on *shB1/SMCs* and *shCTRL/SMCs* at P8 and P15 after 48 hours of culturing. α-tubulin was used as loading control. **(B)** Representative images of *shB1/SMCs* and *shCTRL/SMCs* at P8 and P15 subjected to immunofluorescence (IF) for HMGB1 after acquisition with lower exposure (LOW EXP); scale bars: 20µm. **(C-D)** Enlarged images of the IF showed in B after acquisition with lower exposure (C, LOW EXP) and higher exposure (D, HIGH EXP); scale bars: 10µm. **(E-F)** Quantification of nuclear (C, LOW EXP) and cytosolic (D, HIGH EXP) expression of HMGB1; *shCTRL/SMCs* P8 n=37 cells, *shB1/SMCs* P8 n=27 cells *shCTRL/SMCs* P15 n=35 cells, *shB1/SMCs* P15 n=29 cells. Bars represent values as mean ± SE, ***p<0.001; 1-way ANOVA plus Bonferroni post-hoc test. **(G)** Graph of ELISA assay displaying extracellular HMGB1 protein levels in *shB1/SMCs* and *shCTRL/SMCs* at P8 and P15 after 48 hours of culturing (n=3). Bars represent values as mean ± SE, ***p<0.001; 1-way ANOVA plus Bonferroni post-hoc test.

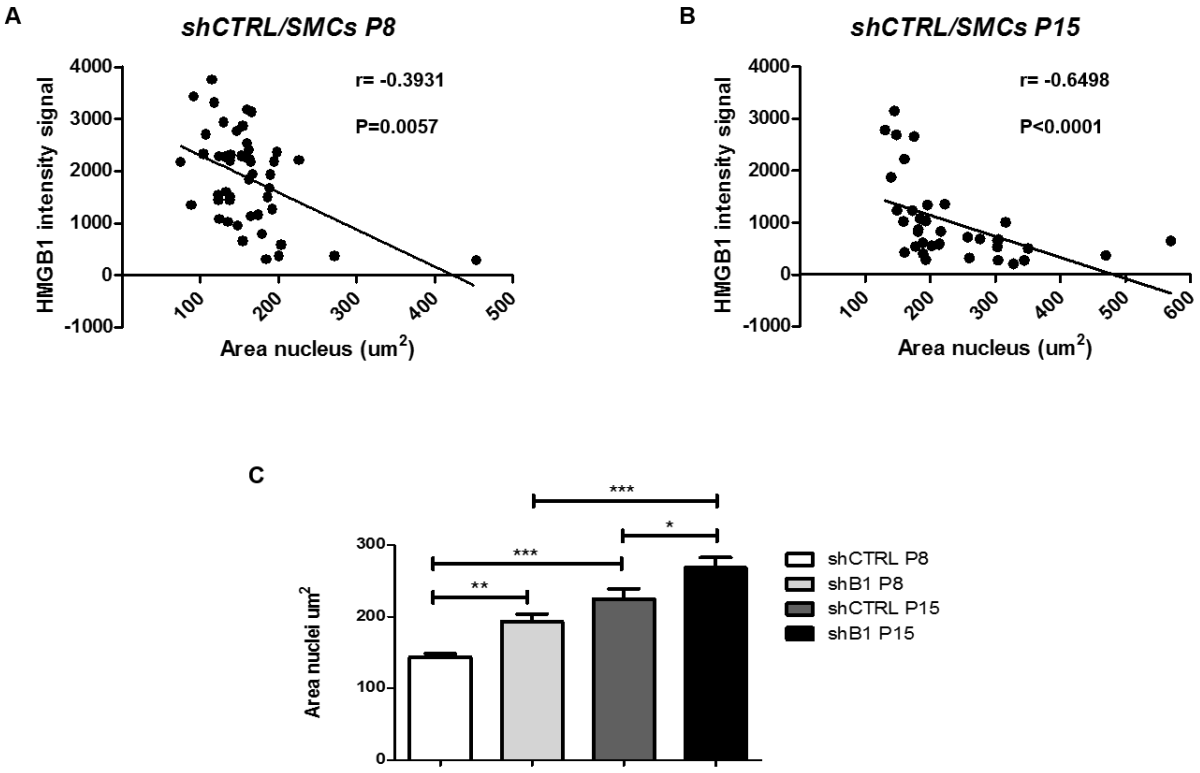


**Figure 4. The down-regulation of HMGB1 augments size of nuclei in HASMCs. (A)** Correlation analysis on P8 *shCTRL/SMCs* showed in Fig. 3B between nuclear area and HMGB1 expression (n=48 cells). Spearman test. **(B)** Correlation analysis on P15 *shCTRL/SMCs* showed in Fig. 3B between nuclear area and HMGB1 expression (n=37 cells). Spearman test. **(C)** Quantification of nuclear sizes of *shB1/SMCs* and *shCTRL/SMCs* at P8 and P15 showed in Fig. 3B; *shCTRL/SMCs* P8 n=37 cells, *shB1/SMCs* P8 n=27 cells *shCTRL/SMCs* P15 n=35 cells, *shB1/SMCs* P15 n=29 cells. Bars represent values as mean ± SE, *p<0.05, **p<0.01 ***p<0.001; 1-way ANOVA plus Bonferroni post-hoc test.

## *4.3. The absence of HMGB1 promotes senescence-like alterations in HASMCs*

Next, we asked whether HMGB1 deficiency could alter HASMCs phenotype, with particular regard to senescence. First, we assessed P8, P13 and P15 *shB1/SMCs* and *shCTRL/SMCs* proliferation for 4 days. *shB1/SMCs* displayed significant lower proliferation rate than *shCTRL/SMCs* at P8, which became less evident but still significant at P13 (Fig. 5A); at P15 we did not observed further differences (Fig. 5A). As expected, proliferation rate decreased along with passages number in *shCTRL/SMCs* (Fig. 5A).

In order to corroborate these data, we performed cell cycle analysis on P8 and P15 *shB1/SMCs* and *shCTRL/SMCs* after 48h of culture. Interestingly, we noticed a significant increase in the percentage of cells in G1 phase and concomitant decrease in S phase (Fig. 5B), together with an augmentation of CDK inhibitor p21 protein levels, but not p16 (Fig. 6A-C), in *shB1/SMCs* compared with *shCTRL/SMCs* at P8 but not at P15. Predictably, we also observed analogue cell cycle variations along with the increase of passages in *shCTRL/SMCs* (Fig. 5B). Finally, *shB1/SMCs* had higher percentage of cells positive for senescence associated β-galactosidase (SA-β-gal) staining than *shCTRL/SMCs* at P8 but not at P15; however, P15 *shCTRL/SMCs* showed a positivity for SA-β-gal that, as expected, was significantly greater in comparison to control cells at P8 (Fig. 6D, E).

Altogether, these data demonstrate that young HASMCs can reduce HMGB1 protein levels to enter in a G0/G1 growth arrest, inhibit their proliferation and acquire senescence-like properties.

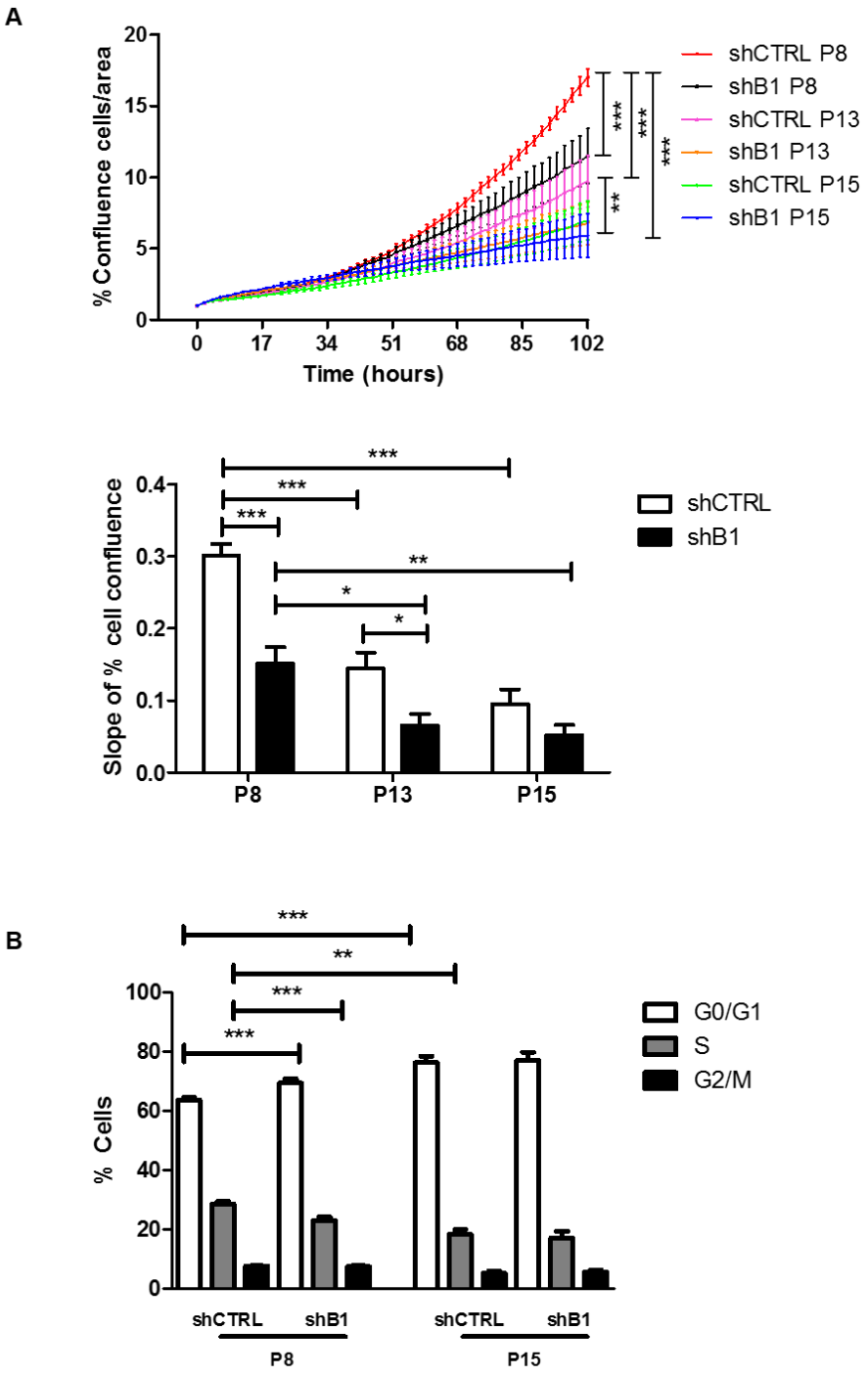


**Figure 5. The absence of HMGB1 inhibits HASMCs proliferation. (A)** Proliferation analysis of indicated HASMCs clones. Graph represents the percentage of cell confluence per area during time; *shCTRL/SMCs* n=3, *shB1/SMCs* n=3. 1-way ANOVA plus Bonferroni post-hoc test for multiple comparisons between same HASMCs clone at different replicative passages; 2-way ANOVA plus Bonferroni post-hoc test for multiple comparisons between *shCTRL/SMCs* and *shB1/SMCs* at the same replicative passage. **(B)** Cell cycle analysis of *shB1/SMCs* and *shCTRL/SMCs* after 48 hours of growth at P8 and P15; n=6.

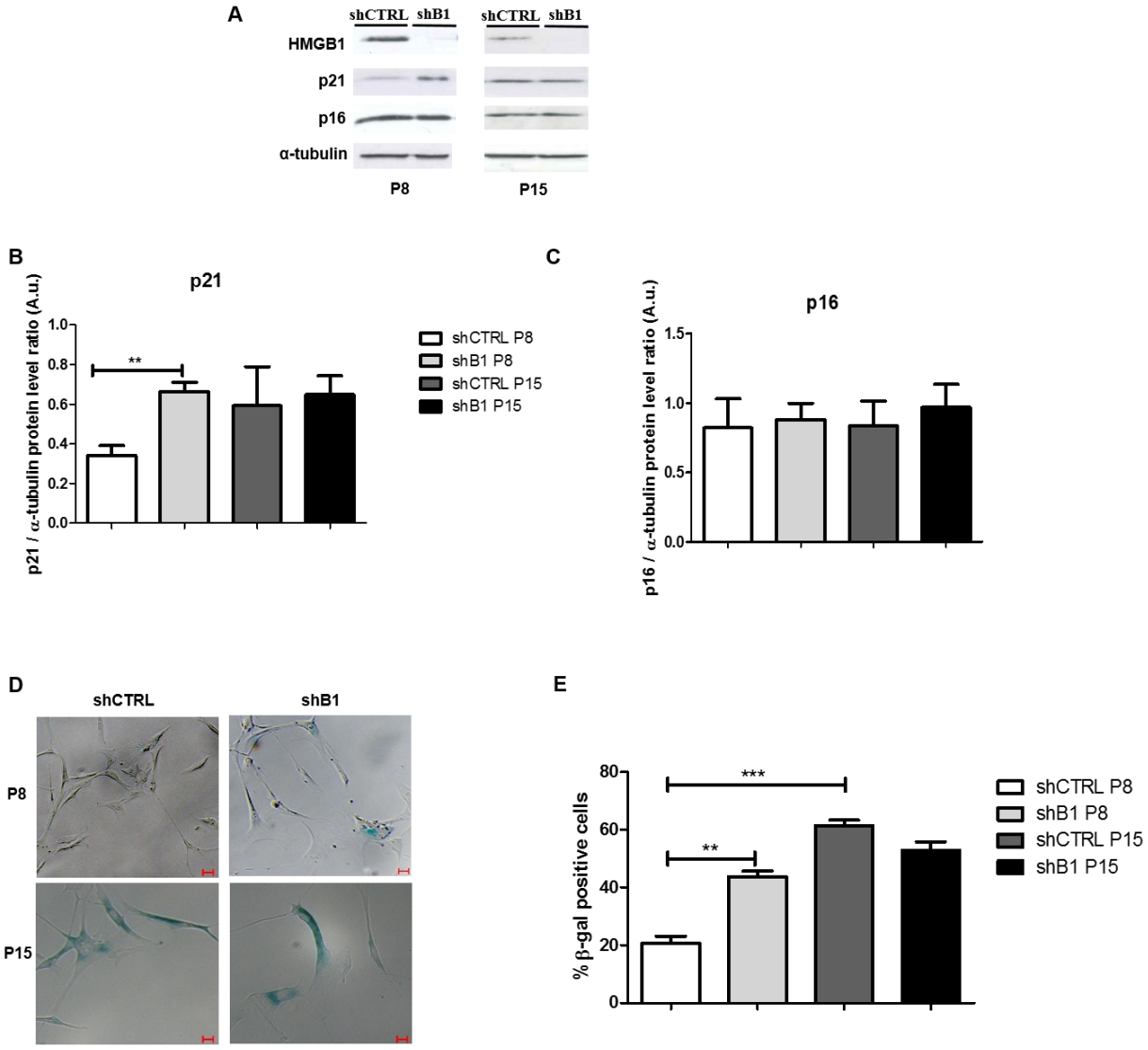


**Figure 6. HMGB1 silencing promotes senescence-like alterations in HASMCs. (A)** Western blot for p21 and p16 protein in *shB1/SMCs* and *shCTRL/SMCs* after 48 hours of growth at P8 (left) and P15 (right). α-tubulin was used as loading control. **(B-C)** Quantification of p21 (B) and p16 (C) protein expression relative to panel A; *shCTRL/SMCs* n=8, *shB1/SMCs* n=7. **(D)** Representative images of *shB1/SMCs* and *shCTRL/SMCs* at P8 and P15 after SA-β-gal staining at 48 hours of growth. Scale bars: 20μm. **(E)** Quantification of SA-β-gal staining relative to panel D; n=3. Bars show values as mean ± SE,*p<0.05, **p<0.01, ***p<0.001. 1-way ANOVA plus Bonferroni post-hoc test for multiple comparisons.

## *4.4. HMGB1 controls the acquisition of SASP in HASMCs*

Production and release of SASP factors is a mechanism of senescence spreading to neighbour cells[109]. Since our data suggest a role for HMGB1 in induction of senescence-like phenotype, we asked whether HMGB1 could alter SASP acquisition in HASMCs. Therefore, we investigate mRNA expression of several SASP factors in *shB1/SMCs* and *shCTRL/SMCs* cells at P8 cultured for 24, 48 and 72 hours by RT-PCR (Fig. 7A). Unexpectedly, *shB1/SMCs* cells display significant lower mRNA expression of inflammatory genes (IL-6, IL-1β, IL-8 and IL-10) and migratory factors (MCP-1), while calcification markers (OPG, OPN, BMP-2) present an anti-calcific expression profile (Fig. 7A). Then, we focused our attention on pro-inflammatory cytokines like IL-6 and IL-1β and molecules like OPG and OPN involved in the VSMCs osteogenic trans-differentiation. Firstly, we compared their mRNA expression in both *shB1/SMCs* and *shCTRL/SMCs* cells at P8 and P15. The analysis revealed that P15 clones present similar trends of IL-6, IL-1β, OPG, and OPN mRNA expression between of P8 cells (Fig. 7B). Next, we determined their extracellular release by ELISA at 72 hours. We found that globally, *shB1/SMCs* secreted less IL-6, in comparison with *shCTRL/SMCs* cells, while they release higher amount of OPN especially at P15 (Fig. 7C). IL-6 extracellular amount was higher in P15 respect to P8 cells, as expected. OPG levels decreased with replicative senescence as well and in P8 *shB1/SMCs* in respect to corresponding control cells (Fig. 7C). IL-1β secretion was barely detectable only in *shCTRL/SMCs* at P8 (Fig. 7C).

Altogether, these data suggest that HMGB1 supports SASP acquisition and hence senescence spreading in HASMCs.

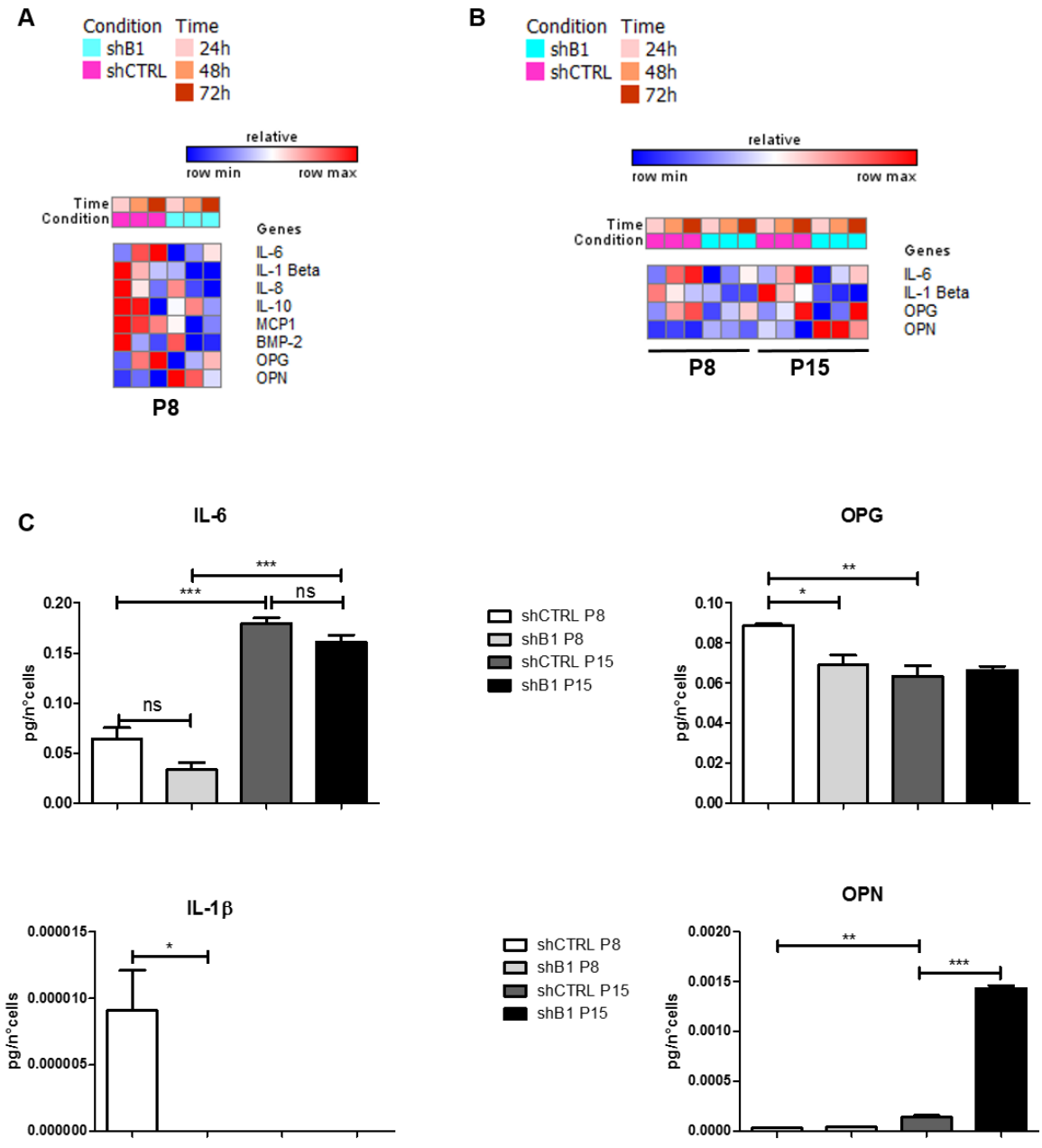


**Figure 7. HMGB1 controls SASP acquisition in HASMCs. (A)** Heatmap representing SASP factors expression in *shB1/SMCs* and *shCTRL/SMCs* at P8 after 24, 48 and 72 hours of growth analyzed by qRT-PCR and normalized to corresponding GAPDH levels. **(B)** Heatmap representing inflammatory (IL-6, IL-1β) SASP factors and calcification markers (OPG, OPN) expression in *shB1/SMC* and *shCTRL/SMCs* at P8 and P15 after 24, 48 and 72 hours of growth analyzed by qRT-PCR and normalized to corresponding GAPDH levels. **(C)** Graphs of ELISA assay displaying extracellular protein levels of indicated SASP factors in *shB1/SMC* and *shCTRL/SMCs* at P8 and P15 after 72 hours of growth. Bars show normalized densitometric ratios. Values are mean ± SE,*p<0.05, **p<0.01, ***p<0.001. *shCTRL/SMCs* n=6; *shB1/SMC* n=6. 1-way ANOVA.

## *4.5. The absence of HMGB1 diminishes basal DNA damage and oxidative stress in HASMCs*

Since DNA damage induces senescence[167] and it is known that HMGB1 regulates the DNA repair[168], we used neutral comet assay to measure basal DNA damage in *shB1/SMCs* and *shCTRL/SMCs* cells at both P8 and P15 after 48 hours of culture. As expected, DNA damage was higher in *shCTRL/SMCs* at passage P15 than P8 (Fig. 8A, B). Interestingly, *shB1/SMCs* cells manifested significant lower DNA damage in comparison with *shCTRL/SMCs* at both P8 and P15 (Fig. 8A, B). Then, we asked whether the discrepancy in DNA damage was due to a better repair machinery present in *shB1/SMCs* respect to *shCTRL/SMCs* cells and/or to a dissimilar content in DNA stressors. Hence, as neutral comet assay detect primarily DSBs, which are frequently caused by ROS[169], we evaluate basal ROS content together with transcriptional expression of several key genes in the NHEJ pathway in *shB1/SMCs* and *shCTRL/SMCs* cells at both P8 and P15 after 48 hours of culture. Remarkably, the difference between *shB1/SMCs* and *shCTRL/SMCs* at P15 respect to P8 was showed in DNA repair genes expression. Indeed, transcriptional levels of XRCC4 and NHEJ factor 1 (NHEJ1) were significantly higher in *shB1/SMCs* respect to *shCTRL/SMCs* only at P15, whereas only a small but not significant difference was observed for P8 cells, and P15 *shCTRL/SMCs* had a tendency to a lower expression of both genes compared to P8 *shCTRL/SMCs* (Fig. 8C).

Basal ROS content in *shB1/SMCs* was lower than *shCTRL/SMCs* in a statistically significant manner both at P8 and at P15 (Fig. 9 E, F). Of note, the difference within P15 cells was much higher respect to P8 cells (14 times vs 3 times); this was justify by the fact that, as expected, P15 *shCTRL/SMCs* presented relevant 10 times higher amount of ROS compared to P8 *shCTRL/SMCs* (Fig. 9F).

Hence, these data propose that HASMCs down-regulate nuclear HMGB1 to reduce basal ROS and DNA damage contents and to modulate DNA repair genes expression in a protective manner for instance when ROS concentrations are particularly high, as happen in senescent cells.

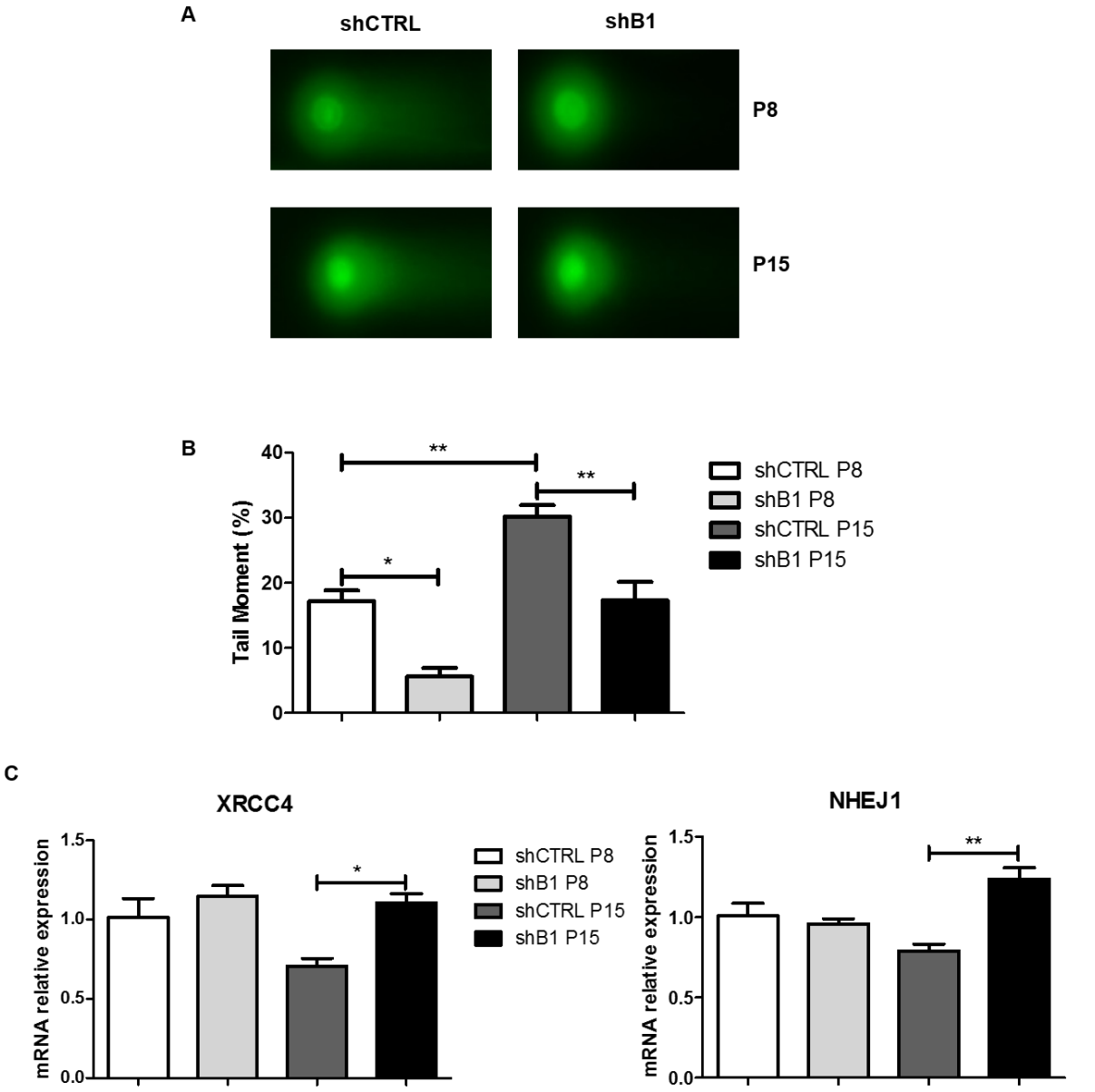


**Figure 8. HMGB1 ablation diminishes DNA damage in HASMCs. (A)** Representative images of *shB1/SMCs* and *shCTRL/SMCs* 48 hours after seeding at P8 and P15 subjected to comet assay to detect DNA damage. **(B)** Quantification of DNA damage relative to panel A; n=3. **(C)** Gene expression of DNA repair factors in *shB1/SMCs* and *shCTRL/SMCs* 48 hours after seeding at P8 and P15 analyzed by qRT-PCR and normalized to corresponding GAPDH levels; n=3. Bars show values as mean ± SE,*p<0.05, **p<0.01. 1-way ANOVA plus Bonferroni post-hoc test for multiple comparisons.

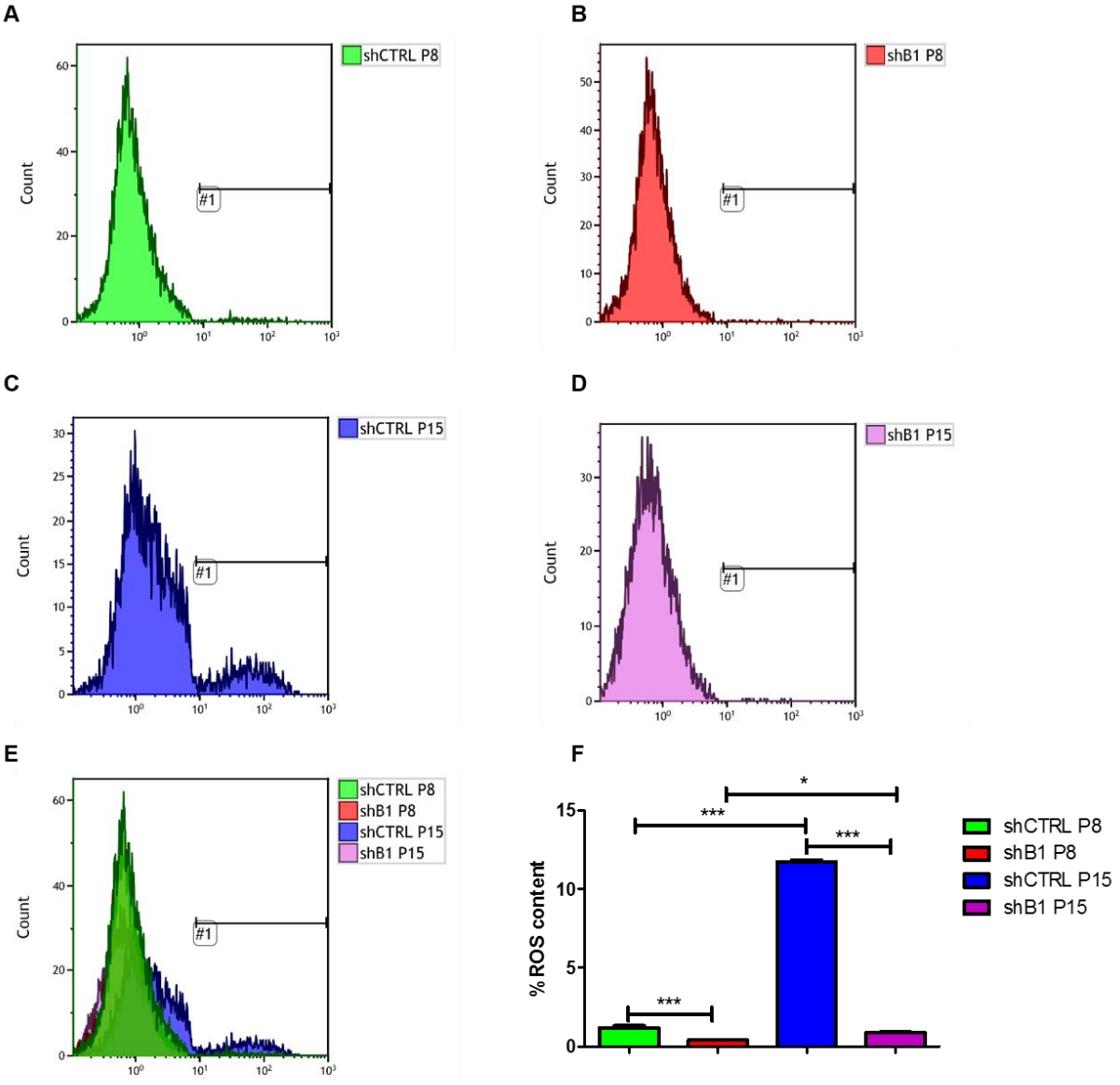


**Figure 9. HMGB1 ablation decreases oxidative stress in HASMCs. (A-E)** Representative image of *shB1/SMCs* and *shCTRL/SMCs* 48 hours after seeding at P8 and P15 subjected to ROS content analysis. **(F)** Quantification of ROS content relative to panel E; n=3. Bars show values as mean ± SE,*p<0.05, ***p<0.001. 1-way ANOVA plus Bonferroni post-hoc test for multiple comparisons.

## *4.6. HMGB1 protein level declines during vascular calcification in vitro and in vivo*

The acquisition of a senescent phenotype is essential for VSMC osteogenic trans-differentiation[108]. Therefore, we investigated the behaviour of HMGB1 in the calcification process. Firstly, we set up an *in vitro* model of HASMCs calcification culturing them in hyperphosphatemia medium (osteogenic medium) or in normal growth medium (as control) for 11 consecutive days. We analysed calcium deposition and HMGB1 expression at day 3, 7 and 11 to follow the kinetic of calcification together with HMGB1 protein fluctuation. As expected, HASMCs cultured in osteogenic medium displayed a time-dependent accumulation of calcium content respect to cells cultured in growth media (Fig. 10A) confirmed also by Von Kossa staining (Fig. 10B). Notably, the increase in calcium accumulation was accompanied by a corresponding downregulation of HMGB1 protein expression, which almost disappeared after 11 days of calcification, while HASMCs cultured in growth medium showed an initial slightly reduction of HMGB1 expression after 7 days (Fig. 10C, D).

To verify HMGB1 decline along with calcification *in vivo*, we take advantage of a well-established rat model of adenine-induced calcification. We fed 12 weeks old Wistar rats with 0.75% adenine diet for 8 weeks and we quantified calcium accumulation and HMGB1 protein amount in rat aortas after 2, 3, 4 and 8 weeks from the beginning of the adenine diet (Fig. 11A-C). In agreement with the *in vitro* data, HMGB1 expression started to drop as the calcification arises in the aortas and then completely disappeared in the late time points of calcification (Fig. 11C). Notably, we also observed a strong negative correlation between calcium content and HMGB1 protein expression in rat aortas (Fig. 11D). Furthermore, we investigated HMGB1 protein levels and calcium content in the human abdominal aneurism of aorta (AAA), which is a vascular alteration characterized by the presence of high levels of calcium[170]. We found an inverse correlation between HMGB1 protein amount and calcium content (Fig. 11E) and a direct correlation between IL-6 mRNA level and calcium content (Fig. 11F).

Thus, these results demonstrate that HMGB1 is downregulated during HASMCs calcification *in vitro* and vascular calcification *in vivo*.

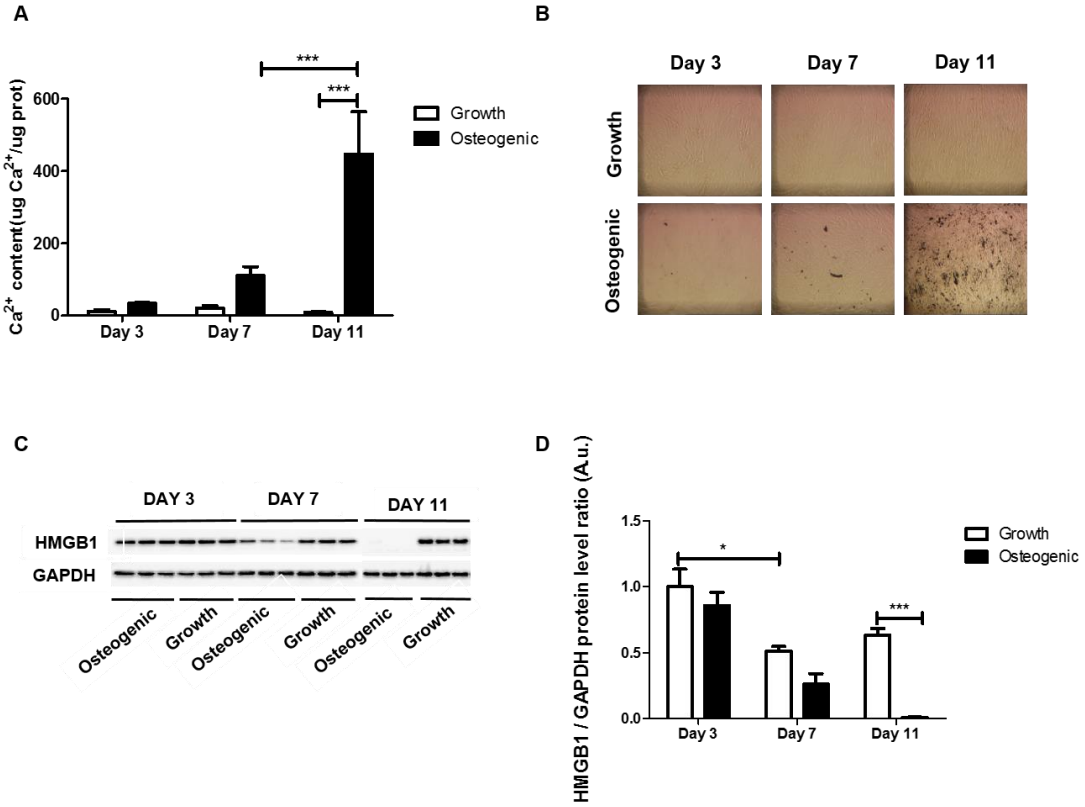


**Figure 10. HMGB1 decreases during VC *in vitro*. (A)** Precipitated calcium of HASMCs cultured in both growth and osteogenic media for 3, 7 and 11 days quantified by colorimetric analysis (n=3). **(B)** Representative images of Von Kossa staining to reveal calcium deposition (black). **(C)** Protein extracts of HASMCs were subjected to WB with anti-HMGB1 antibody. GAPDH was used as loading control. **(D)** Quantification of HMGB1 protein expression relative to panel C (n=3). Values are mean ± SE, *p<0.05; ***p<0.001. 1-way ANOVA plus Bonferroni post-hoc test for multiple comparisons between Growth or Osteogenic sample during different Days of calcification; 2-way ANOVA plus Bonferroni post-hoc test for multiple comparisons between Growth and Osteogenic at the same Day of calcification.

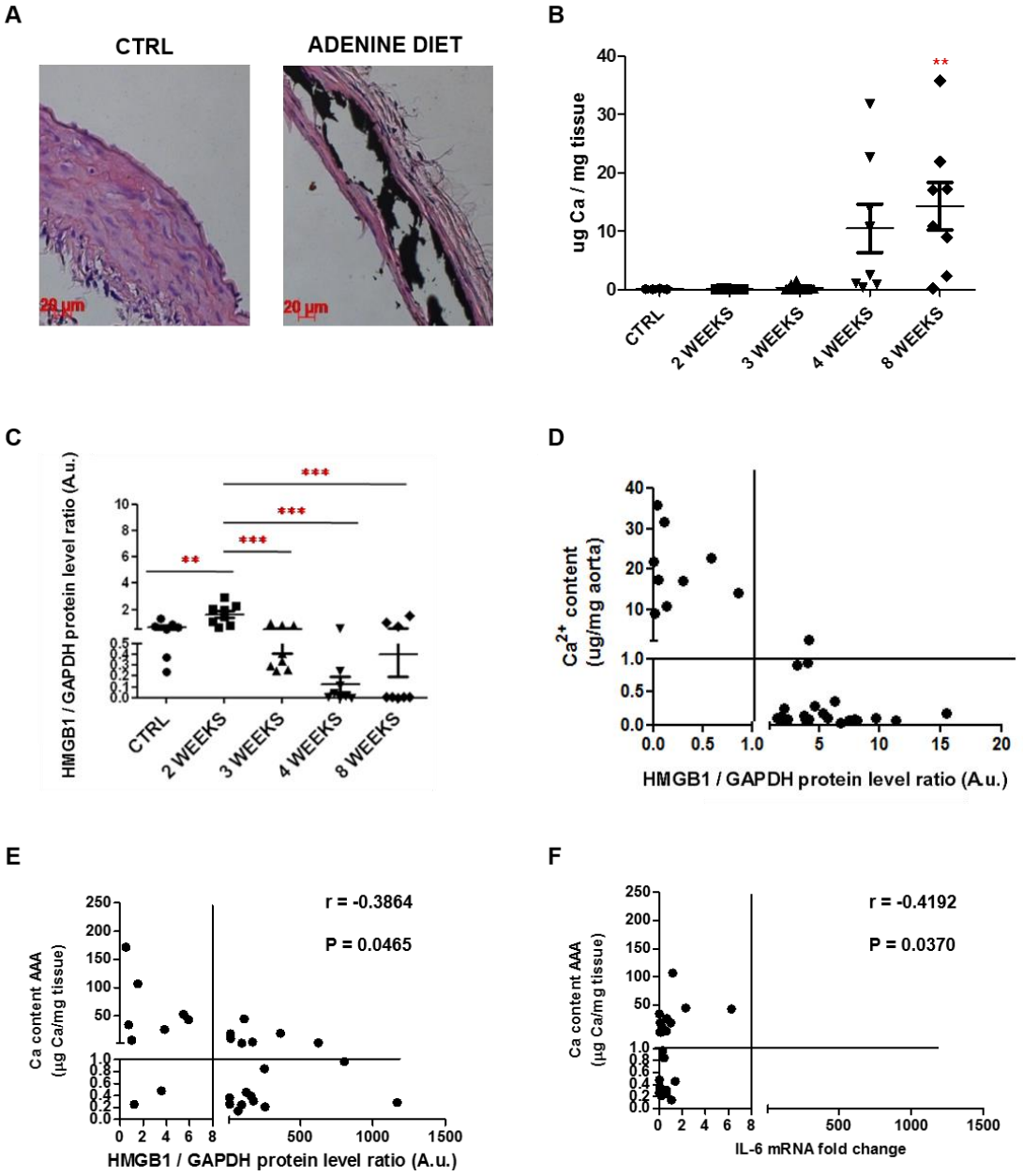


**Figure 11. HMGB1 decreases during VC *in vivo*. (A)** Representative images of 12 weeks old uremic rat aortas subjected to Von Kossa staining to reveal calcium deposition (black); scale bars: 20µm. **(B)** Calcium content was quantified by colorimetric analysis (CTRL n=5; 2 WEEKS n=8; 3 WEEKS n=8; 4 WEEKS n=8; 8 WEEKS n=8). Values are mean ± SE, **p<0.01, WEEKS of Diet *vs* CTRL, 2-way ANOVA. **(C)** Tissues extracts of rat aortas showed in A were subjected to WB with anti-HMGB1 and GAPDH (loading control) antibody (CTRL n=5; 2 WEEKS n=8; 3 WEEKS n=8; 4 WEEKS n=8; 8 WEEKS n=8). Values are mean ± SE, **p<0.01; ***p<0.001. 2-way ANOVA. **(D)** Correlation analysis on uremic rat aortas showed in panel A between HMGB1 protein levels and calcium content (Pearson test). **(E)** Correlation analysis between HMGB1 protein expression and calcium content in AAA specimens (Spearman test). **(F)** Correlation analysis between IL-6 mRNA expression and calcium content in AAA specimens (Pearson test). Values are mean ± SE, **p<0.01; ***p<0.001.

## *4.7. HMGB1 down-regulation is protective in the early phases of HASMCs calcification, but favours it in the late phases*

Next, we investigated the effect of HMGB1 ablation during HASMCs calcification. We cultured P8 *shB1/SMCs* and *shCTRL/SMCs* in osteogenic media for 3, 5, 7 and 11 consecutive days and analysed calcium deposition by qualitative Alizarin red staining and quantitative colorimetric assay (Fig. 12A and B, respectively). The analysis displayed that *shB1/SMCs* accumulated lower amount of calcium at Day 5 and 7 in comparison to *shCTRL/SMCs* (Fig. 12A, B). However, after 11 days of calcification, *shB1/SMCs* displayed significantly higher calcium content than control cells (Fig. 12A, B).

Since we verified that HMGB1 could alter the secretion of some pro-calcification SASP factors (Fig. 7C), we analysed the release of IL-6, IL-1β, OPG and OPN in the supernatant of P8 *shB1/SMCs* and *shCTRL/SMCs* during calcification by ELISA. Extracellular IL-6 amount increased during calcification in *shCTRL/SMCs* from Day 0 to Day 5 and then decreased in the late days (Fig. 13A). On the other hand, IL-6 content was significantly lower in *shB1/SMCs* respect to corresponding *shCTRL/SMCs* from Day 0 to Day 5 (Fig. 13A) but kept increasing during calcification reaching higher extracellular levels at Day 11 in respect to *shCTRL/SMCs* (Fig. 13A). IL-1β secretion diminished during calcification in both *shCTRL/SMCs* and *shB1/SMCs* but remained higher in the former cells after 11 days of calcification (Fig. 13A). Secretion of OPG increased during calcification in *shCTRL/SMCs* but not in *shB1/SMCs* (Fig. 13A). Finally, OPN levels clearly augmented in the extracellular media at Day 7 and 11 in *shB1/SMCs* in respect to corresponding control cells (Fig. 13A).

Then, we checked mRNA expression of specific osteoblastic markers such as Runx-2, Msx-2 and ALP. We observe that the levels of Runx-2 and ALP were lower in *shB1/SMCs* compared to *shCTRL/SMCs* already at Day 0 and across the calcification timing (Fig. 13B), while Msx-2 was downregulated at the basal condition (Day 0) but resulted clearly upregulated at Day 11 in *shB1/SMCs* in respect to *shCTRL/SMCs* (Fig. 13B).

Overall, these data suggest that HMGB1 downregulation is protective in the early phase of HASMCs calcification but favours it in the late phase, probably because it alters pro-calcification SASP release.

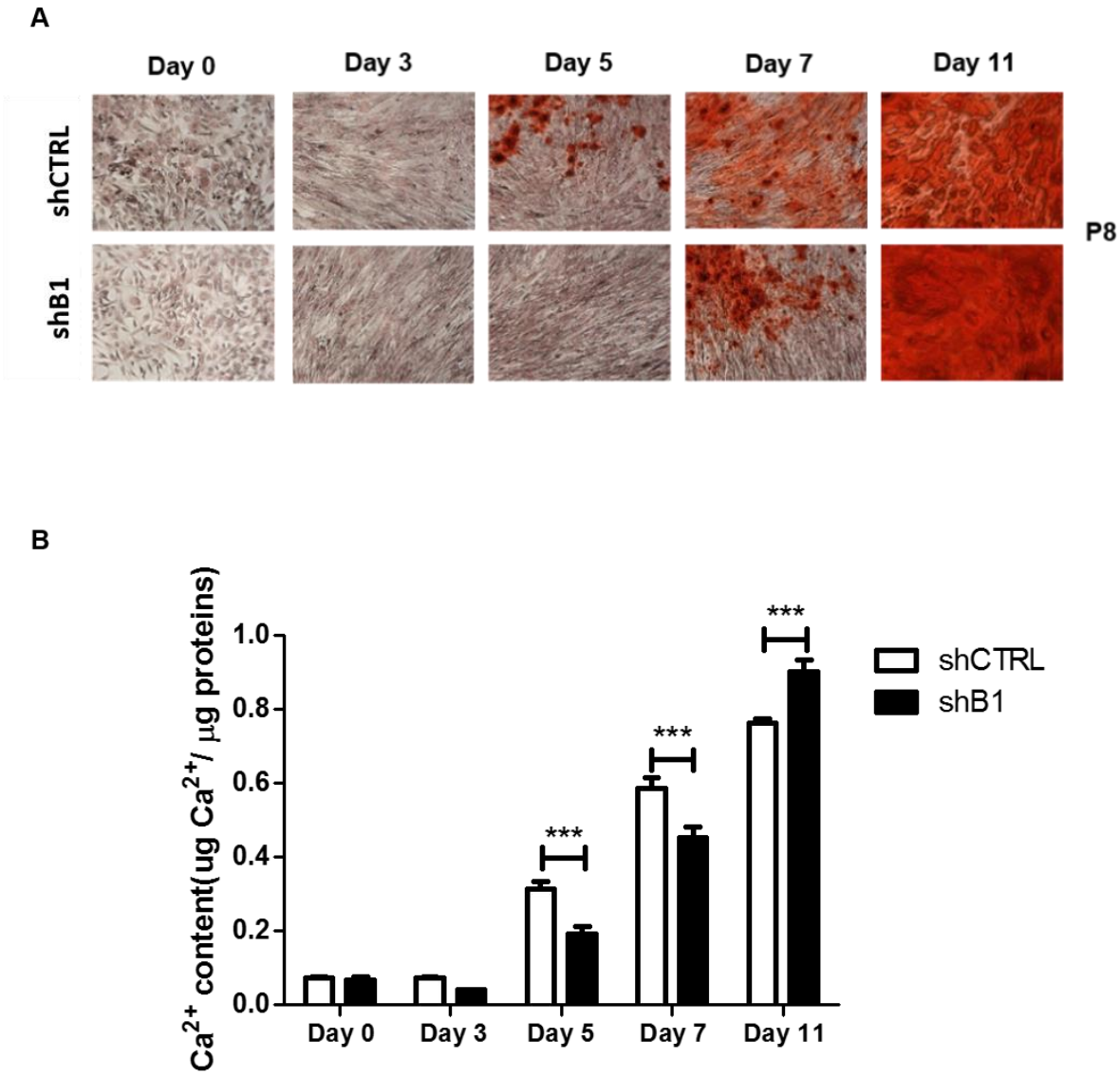


**Figure 12. HMGB1 downregulation is protective in the early phase of HASMCs calcification but favours it in the late phase. (A)** Representative images of *shB1/SMCs* and *shCTRL/SMCs* at P8 cultured in osteogenic media for 3, 7 and 11 days after alizarin red staining to reveal calcium deposits (red). **(B)** Calcium content of P8 HASMCs clones was quantified by colorimetric analysis (*shCTRL/SMCs* n=3, *shB1/SMCs* n=3). Bars show values as mean ± SE, ***p<0.001. Two-way ANOVA plus Bonferroni post-hoc test for multiple comparisons.

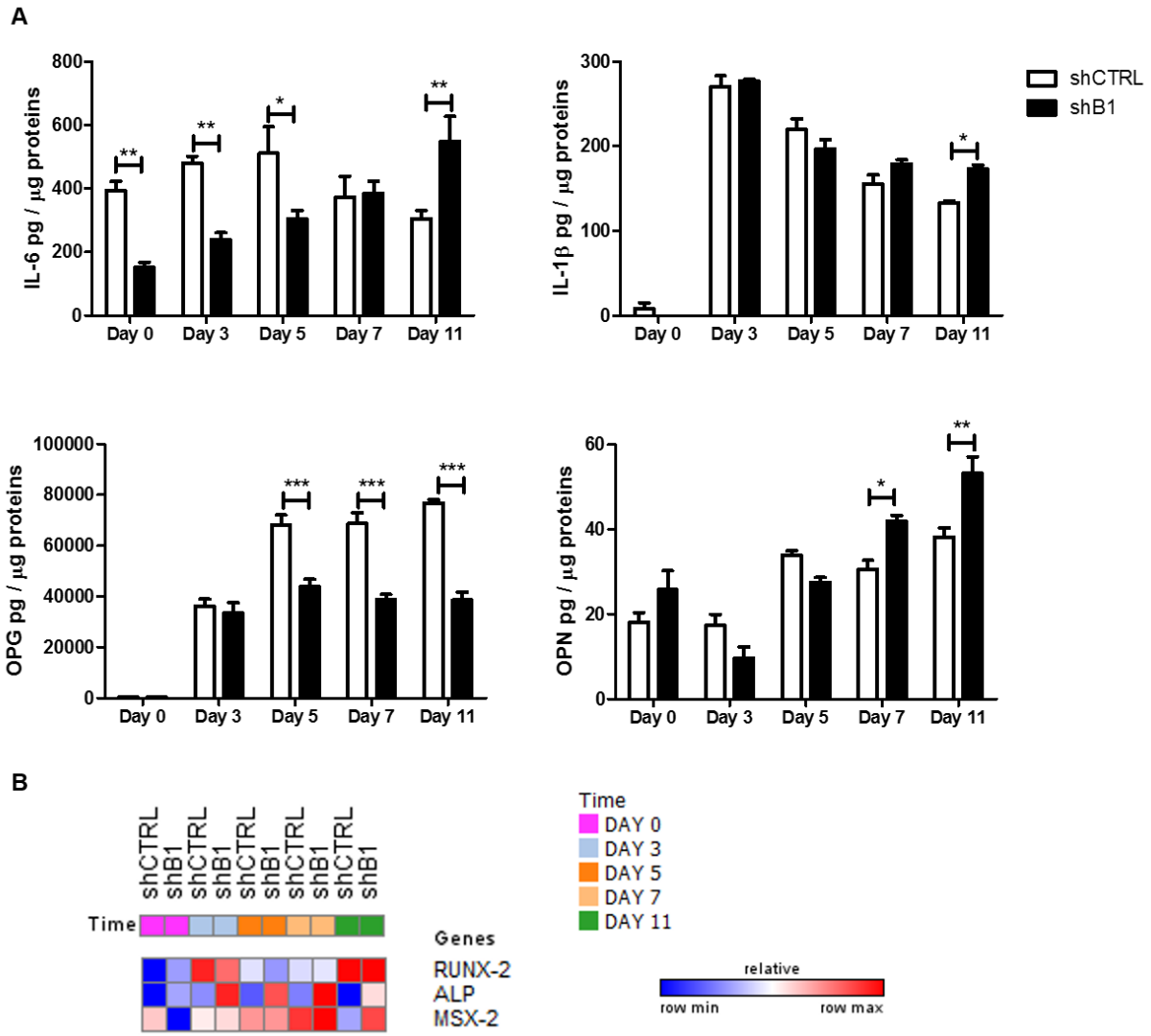


**Figure 13. HMGB1 affects SASP secretion during HASMCs calcification. (A)** Supernatants of P8 HASMCs clones showed in Fig. 12 were subjected to ELISA assay for IL-6, IL-1β, OPG and OPN (*shCTRL/SMCs* n=3, *shB1/SMCs* n=3) Values are mean ± SE, *p<0.05; ** p<0.01; ***p<0.001; 2-way ANOVA plus Bonferroni post-hoc test for multiple comparisons between *shCTRL/SMCs* and *shB1/SMCs* at the same Day of calcification. **(B)** Heatmap representing SASP factors and calcification markers expression in *shB1/SMCs* and *shCTRL/SMCs* at P8 cultured in osteogenic media for 3, 7 and 11 days analyzed by qRT-PCR and normalized to corresponding GAPDH levels (*shCTRL/SMCs* n=3, *shB1/SMCs* n=3). Bars show values as mean ± SE,*p<0.05, ***p<0.001. 2-way ANOVA plus Bonferroni post-hoc test for multiple comparisons.

## *4.8. HMGB1 affects calcification of aortas in vivo*

In order to verify if HMGB1 could also alter VC *in vivo*, we take advantage of a well-established model of soft tissue calcification[74, 171], by subcutaneously injecting for three consecutive days high doses of vitamin D (VIT D) or a mock solution as control (CTRL) in *Hmgb1*$^{+/+}$ and *Hmgb1*$^{+/-}$ mice. To follow the kinetic of calcification *in vivo*, we sacrificed mice after five (Day 5) and seven (Day 7) days from the first injection. VIT D-treated mice displayed significant body weight loss respected to CTRL animals (Fig. 14A, B). Of note, *Hmgb1*$^{+/-}$ VIT D-treated mice showed significantly higher bodyweight loss in comparison to the corresponding *Hmgb1*$^{+/+}$ animals at Day 7, suggesting that HMGB1 is protective to VIT D treatment (Fig. 14B). Then, we checked aortas calcium deposition by Von Kossa staining and, as expected, aortic calcium content increased with the treatment (Fig. 14C, D). Interestingly, *Hmgb1*$^{+/-}$ VIT D-injected mice presented lower calcium deposits then *Hmgb1*$^{+/+}$ at Day 5, while accumulated more calcium at Day 7 (Fig. 14C, D).

Together, these data suggest that HMGB1 alters aortas calcification *in vivo* and, in particular, its deficiency worsen the long-term response to a pro-calcification stimulus.

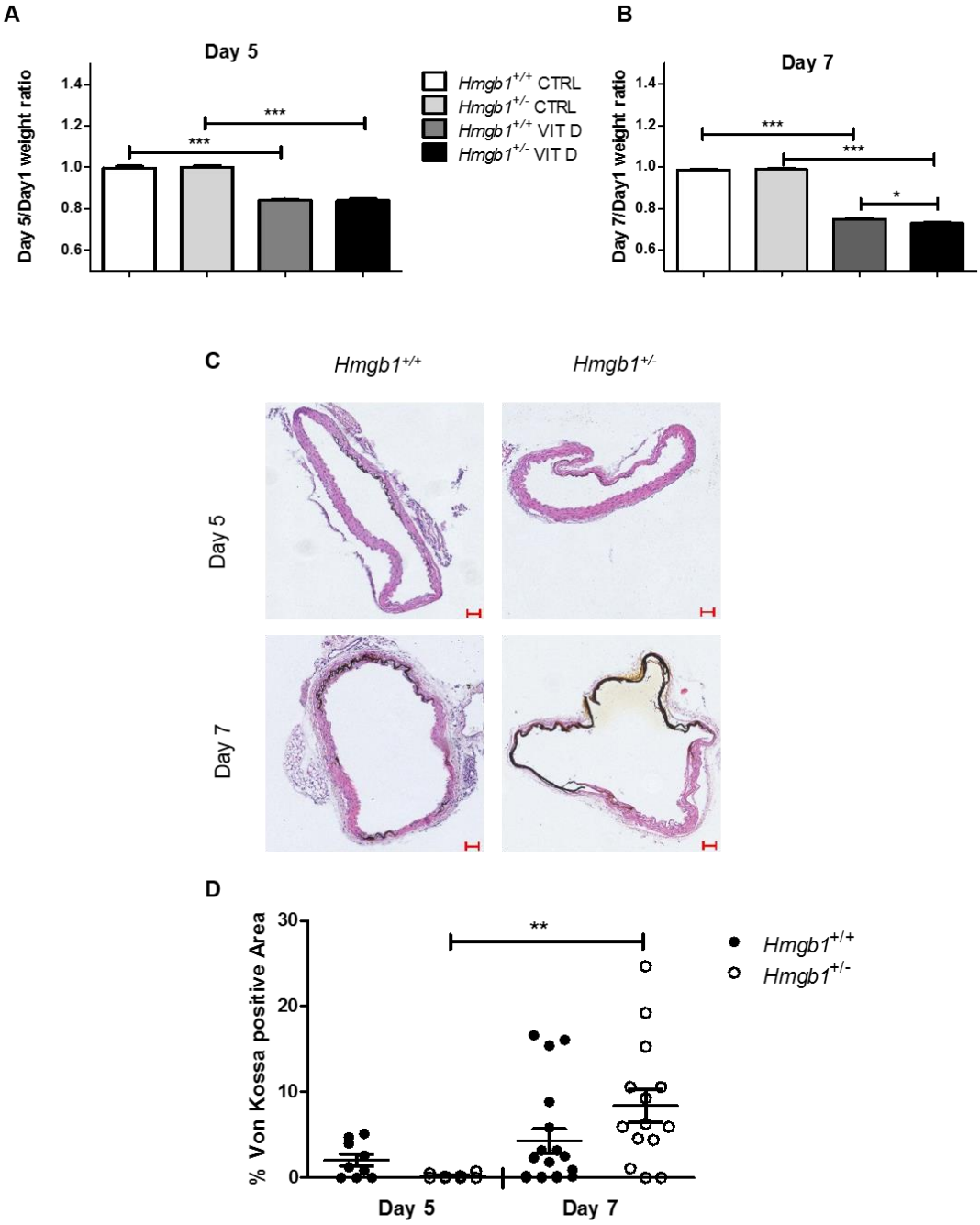


**Figure 14. HMGB1 alters aortas calcification *in vivo*. (A-D)** Sixteen week-old *Hmgb1*$^{+/+}$ and *Hmgb1*$^{+/-}$ male mice were treated subcutaneously with either vitamin D (VIT D) or a mock solution (CTRL) for three consecutive days and sacrificed 5 (Day 5) and 7 (Day 7) days after the first injection. **(A)** Mice weight ratio at the fifth day (Day 5) and before the first vitamin D injection (Day 1) (n= 13, 10, 18, 15). **(B)** Mice weight ratio at the seventh day (Day 7) and before the first vitamin D injection (Day 1) (n= 18, 14, 27, 26). **(C)** Representative images of Von Kossa staining to reveal calcium deposits (black) on section from distal thoracic aortas; scale bar: 50µm **(D)** Bars show the percentage of Von Kossa positive area to the total aortic area (*Hmgb1*$^{+/+}$ Day 5 n=9, *Hmgb1*$^{+/-}$ Day 5 n=9, *Hmgb1*$^{+/+}$ Day 7 n=18, *Hmgb1*$^{+/-}$ Day 7 n=14). Values are mean ± SE, *p<0.05; ***p<0.001. 1-way ANOVA plus Kruskal-Wallis post-hoc test for multiple comparisons.

# 5. Discussion

Vascular aging is a detrimental process characterized by progressive degeneration of vascular tissue and cell functions. During aging, vasculature undergoes different structural and molecular modifications that predispose to several pathologies, primarily CVDs, or/and vascular complications, like VC. Since the blood vessels are composed mainly by VSMCs, understanding their phenotypic alterations during aging and calcification is important in order to prevent or cure such diseases.

In this study, we investigated for the first-time changes of HMGB1 expression and its role in vascular aging and calcification and in particular, in VSMCs senescence and osteogenic transition.

HMGB1 is a highly conserved protein and a member of the HMG protein super-families. It is localized mainly in the nucleus, but it can translocate to the cytosol and the extracellular environment after pro-inflammatory or stress stimuli[126]. Different studies have demonstrated that nuclear HMGB1 declines in replicative senescence in several cell types like human fibroblasts WI-38[148] and murine fibroblasts IMR-90[148] because of an active secretion outside the cell after acetylation in a p53-dependent manner[148].

Herein, we found that HMGB1 protein expression decreases in aged mouse aortas and in replicative senescent HASMCs (Fig. 1). Interestingly, unlike human and murine senescent fibroblasts that have been demonstrated to secrete HMGB1[148], HMGB1 downregulation in HASMCs during senescence is not due to re-localization of the protein from the nucleus to the cytosol and eventually to the extracellular environment, as its cytosolic and extracellular content is very low and does not raise in old (P15) compared to young (P8) HASMCs but rather decreases (Fig. 3E-G). Further, we observed that HMGB1 mRNA expression is downregulated during HASMCs senescence indicating a transcriptional mechanism of regulation (Fig. 2C). Thus, our data confirms that HMGB1 reduction occurs during the onset of replicative senescence but the mechanism that regulates the protein decline depends on the cell type.

Several studies have indicated HMGB1 as a senescence marker[172, 173] and we expand these findings to HASMCs as well. Indeed, we found that HMGB1 levels decline with the age of HASMCs donors (Fig. 2A, G) and inversely correlate with nucleus and cytosolic areas of cells that are known to augment with senescence[57] (Fig. 4).

Furthermore, our experiments with HASMCs silenced for HMGB1 show its direct involvement in promoting senescence (Fig. 5, 6). *shB1/SMCs* have bigger nucleus and cytosol, proliferate less, are partially blocked in G0/G1 phase of the cell cycle and express higher levels of senescent marker, like p21 and SA-β-gal, compared to control cells (Fig. 5, 6). Of note, these differences were observed only in young P8 HASMCs clones, which are characterized by high difference in HMGB1 protein level (*shB1/SMCs vs shCTRL/SMCs;* Fig. 5, 6), and were progressively lost with the increase of passages number. Indeed, P15 *shB1/SMCs* and *shCTRL/SMCs* show no major discrepancies in terms of proliferation and senescence markers expression (Fig. 5, 6). A senescent cell is also characterized by DNA damage and by the acquisition of a SASP phenotype that consists in the production and secretion in the extracellular environment of pro-inflammatory soluble factors. SASP contributes to the spreading of senescence to nearby cells[109], chronic inflammation and organ damage typical of age-related diseases[109]. Our results display that HASMCs can reduce both their SASP expression and secretion through HMGB1 downregulation (Fig. 7), suggesting that HMGB1 is involved not only in the onset of VSMCs senescence, but also in its spreading and chronic inflammation.

Altogether, our findings suggest that the senescence-like alterations that we observe in *shB1/SMCs* cells (Fig. 3-7) could exert beneficial effects. On one hand, the reduction of VSMCs proliferation induced by HMGB1 depletion could be helpful, for instance, in a pathological context like atherosclerosis, slowing down the formation and the progression of the atherosclerotic plaque[174]. This is in accordance to recent studies showing that the increase of senescence is beneficial, in cardiac fibroblast, as it reduces their differentiation in myofibroblasts and eventually fibrosis[175]. On the other hand, the reduction of SASP synthesis and release caused by HMGB1 ablation could decrease chronic inflammation.

Furthermore, our data also display that HMGB1 ablation results in significantly lower DNA damage and ROS content, even in P15 cells, which are clearly senescent (Fig. 8, 9), strongly corroborating the hypothesis of advantageous effects of HMGB1 depletion in HASMCs. Literature is still controversial about the role of HMGB1 in DNA damage and repair. For instance, several works demonstrate that HMGB1 enhances DNA repair[168] and its depletion increases DNA damage[176]. Conversely, other studies show that HMGB1 inhibits the repair of DNA damaged by cis-platin[177]. We investigated in our HASMCs clones the expression of two of the most important key genes of the NHEJ pathway, XRCC4 and NHEJ1[21], since lower levels or structural modifications of these two factors are associated with impaired DNA repair,

diseases and cancer[178]. We found that XRCC4 and NHEJ1 mRNA expression have a tendency to decrease with passages in *shCTRL/SMCs* but not in *shB1/SMCs* (Fig. 8C). Thus, we could speculate that the longer time spent by P8 *shB1/SMCs* in G0/G1 phase and the increase in the expression of XRCC4 and NHEJ1 in P15 *shB1/SMCs*, respectively, could help DNA repair after damage.

How HMGB1 reduction could decrease ROS content and DNA damage is under investigation. ROS are produced mainly by mitochondria, because of oxidative phosphorylation reactions, which are necessary to provide ATP for cells[179]. Therefore, it might be that HMGB1 downregulation during senescence in HASMCs decelerates these metabolic reactions, resulting in a reduction of ROS generation. Moreover, as ROS activities are counteracted by a well-organized antioxidant system composed by several enzymes, HMGB1 down-regulation could enhance the antioxidant response as well.

Our results also demonstrated that HMGB1 decreases during HASMCs calcification induced by hyperphosphatemia (Fig. 10) and in aortas of uremic rats (Fig. 11A-D). Notably, HMGB1 levels inversely correlate with calcium content in both uremic rats and human AAA (Fig. 11D, E) suggesting that HMGB1 can be proposed as marker of tissue calcification too.

As we demonstrated that HMGB1 reduction alters HASMCs senescence and synthesis/secretion of pro-inflammatory SASP factors (Fig. 7), which are known to elicit VSMCs osteoblastic transition and VC[180], we investigated the calcification in P8 *shCTRL/SMCs* and *shB1/SMCs* along with SASP factors secretion. Following the kinetic of calcification, we could appreciate that HMGB1-silenced cells initially deposit less calcium than the corresponding control cells and that they reverse this trend, accumulating conspicuous quantity of calcium in the late time of calcification (Fig. 12). Of note, IL-6 and IL-1β secretion exhibit similar behavior (Fig. 13A). Then we analyzed the expression and release of SASP molecules directly related to calcification such as OPN and OPG. OPG secretion increased during calcification in *shCTRL/SMCs* but not in *shB1/SMCs* while OPN levels clearly augmented in *shB1/SMCs* in respect to corresponding control cells (Fig. 13A). OPG is known to act as a decoy receptor for RANKL[97], thus its absence in HMGB1 silenced cells could augment the possibility of RANKL to bind and activate RANK receptor promoting osteoblastic differentiation and thus calcification. OPN contribute is still debated. The behavior of these molecules reflects the complexity of VC that arises from the conspicuous number of players that interact with each other in order to promote or inhibit calcification and the outcome is determined by the resultant of each single contribute[86]. As our data demonstrate that HMGB1

could influence several of these players both pro- and anti-calcification, it is complicated to identify precisely the mechanism of HMGB1 action in VC, so deeper investigations are needed.

Our *in vivo* model of soft tissues calcification induced in *Hmgb1*$^{+/+}$ and *Hmgb1*$^{+/-}$ mice strongly corroborates the *in vitro* data. Indeed, aortas of *Hmgb1*$^{+/-}$ mice are characterized by a lower calcium deposition in the first days after treatment, and a more rapidly tissue mineralization in the later days compared to *Hmgb1*$^{+/+}$ animals (Fig. 14C, D). It is important to underline that we observed those differences in *Hmgb1*$^{+/-}$ mice, which express 50% of HMGB1 protein. Therefore, in a model of HMGB1 inducible knockout mice, the effects on aortas calcification would be likely much stronger.

Nevertheless, further studies are necessary to better understand the consequences of HMGB1 reduction in osteogenic trans-differentiation of HASMCs and during calcification *in vivo* with the regards to DNA damage and ROS content.

HMGB1 is known to be involved in chromatin remodeling and mRNA modulation [153] and it has been demonstrated by our data (Fig. 5-7) that its premature ablation could induce a modification in genes transcription related to senescence entry and SASP induction. Hence, it is possible that chromatin remodeling induced by lack of HMGB1 could similarly affect the expression of genes related to osteogenic trans-differentiation. Indeed, we found that the mRNA expression of Runx-2, Msx-2 and ALP are altered in *shB1/SMCs* and in particular, ALP and Msx-2 are clearly upregulated in the late days of calcification in *shB1/SMCs*, contributing to their greater mineralization (Fig. 7D). Gene expression analysis in *shB1/SMCs* and *shCTRL/SMCs* both in basal condition and during calcification are ongoing in the lab and will help to further dissect our hypothesis.

To conclude, we suggest that HMGB1 represents an important player in vascular aging and calcification, modulating senescence, proliferation, SASP molecules expression/release and calcium accumulation in HASMCs. We also propose that in response to a pro-calcification stimulus, VSMCs reduce nuclear HMGB1 to limit initial phases of mineralization that however, become ineffective and deleterious later.

In the future, it will be challenging uncover if the positive effects of HMGB1 silencing that we found in HASMCs could be also extended to other cell types as the effects are cell specific. Moreover, since we observed that these effects are limited during time it will be fascinating manage to modulate them to avoid the side effects that arise in the late time. Hence, our study could be useful to pave the way for new research in the therapeutic field to modulate the positive effects of senescence through HMGB1 not only in vascular calcification but also

in other processes like fibrosis, that are ultimately emerging to be regulated by senescence. Furthermore, as HMGB1 interacts with histones and its modulation affects gene expression, it will be interesting analyze if gene expression alteration in HASMCs influences genes that are involved in other age-related diseases than vascular calcification. Therefore, our research may have another great therapeutic potential because understanding the role of HMGB1 in aging and age-related diseases contributes to enlarge the knowledge of such diseases and so offers new possibilities and perspectives to cure them.

# *References*


1. Zainabadi K. A brief history of modern aging research. *Experimental gerontology*. 2018;104:35-42
2. Ayyadevara S, Alla R, Thaden JJ, Shmookler Reis RJ. Remarkable longevity and stress resistance of nematode pi3k-null mutants. *Aging cell*. 2008;7:13-22
3. Wheeler HE, Kim SK. Genetics and genomics of human ageing. *Philosophical transactions of the Royal Society of London. Series B, Biological sciences*. 2011;366:43-50
4. Corder EH, Saunders AM, Strittmatter WJ, Schmechel DE, Gaskell PC, Small GW, Roses AD, Haines JL, Pericak-Vance MA. Gene dose of apolipoprotein e type 4 allele and the risk of alzheimer's disease in late onset families. *Science*. 1993;261:921-923
5. Kervinen K, Savolainen MJ, Salokannel J, Hynninen A, Heikkinen J, Ehnholm C, Koistinen MJ, Kesaniemi YA. Apolipoprotein e and b polymorphisms--longevity factors assessed in nonagenarians. *Atherosclerosis*. 1994;105:89-95
6. Hsin H, Kenyon C. Signals from the reproductive system regulate the lifespan of c. Elegans. *Nature*. 1999;399:362-366
7. Guarente L, Kenyon C. Genetic pathways that regulate ageing in model organisms. *Nature*. 2000;408:255-262
8. Willcox BJ, Donlon TA, He Q, Chen R, Grove JS, Yano K, Masaki KH, Willcox DC, Rodriguez B, Curb JD. Foxo3a genotype is strongly associated with human longevity. *Proceedings of the National Academy of Sciences of the United States of America*. 2008;105:13987-13992
9. Cournil A, Kirkwood TB. If you would live long, choose your parents well. *Trends in genetics : TIG*. 2001;17:233-235
10. North BJ, Sinclair DA. The intersection between aging and cardiovascular disease. *Circulation research*. 2012;110:1097-1108
11. Kovacic JC, Moreno P, Hachinski V, Nabel EG, Fuster V. Cellular senescence, vascular disease, and aging: Part 1 of a 2-part review. *Circulation*. 2011;123:1650-1660
12. Lacolley P, Regnault V, Segers P, Laurent S. Vascular smooth muscle cells and arterial stiffening: Relevance in development, aging, and disease. *Physiological reviews*. 2017;97:1555-1617
13. Cheung C, Bernardo AS, Trotter MW, Pedersen RA, Sinha S. Generation of human vascular smooth muscle subtypes provides insight into embryological origin-dependent disease susceptibility. *Nature biotechnology*. 2012;30:165-173
14. Chamley-Campbell J, Campbell GR, Ross R. The smooth muscle cell in culture. *Physiological reviews*. 1979;59:1-61
15. Majesky MW. Developmental basis of vascular smooth muscle diversity. *Arteriosclerosis, thrombosis, and vascular biology*. 2007;27:1248-1258
16. Moskalev AA, Shaposhnikov MV, Plyusnina EN, Zhavoronkov A, Budovsky A, Yanai H, Fraifeld VE. The role of DNA damage and repair in aging through the prism of koch-like criteria. *Ageing research reviews*. 2013;12:661-684
17. Lieber MR. The mechanism of double-strand DNA break repair by the nonhomologous DNA end-joining pathway. *Annual review of biochemistry*. 2010;79:181-211

18. Chang HHY, Pannunzio NR, Adachi N, Lieber MR. Non-homologous DNA end joining and alternative pathways to double-strand break repair. *Nature reviews. Molecular cell biology*. 2017;18:495-506
19. Meek K, Dang V, Lees-Miller SP. DNA-pk: The means to justify the ends? *Advances in immunology*. 2008;99:33-58
20. Bebenek K, Pedersen LC, Kunkel TA. Structure-function studies of DNA polymerase lambda. *Biochemistry*. 2014;53:2781-2792
21. Lieber MR, Ma Y, Pannicke U, Schwarz K. The mechanism of vertebrate nonhomologous DNA end joining and its role in v(d)j recombination. *DNA repair*. 2004;3:817-826
22. Lord CJ, Ashworth A. The DNA damage response and cancer therapy. *Nature*. 2012;481:287-294
23. Linnane AW, Marzuki S, Ozawa T, Tanaka M. Mitochondrial DNA mutations as an important contributor to ageing and degenerative diseases. *Lancet*. 1989;1:642-645
24. Dechat T, Pfleghaar K, Sengupta K, Shimi T, Shumaker DK, Solimando L, Goldman RD. Nuclear lamins: Major factors in the structural organization and function of the nucleus and chromatin. *Genes & development*. 2008;22:832-853
25. Blackburn EH, Greider CW, Szostak JW. Telomeres and telomerase: The path from maize, tetrahymena and yeast to human cancer and aging. *Nature medicine*. 2006;12:1133-1138
26. Hayflick L, Moorhead PS. The serial cultivation of human diploid cell strains. *Experimental cell research*. 1961;25:585-621
27. Bodnar AG, Ouellette M, Frolkis M, Holt SE, Chiu CP, Morin GB, Harley CB, Shay JW, Lichtsteiner S, Wright WE. Extension of life-span by introduction of telomerase into normal human cells. *Science*. 1998;279:349-352
28. Jaskelioff M, Muller FL, Paik JH, Thomas E, Jiang S, Adams AC, Sahin E, Kost-Alimova M, Protopopov A, Cadinanos J, Horner JW, Maratos-Flier E, Depinho RA. Telomerase reactivation reverses tissue degeneration in aged telomerase-deficient mice. *Nature*. 2011;469:102-106
29. Bernardes de Jesus B, Vera E, Schneeberger K, Tejera AM, Ayuso E, Bosch F, Blasco MA. Telomerase gene therapy in adult and old mice delays aging and increases longevity without increasing cancer. *EMBO molecular medicine*. 2012;4:691-704
30. Palm W, de Lange T. How shelterin protects mammalian telomeres. *Annual review of genetics*. 2008;42:301-334
31. Talens RP, Christensen K, Putter H, Willemsen G, Christiansen L, Kremer D, Suchiman HE, Slagboom PE, Boomsma DI, Heijmans BT. Epigenetic variation during the adult lifespan: Cross-sectional and longitudinal data on monozygotic twin pairs. *Aging cell*. 2012;11:694-703
32. Fraga MF, Esteller M. Epigenetics and aging: The targets and the marks. *Trends in genetics : TIG*. 2007;23:413-418
33. Maegawa S, Hinkal G, Kim HS, Shen L, Zhang L, Zhang J, Zhang N, Liang S, Donehower LA, Issa JP. Widespread and tissue specific age-related DNA methylation changes in mice. *Genome research*. 2010;20:332-340
34. Oberdoerffer P, Sinclair DA. The role of nuclear architecture in genomic instability and ageing. *Nature reviews. Molecular cell biology*. 2007;8:692-702
35. Rando TA, Chang HY. Aging, rejuvenation, and epigenetic reprogramming: Resetting the aging clock. *Cell*. 2012;148:46-57
36. Powers ET, Morimoto RI, Dillin A, Kelly JW, Balch WE. Biological and chemical approaches to diseases of proteostasis deficiency. *Annual review of biochemistry*. 2009;78:959-991

37. Hartl FU, Bracher A, Hayer-Hartl M. Molecular chaperones in protein folding and proteostasis. *Nature*. 2011;475:324-332
38. Koga H, Kaushik S, Cuervo AM. Protein homeostasis and aging: The importance of exquisite quality control. *Ageing research reviews*. 2011;10:205-215
39. Chiang WC, Ching TT, Lee HC, Mousigian C, Hsu AL. Hsf-1 regulators ddl-1/2 link insulin-like signaling to heat-shock responses and modulation of longevity. *Cell*. 2012;148:322-334
40. Hekimi S, Lapointe J, Wen Y. Taking a "good" look at free radicals in the aging process. *Trends in cell biology*. 2011;21:569-576
41. Doonan R, McElwee JJ, Matthijssens F, Walker GA, Houthoofd K, Back P, Matscheski A, Vanfleteren JR, Gems D. Against the oxidative damage theory of aging: Superoxide dismutases protect against oxidative stress but have little or no effect on life span in caenorhabditis elegans. *Genes & development*. 2008;22:3236-3241
42. Edgar D, Trifunovic A. The mtdna mutator mouse: Dissecting mitochondrial involvement in aging. *Aging*. 2009;1:1028-1032
43. Qiu X, Brown K, Hirschey MD, Verdin E, Chen D. Calorie restriction reduces oxidative stress by sirt3-mediated sod2 activation. *Cell metabolism*. 2010;12:662-667
44. Wang YC, Lee CM, Lee LC, Tung LC, Hsieh-Li HM, Lee-Chen GJ, Su MT. Mitochondrial dysfunction and oxidative stress contribute to the pathogenesis of spinocerebellar ataxia type 12 (sca12). *The Journal of biological chemistry*. 2011;286:21742-21754
45. Shaw RL, Kohlmaier A, Polesello C, Veelken C, Edgar BA, Tapon N. The hippo pathway regulates intestinal stem cell proliferation during drosophila adult midgut regeneration. *Development*. 2010;137:4147-4158
46. Chen C, Liu Y, Zheng P. Mtor regulation and therapeutic rejuvenation of aging hematopoietic stem cells. *Science signaling*. 2009;2:ra75
47. Salminen A, Kaarniranta K, Kauppinen A. Inflammaging: Disturbed interplay between autophagy and inflammasomes. *Aging*. 2012;4:166-175
48. Deeks SG. Hiv infection, inflammation, immunosenescence, and aging. *Annual review of medicine*. 2011;62:141-155
49. Coppe JP, Desprez PY, Krtolica A, Campisi J. The senescence-associated secretory phenotype: The dark side of tumor suppression. *Annual review of pathology*. 2010;5:99-118
50. Kuilman T, Michaloglou C, Vredeveld LC, Douma S, van Doorn R, Desmet CJ, Aarden LA, Mooi WJ, Peeper DS. Oncogene-induced senescence relayed by an interleukin-dependent inflammatory network. *Cell*. 2008;133:1019-1031
51. Coppe JP, Patil CK, Rodier F, Sun Y, Munoz DP, Goldstein J, Nelson PS, Desprez PY, Campisi J. Senescence-associated secretory phenotypes reveal cell-nonautonomous functions of oncogenic ras and the p53 tumor suppressor. *PLoS biology*. 2008;6:2853-2868
52. Rodier F, Coppe JP, Patil CK, Hoeijmakers WA, Munoz DP, Raza SR, Freund A, Campeau E, Davalos AR, Campisi J. Persistent DNA damage signalling triggers senescence-associated inflammatory cytokine secretion. *Nature cell biology*. 2009;11:973-979
53. Hayflick L. The limited in vitro lifetime of human diploid cell strains. *Experimental cell research*. 1965;37:614-636
54. Campisi J. Cellular senescence as a tumor-suppressor mechanism. *Trends in cell biology*. 2001;11:S27-31

55. Campisi J. Senescent cells, tumor suppression, and organismal aging: Good citizens, bad neighbors. *Cell*. 2005;120:513-522
56. Kirkwood TB, Austad SN. Why do we age? *Nature*. 2000;408:233-238
57. Campisi J, d'Adda di Fagagna F. Cellular senescence: When bad things happen to good cells. *Nature reviews. Molecular cell biology*. 2007;8:729-740
58. Zhang H, Pan KH, Cohen SN. Senescence-specific gene expression fingerprints reveal cell-type-dependent physical clustering of up-regulated chromosomal loci. *Proceedings of the National Academy of Sciences of the United States of America*. 2003;100:3251-3256
59. Wada T, Joza N, Cheng HY, Sasaki T, Kozieradzki I, Bachmaier K, Katada T, Schreiber M, Wagner EF, Nishina H, Penninger JM. Mkk7 couples stress signalling to g2/m cell-cycle progression and cellular senescence. *Nature cell biology*. 2004;6:215-226
60. Roninson IB. Tumor cell senescence in cancer treatment. *Cancer research*. 2003;63:2705-2715
61. Green DR, Evan GI. A matter of life and death. *Cancer cell*. 2002;1:19-30
62. Hampel B, Malisan F, Niederegger H, Testi R, Jansen-Durr P. Differential regulation of apoptotic cell death in senescent human cells. *Experimental gerontology*. 2004;39:1713-1721
63. Rebbaa A, Zheng X, Chou PM, Mirkin BL. Caspase inhibition switches doxorubicin-induced apoptosis to senescence. *Oncogene*. 2003;22:2805-2811
64. Dimri GP, Lee X, Basile G, Acosta M, Scott G, Roskelley C, Medrano EE, Linskens M, Rubelj I, Pereira-Smith O, et al. A biomarker that identifies senescent human cells in culture and in aging skin in vivo. *Proceedings of the National Academy of Sciences of the United States of America*. 1995;92:9363-9367
65. Lee BY, Han JA, Im JS, Morrone A, Johung K, Goodwin EC, Kleijer WJ, DiMaio D, Hwang ES. Senescence-associated beta-galactosidase is lysosomal beta-galactosidase. *Aging cell*. 2006;5:187-195
66. Narita M, Nunez S, Heard E, Lin AW, Hearn SA, Spector DL, Hannon GJ, Lowe SW. Rb-mediated heterochromatin formation and silencing of e2f target genes during cellular senescence. *Cell*. 2003;113:703-716
67. Sherr CJ, McCormick F. The rb and p53 pathways in cancer. *Cancer cell*. 2002;2:103-112
68. Jacobs JJ, de Lange T. Significant role for p16ink4a in p53-independent telomere-directed senescence. *Current biology : CB*. 2004;14:2302-2308
69. Smogorzewska A, de Lange T. Different telomere damage signaling pathways in human and mouse cells. *The EMBO journal*. 2002;21:4338-4348
70. Di Micco R, Fumagalli M, Cicalese A, Piccinin S, Gasparini P, Luise C, Schurra C, Garre M, Nuciforo PG, Bensimon A, Maestro R, Pelicci PG, d'Adda di Fagagna F. Oncogene-induced senescence is a DNA damage response triggered by DNA hyper-replication. *Nature*. 2006;444:638-642
71. Beausejour CM, Krtolica A, Galimi F, Narita M, Lowe SW, Yaswen P, Campisi J. Reversal of human cellular senescence: Roles of the p53 and p16 pathways. *The EMBO journal*. 2003;22:4212-4222
72. Zeggini E. A new era for type 2 diabetes genetics. *Diabetic medicine : a journal of the British Diabetic Association*. 2007;24:1181-1186
73. Bianchessi V, Badi I, Bertolotti M, Nigro P, D'Alessandra Y, Capogrossi MC, Zanobini M, Pompilio G, Raucci A, Lauri A. The mitochondrial lncrna asncmtrna-2 is induced in aging and replicative senescence in endothelial cells. *Journal of molecular and cellular cardiology*. 2015;81:62-70

74. Badi I, Mancinelli L, Polizzotto A, Ferri D, Zeni F, Burba I, Milano G, Brambilla F, Saccu C, Bianchi ME, Pompilio G, Capogrossi MC, Raucci A. Mir-34a promotes vascular smooth muscle cell calcification by downregulating sirt1 (sirtuin 1) and axl (axl receptor tyrosine kinase). *Arteriosclerosis, thrombosis, and vascular biology*. 2018;38:2079-2090
75. Bochaton-Piallat ML, Gabbiani F, Ropraz P, Gabbiani G. Age influences the replicative activity and the differentiation features of cultured rat aortic smooth muscle cell populations and clones. *Arteriosclerosis and thrombosis : a journal of vascular biology*. 1993;13:1449-1455
76. Torella D, Leosco D, Indolfi C, Curcio A, Coppola C, Ellison GM, Russo VG, Torella M, Li Volti G, Rengo F, Chiariello M. Aging exacerbates negative remodeling and impairs endothelial regeneration after balloon injury. *American journal of physiology. Heart and circulatory physiology*. 2004;287:H2850-2860
77. Schwartz SM, Campbell GR, Campbell JH. Replication of smooth muscle cells in vascular disease. *Circulation research*. 1986;58:427-444
78. Spinetti G, Wang M, Monticone R, Zhang J, Zhao D, Lakatta EG. Rat aortic mcp-1 and its receptor ccr2 increase with age and alter vascular smooth muscle cell function. *Arteriosclerosis, thrombosis, and vascular biology*. 2004;24:1397-1402
79. Wang M, Spinetti G, Monticone RE, Zhang J, Wu J, Jiang L, Khazan B, Telljohann R, Lakatta EG. A local proinflammatory signalling loop facilitates adverse age-associated arterial remodeling. *PloS one*. 2011;6:e16653
80. Moon SK, Thompson LJ, Madamanchi N, Ballinger S, Papaconstantinou J, Horaist C, Runge MS, Patterson C. Aging, oxidative responses, and proliferative capacity in cultured mouse aortic smooth muscle cells. *American journal of physiology. Heart and circulatory physiology*. 2001;280:H2779-2788
81. Duca L, Blaise S, Romier B, Laffargue M, Gayral S, El Btaouri H, Kawecki C, Guillot A, Martiny L, Debelle L, Maurice P. Matrix ageing and vascular impacts: Focus on elastin fragmentation. *Cardiovascular research*. 2016;110:298-308
82. Schlieper G, Schurgers L, Brandenburg V, Reutelingsperger C, Floege J. Vascular calcification in chronic kidney disease: An update. *Nephrology, dialysis, transplantation : official publication of the European Dialysis and Transplant Association - European Renal Association*. 2016;31:31-39
83. Bostrom K, Watson KE, Horn S, Wortham C, Herman IM, Demer LL. Bone morphogenetic protein expression in human atherosclerotic lesions. *The Journal of clinical investigation*. 1993;91:1800-1809
84. Alique M, Ruiz-Torres MP, Bodega G, Noci MV, Troyano N, Bohorquez L, Luna C, Luque R, Carmona A, Carracedo J, Ramirez R. Microvesicles from the plasma of elderly subjects and from senescent endothelial cells promote vascular calcification. *Aging*. 2017;9:778-789
85. Virmani R, Kolodgie FD, Burke AP, Farb A, Schwartz SM. Lessons from sudden coronary death: A comprehensive morphological classification scheme for atherosclerotic lesions. *Arteriosclerosis, thrombosis, and vascular biology*. 2000;20:1262-1275
86. Lanzer P, Boehm M, Sorribas V, Thiriet M, Janzen J, Zeller T, St Hilaire C, Shanahan C. Medial vascular calcification revisited: Review and perspectives. *European heart journal*. 2014;35:1515-1525
87. Epstein M. Aging and the kidney. *Journal of the American Society of Nephrology : JASN*. 1996;7:1106-1122
88. Zhou XJ, Rakheja D, Yu X, Saxena R, Vaziri ND, Silva FG. The aging kidney. *Kidney international*. 2008;74:710-720

89. Proudfoot D, Skepper JN, Hegyi L, Bennett MR, Shanahan CM, Weissberg PL. Apoptosis regulates human vascular calcification in vitro: Evidence for initiation of vascular calcification by apoptotic bodies. *Circulation research*. 2000;87:1055-1062
90. Luo G, Ducy P, McKee MD, Pinero GJ, Loyer E, Behringer RR, Karsenty G. Spontaneous calcification of arteries and cartilage in mice lacking matrix gla protein. *Nature*. 1997;386:78-81
91. Schafer C, Heiss A, Schwarz A, Westenfeld R, Ketteler M, Floege J, Muller-Esterl W, Schinke T, Jahnen-Dechent W. The serum protein alpha 2-heremans-schmid glycoprotein/fetuin-a is a systemically acting inhibitor of ectopic calcification. *The Journal of clinical investigation*. 2003;112:357-366
92. Bucay N, Sarosi I, Dunstan CR, Morony S, Tarpley J, Capparelli C, Scully S, Tan HL, Xu W, Lacey DL, Boyle WJ, Simonet WS. Osteoprotegerin-deficient mice develop early onset osteoporosis and arterial calcification. *Genes & development*. 1998;12:1260-1268
93. Reynolds JL, Skepper JN, McNair R, Kasama T, Gupta K, Weissberg PL, Jahnen-Dechent W, Shanahan CM. Multifunctional roles for serum protein fetuin-a in inhibition of human vascular smooth muscle cell calcification. *Journal of the American Society of Nephrology : JASN*. 2005;16:2920-2930
94. Scatena M, Liaw L, Giachelli CM. Osteopontin: A multifunctional molecule regulating chronic inflammation and vascular disease. *Arteriosclerosis, thrombosis, and vascular biology*. 2007;27:2302-2309
95. Speer MY, McKee MD, Guldberg RE, Liaw L, Yang HY, Tung E, Karsenty G, Giachelli CM. Inactivation of the osteopontin gene enhances vascular calcification of matrix gla protein-deficient mice: Evidence for osteopontin as an inducible inhibitor of vascular calcification in vivo. *The Journal of experimental medicine*. 2002;196:1047-1055
96. Jono S, Peinado C, Giachelli CM. Phosphorylation of osteopontin is required for inhibition of vascular smooth muscle cell calcification. *The Journal of biological chemistry*. 2000;275:20197-20203
97. Lacey DL, Timms E, Tan HL, Kelley MJ, Dunstan CR, Burgess T, Elliott R, Colombero A, Elliott G, Scully S, Hsu H, Sullivan J, Hawkins N, Davy E, Capparelli C, Eli A, Qian YX, Kaufman S, Sarosi I, Shalhoub V, Senaldi G, Guo J, Delaney J, Boyle WJ. Osteoprotegerin ligand is a cytokine that regulates osteoclast differentiation and activation. *Cell*. 1998;93:165-176
98. Schneeweis LA, Willard D, Milla ME. Functional dissection of osteoprotegerin and its interaction with receptor activator of nf-kappab ligand. *The Journal of biological chemistry*. 2005;280:41155-41164
99. Bennett BJ, Scatena M, Kirk EA, Rattazzi M, Varon RM, Averill M, Schwartz SM, Giachelli CM, Rosenfeld ME. Osteoprotegerin inactivation accelerates advanced atherosclerotic lesion progression and calcification in older apoe-/- mice. *Arteriosclerosis, thrombosis, and vascular biology*. 2006;26:2117-2124
100. Jia J, Zhou H, Zeng X, Feng S. Estrogen stimulates osteoprotegerin expression via the suppression of mir-145 expression in mg-63 cells. *Molecular medicine reports*. 2017;15:1539-1546
101. Harmey D, Hessle L, Narisawa S, Johnson KA, Terkeltaub R, Millan JL. Concerted regulation of inorganic pyrophosphate and osteopontin by akp2, enpp1, and ank: An integrated model of the pathogenesis of mineralization disorders. *The American journal of pathology*. 2004;164:1199-1209

102. Johnson K, Polewski M, van Etten D, Terkeltaub R. Chondrogenesis mediated by ppi depletion promotes spontaneous aortic calcification in npp1-/- mice. *Arteriosclerosis, thrombosis, and vascular biology*. 2005;25:686-691
103. St Hilaire C, Ziegler SG, Markello TC, Brusco A, Groden C, Gill F, Carlson-Donohoe H, Lederman RJ, Chen MY, Yang D, Siegenthaler MP, Arduino C, Mancini C, Freudenthal B, Stanescu HC, Zdebik AA, Chaganti RK, Nussbaum RL, Kleta R, Gahl WA, Boehm M. Nt5e mutations and arterial calcifications. *The New England journal of medicine*. 2011;364:432-442
104. Bostrom KI, Rajamannan NM, Towler DA. The regulation of valvular and vascular sclerosis by osteogenic morphogens. *Circulation research*. 2011;109:564-577
105. Komori T. Regulation of osteoblast differentiation by transcription factors. *Journal of cellular biochemistry*. 2006;99:1233-1239
106. Lian JB, Stein GS, Javed A, van Wijnen AJ, Stein JL, Montecino M, Hassan MQ, Gaur T, Lengner CJ, Young DW. Networks and hubs for the transcriptional control of osteoblastogenesis. *Reviews in endocrine & metabolic disorders*. 2006;7:1-16
107. Nakashima K, Zhou X, Kunkel G, Zhang Z, Deng JM, Behringer RR, de Crombrugghe B. The novel zinc finger-containing transcription factor osterix is required for osteoblast differentiation and bone formation. *Cell*. 2002;108:17-29
108. Speer MY, Yang HY, Brabb T, Leaf E, Look A, Lin WL, Frutkin A, Dichek D, Giachelli CM. Smooth muscle cells give rise to osteochondrogenic precursors and chondrocytes in calcifying arteries. *Circulation research*. 2009;104:733-741
109. Liu Y, Drozdov I, Shroff R, Beltran LE, Shanahan CM. Prelamin a accelerates vascular calcification via activation of the DNA damage response and senescence-associated secretory phenotype in vascular smooth muscle cells. *Circulation research*. 2013;112:e99-109
110. Goodwin GH, Sanders C, Johns EW. A new group of chromatin-associated proteins with a high content of acidic and basic amino acids. *Eur J Biochem*. 1973;38:14-19
111. Hock R, Furusawa T, Ueda T, Bustin M. Hmg chromosomal proteins in development and disease. *Trends in cell biology*. 2007;17:72-79
112. Sessa L, Bianchi ME. The evolution of high mobility group box (hmgb) chromatin proteins in multicellular animals. *Gene*. 2007;387:133-140
113. Bianchi ME, Agresti A. Hmg proteins: Dynamic players in gene regulation and differentiation. *Current opinion in genetics & development*. 2005;15:496-506
114. Tang D, Kang R, Livesey KM, Cheh CW, Farkas A, Loughran P, Hoppe G, Bianchi ME, Tracey KJ, Zeh HJ, 3rd, Lotze MT. Endogenous hmgb1 regulates autophagy. *The Journal of cell biology*. 2010;190:881-892
115. Harris HE, Raucci A. Alarmin(g) news about danger: Workshop on innate danger signals and hmgb1. *EMBO Rep*. 2006;7:774-778
116. Raucci A, Di Maggio S, Scavello F, D'Ambrosio A, Bianchi ME, Capogrossi MC. The janus face of hmgb1 in heart disease: A necessary update. *Cellular and molecular life sciences : CMLS*. 2019;76:211-229
117. Andersson U, Tracey KJ. Hmgb1 is a therapeutic target for sterile inflammation and infection. *Annual review of immunology*. 2011;29:139-162
118. Venereau E, Casalgrandi M, Schiraldi M, Antoine DJ, Cattaneo A, De Marchis F, Liu J, Antonelli A, Preti A, Raeli L, Shams SS, Yang H, Varani L, Andersson U, Tracey KJ, Bachi A, Uguccioni M, Bianchi ME. Mutually exclusive redox forms of hmgb1 promote cell recruitment or proinflammatory cytokine release. *The Journal of experimental medicine*. 2012;209:1519-1528

119. Calogero S, Grassi F, Aguzzi A, Voigtlander T, Ferrier P, Ferrari S, Bianchi ME. The lack of chromosomal protein hmg1 does not disrupt cell growth but causes lethal hypoglycaemia in newborn mice. *Nat Genet*. 1999;22:276-280
120. Agresti A, Bianchi ME. Hmgb proteins and gene expression. *Current opinion in genetics & development*. 2003;13:170-178
121. Iacomino G, Picariello G, Sbrana F, Raiteri R, D'Agostino L. DNA-hmgb1 interaction: The nuclear aggregates of polyamine mediation. *Biochimica et biophysica acta*. 2016;1864:1402-1410
122. Scaffidi P, Misteli T, Bianchi ME. Release of chromatin protein hmgb1 by necrotic cells triggers inflammation. *Nature*. 2002;418:191-195
123. Celona B, Weiner A, Di Felice F, Mancuso FM, Cesarini E, Rossi RL, Gregory L, Baban D, Rossetti G, Grianti P, Pagani M, Bonaldi T, Ragoussis J, Friedman N, Camilloni G, Bianchi ME, Agresti A. Substantial histone reduction modulates genomewide nucleosomal occupancy and global transcriptional output. *PLoS biology*. 2011;9:e1001086
124. Hu Z, Chen K, Xia Z, Chavez M, Pal S, Seol JH, Chen CC, Li W, Tyler JK. Nucleosome loss leads to global transcriptional up-regulation and genomic instability during yeast aging. *Genes & development*. 2014;28:396-408
125. De Toma I, Rossetti G, Zambrano S, Bianchi ME, Agresti A. Nucleosome loss facilitates the chemotactic response of macrophages. *J Intern Med*. 2014;276:454-469
126. Bonaldi T, Talamo F, Scaffidi P, Ferrera D, Porto A, Bachi A, Rubartelli A, Agresti A, Bianchi ME. Monocytic cells hyperacetylate chromatin protein hmgb1 to redirect it towards secretion. *The EMBO journal*. 2003;22:5551-5560
127. Lotze MT, Tracey KJ. High-mobility group box 1 protein (hmgb1): Nuclear weapon in the immune arsenal. *Nature reviews. Immunology*. 2005;5:331-342
128. Little AJ, Corbett E, Ortega F, Schatz DG. Cooperative recruitment of hmgb1 during v(d)j recombination through interactions with rag1 and DNA. *Nucleic acids research*. 2013;41:3289-3301
129. Stros M, Ozaki T, Bacikova A, Kageyama H, Nakagawara A. Hmgb1 and hmgb2 cell-specifically down-regulate the p53- and p73-dependent sequence-specific transactivation from the human bax gene promoter. *The Journal of biological chemistry*. 2002;277:7157-7164
130. Thomas JO, Stott K. H1 and hmgb1: Modulators of chromatin structure. *Biochemical Society transactions*. 2012;40:341-346
131. Polanska E, Pospisilova S, Stros M. Binding of histone h1 to DNA is differentially modulated by redox state of hmgb1. *PloS one*. 2014;9:e89070
132. Wang H, Bloom O, Zhang M, Vishnubhakat JM, Ombrellino M, Che J, Frazier A, Yang H, Ivanova S, Borovikova L, Manogue KR, Faist E, Abraham E, Andersson J, Andersson U, Molina PE, Abumrad NN, Sama A, Tracey KJ. Hmg-1 as a late mediator of endotoxin lethality in mice. *Science*. 1999;285:248-251
133. Bianchi ME, Manfredi AA. High-mobility group box 1 (hmgb1) protein at the crossroads between innate and adaptive immunity. *Immunol Rev*. 2007;220:35-46
134. Treutiger CJ, Mullins GE, Johansson AS, Rouhiainen A, Rauvala HM, Erlandsson-Harris H, Andersson U, Yang H, Tracey KJ, Andersson J, Palmblad JE. High mobility group 1 b-box mediates activation of human endothelium. *J Intern Med*. 2003;254:375-385
135. Andrassy M, Volz HC, Igwe JC, Funke B, Eichberger SN, Kaya Z, Buss S, Autschbach F, Pleger ST, Lukic IK, Bea F, Hardt SE, Humpert PM, Bianchi ME, Mairbaurl H, Nawroth PP, Remppis A, Katus HA, Bierhaus A. High-mobility group box-1 in ischemia-reperfusion injury of the heart. *Circulation*. 2008;117:3216-3226

136. Wang WK, Lu QH, Zhang JN, Wang B, Liu XJ, An FS, Qin WD, Chen XY, Dong WQ, Zhang C, Zhang Y, Zhang MX. Hmgb1 mediates hyperglycaemia-induced cardiomyocyte apoptosis via erk/ets-1 signalling pathway. *J Cell Mol Med*. 2014;18:2311-2320
137. Ulloa L, Batliwalla FM, Andersson U, Gregersen PK, Tracey KJ. High mobility group box chromosomal protein 1 as a nuclear protein, cytokine, and potential therapeutic target in arthritis. *Arthritis Rheum*. 2003;48:876-881
138. Maroso M, Balosso S, Ravizza T, Liu J, Aronica E, Iyer AM, Rossetti C, Molteni M, Casalgrandi M, Manfredi AA, Bianchi ME, Vezzani A. Toll-like receptor 4 and high-mobility group box-1 are involved in ictogenesis and can be targeted to reduce seizures. *Nature medicine*. 2010;16:413-419
139. Yang H, Lundback P, Ottosson L, Erlandsson-Harris H, Venereau E, Bianchi ME, Al-Abed Y, Andersson U, Tracey KJ, Antoine DJ. Redox modification of cysteine residues regulates the cytokine activity of high mobility group box-1 (hmgb1). *Mol Med*. 2012;18:250-259
140. Tsung A, Tohme S, Billiar TR. High-mobility group box-1 in sterile inflammation. *J Intern Med*. 2014;276:425-443
141. Fritz G. Rage: A single receptor fits multiple ligands. *Trends Biochem Sci*. 2011;36:625-632
142. Kang R, Chen R, Zhang Q, Hou W, Wu S, Cao L, Huang J, Yu Y, Fan XG, Yan Z, Sun X, Wang H, Wang Q, Tsung A, Billiar TR, Zeh HJ, 3rd, Lotze MT, Tang D. Hmgb1 in health and disease. *Mol Aspects Med*. 2014;40:1-116
143. Tirone M, Tran NL, Ceriotti C, Gorzanelli A, Canepari M, Bottinelli R, Raucci A, Di Maggio S, Santiago C, Mellado M, Saclier M, Francois S, Careccia G, He M, De Marchis F, Conti V, Ben Larbi S, Cuvellier S, Casalgrandi M, Preti A, Chazaud B, Al-Abed Y, Messina G, Sitia G, Brunelli S, Bianchi ME, Venereau E. High mobility group box 1 orchestrates tissue regeneration via cxcr4. *The Journal of experimental medicine*. 2018;215:303-318
144. Leifer CA, Medvedev AE. Molecular mechanisms of regulation of toll-like receptor signaling. *J Leukoc Biol*. 2016;100:927-941
145. Park JS, Svetkauskaite D, He Q, Kim JY, Strassheim D, Ishizaka A, Abraham E. Involvement of toll-like receptors 2 and 4 in cellular activation by high mobility group box 1 protein. *The Journal of biological chemistry*. 2004;279:7370-7377
146. Conti L, Lanzardo S, Arigoni M, Antonazzo R, Radaelli E, Cantarella D, Calogero RA, Cavallo F. The noninflammatory role of high mobility group box 1/toll-like receptor 2 axis in the self-renewal of mammary cancer stem cells. *FASEB journal : official publication of the Federation of American Societies for Experimental Biology*. 2013;27:4731-4744
147. Hummel S, Van Aken H, Zarbock A. Inhibitors of cxc chemokine receptor type 4: Putative therapeutic approaches in inflammatory diseases. *Curr Opin Hematol*. 2014;21:29-36
148. Davalos AR, Kawahara M, Malhotra GK, Schaum N, Huang J, Ved U, Beausejour CM, Coppe JP, Rodier F, Campisi J. P53-dependent release of alarmin hmgb1 is a central mediator of senescent phenotypes. *The Journal of cell biology*. 2013;201:613-629
149. Lee JJ, Park IH, Rhee WJ, Kim HS, Shin JS. Hmgb1 modulates the balance between senescence and apoptosis in response to genotoxic stress. *FASEB journal : official publication of the Federation of American Societies for Experimental Biology*. 2019;33:10942-10953

150. Ji J, Fu T, Dong C, Zhu W, Yang J, Kong X, Zhang Z, Bao Y, Zhao R, Ge X, Sha X, Lu Z, Li J, Gu Z. Targeting hmgb1 by ethyl pyruvate ameliorates systemic lupus erythematosus and reverses the senescent phenotype of bone marrow-mesenchymal stem cells. *Aging*. 2019;11:4338-4353
151. Fang T, Li Y, Peng Z, Zhang Z, Chen F. [role of high mobility group protein b1 in il-1alpha-induced endothelial cell senescence]. *Zhong nan da xue xue bao. Yi xue ban = Journal of Central South University. Medical sciences*. 2017;42:1361-1366
152. Zirkel A, Nikolic M, Sofiadis K, Mallm JP, Brackley CA, Gothe H, Drechsel O, Becker C, Altmuller J, Josipovic N, Georgomanolis T, Brant L, Franzen J, Koker M, Gusmao EG, Costa IG, Ullrich RT, Wagner W, Roukos V, Nurnberg P, Marenduzzo D, Rippe K, Papantonis A. Hmgb2 loss upon senescence entry disrupts genomic organization and induces ctcf clustering across cell types. *Molecular cell*. 2018;70:730-744 e736
153. Castello A, Fischer B, Frese CK, Horos R, Alleaume AM, Foehr S, Curk T, Krijgsveld J, Hentze MW. Comprehensive identification of rna-binding domains in human cells. *Molecular cell*. 2016;63:696-710
154. Mohammad G, Alam K, Nawaz MI, Siddiquei MM, Mousa A, Abu El-Asrar AM. Mutual enhancement between high-mobility group box-1 and nadph oxidase-derived reactive oxygen species mediates diabetes-induced upregulation of retinal apoptotic markers. *Journal of physiology and biochemistry*. 2015;71:359-372
155. Yu Y, Tang D, Kang R. Oxidative stress-mediated hmgb1 biology. *Frontiers in physiology*. 2015;6:93
156. Bostrom KI. Where do we stand on vascular calcification? *Vascular pharmacology*. 2016;84:8-14
157. Qi SC, Cui C, Yan YH, Sun GH, Zhu SR. Effects of high-mobility group box 1 on the proliferation and odontoblastic differentiation of human dental pulp cells. *International endodontic journal*. 2013;46:1153-1163
158. Hernanz R, Martinez-Revelles S, Palacios R, Martin A, Cachofeiro V, Aguado A, Garcia-Redondo L, Barrus MT, de Batista PR, Briones AM, Salaices M, Alonso MJ. Toll-like receptor 4 contributes to vascular remodelling and endothelial dysfunction in angiotensin ii-induced hypertension. *British journal of pharmacology*. 2015;172:3159-3176
159. Li FJ, Zhang CL, Luo XJ, Peng J, Yang TL. Involvement of the mir-181b-5p/hmgb1 pathway in ang ii-induced phenotypic transformation of smooth muscle cells in hypertension. *Aging and disease*. 2019;10:231-248
160. Jin X, Rong S, Yuan W, Gu L, Jia J, Wang L, Yu H, Zhuge Y. High mobility group box 1 promotes aortic calcification in chronic kidney disease via the wnt/beta-catenin pathway. *Frontiers in physiology*. 2018;9:665
161. Yang J, Shah R, Robling AG, Templeton E, Yang H, Tracey KJ, Bidwell JP. Hmgb1 is a bone-active cytokine. *Journal of cellular physiology*. 2008;214:730-739
162. Passmore M, Nataatmadja M, Fung YL, Pearse B, Gabriel S, Tesar P, Fraser JF. Osteopontin alters endothelial and valvular interstitial cell behaviour in calcific aortic valve stenosis through hmgb1 regulation. *European journal of cardio-thoracic surgery : official journal of the European Association for Cardio-thoracic Surgery*. 2015;48:e20-29
163. Wang B, Li F, Zhang C, Wei G, Liao P, Dong N. High-mobility group box-1 protein induces osteogenic phenotype changes in aortic valve interstitial cells. *The Journal of thoracic and cardiovascular surgery*. 2016;151:255-262

164. Wang Y, Shan J, Yang W, Zheng H, Xue S. High mobility group box 1 (hmgb1) mediates high-glucose-induced calcification in vascular smooth muscle cells of saphenous veins. *Inflammation*. 2013;36:1592-1604
165. Chen Q, Bei JJ, Liu C, Feng SB, Zhao WB, Zhou Z, Yu ZP, Du XJ, Hu HY. Hmgb1 induces secretion of matrix vesicles by macrophages to enhance ectopic mineralization. *PloS one*. 2016;11:e0156686
166. Zhu X, Messer JS, Wang Y, Lin F, Cham CM, Chang J, Billiar TR, Lotze MT, Boone DL, Chang EB. Cytosolic hmgb1 controls the cellular autophagy/apoptosis checkpoint during inflammation. *The Journal of clinical investigation*. 2015;125:1098-1110
167. Rodier F, Munoz DP, Teachenor R, Chu V, Le O, Bhaumik D, Coppe JP, Campeau E, Beausejour CM, Kim SH, Davalos AR, Campisi J. DNA-scars: Distinct nuclear structures that sustain damage-induced senescence growth arrest and inflammatory cytokine secretion. *Journal of cell science*. 2011;124:68-81
168. Lange SS, Vasquez KM. Hmgb1: The jack-of-all-trades protein is a master DNA repair mechanic. *Molecular carcinogenesis*. 2009;48:571-580
169. Lindahl T. Instability and decay of the primary structure of DNA. *Nature*. 1993;362:709-715
170. Bastos Goncalves F, Voute MT, Hoeks SE, Chonchol MB, Boersma EE, Stolker RJ, Verhagen HJ. Calcification of the abdominal aorta as an independent predictor of cardiovascular events: A meta-analysis. *Heart*. 2012;98:988-994
171. Kang YH, Jin JS, Yi DW, Son SM. Bone morphogenetic protein-7 inhibits vascular calcification induced by high vitamin d in mice. *The Tohoku journal of experimental medicine*. 2010;221:299-307
172. Wiley CD, Velarde MC, Lecot P, Liu S, Sarnoski EA, Freund A, Shirakawa K, Lim HW, Davis SS, Ramanathan A, Gerencser AA, Verdin E, Campisi J. Mitochondrial dysfunction induces senescence with a distinct secretory phenotype. *Cell metabolism*. 2016;23:303-314
173. Biran A, Zada L, Abou Karam P, Vadai E, Roitman L, Ovadya Y, Porat Z, Krizhanovsky V. Quantitative identification of senescent cells in aging and disease. *Aging cell*. 2017;16:661-671
174. Rudijanto A. The role of vascular smooth muscle cells on the pathogenesis of atherosclerosis. *Acta medica Indonesiana*. 2007;39:86-93
175. Sawaki D, Czibik G, Pini M, Ternacle J, Suffee N, Mercedes R, Marcelin G, Surenaud M, Marcos E, Gual P, Clement K, Hue S, Adnot S, Hatem SN, Tsuchimochi I, Yoshimitsu T, Henegar C, Derumeaux G. Visceral adipose tissue drives cardiac aging through modulation of fibroblast senescence by osteopontin production. *Circulation*. 2018;138:809-822
176. Polanska E, Dobsakova Z, Dvorackova M, Fajkus J, Stros M. Hmgb1 gene knockout in mouse embryonic fibroblasts results in reduced telomerase activity and telomere dysfunction. *Chromosoma*. 2012;121:419-431
177. Yusein-Myashkova S, Ugrinova I, Pasheva E. Non-histone protein hmgb1 inhibits the repair of damaged DNA by cisplatin in nih-3t3 murine fibroblasts. *BMB reports*. 2016;49:99-104
178. Bee L, Nasca A, Zanolini A, Cendron F, d'Adamo P, Costa R, Lamperti C, Celotti L, Ghezzi D, Zeviani M. A nonsense mutation of human xrcc4 is associated with adult-onset progressive encephalocardiomyopathy. *EMBO molecular medicine*. 2015;7:918-929
179. Murphy MP. How mitochondria produce reactive oxygen species. *The Biochemical journal*. 2009;417:1-13

180. Dai L, Qureshi AR, Witasp A, Lindholm B, Stenvinkel P. Early vascular ageing and cellular senescence in chronic kidney disease. *Computational and structural biotechnology journal*. 2019;17:721-729

# *List of original manuscripts*

**Badi I, Mancinelli L, Polizzotto A, Ferri D, Zeni F, Burba I, Milano G, Brambilla F, Saccu C, Bianchi ME, Pompilio G, Capogrossi MC, Raucci A** "Mir 34a promotes vascular calcification by downregulating Sirt1 (sirtuin 1) and Axl (Axl receptor tyrosine kinase)". (2018) Arterioscler Thromb Vasc Biol. 2018 Jul 19. doi: 10.1161/ATVBAHA.118.311298. PMID: 30026277.

OPEN

# miR-34a Promotes Vascular Smooth Muscle Cell Calcification by Downregulating SIRT1 (Sirtuin 1) and Axl (AXL Receptor Tyrosine Kinase)

Ileana Badi, Luigi Mancinelli, Andrea Polizzotto, Debora Ferri, Filippo Zeni, Ilaria Burba, Giuseppina Milano, Francesca Brambilla, Claudio Saccu, Marco E. Bianchi, Giulio Pompilio, Maurizio C. Capogrossi, Angela Raucci

***Objective***—Vascular calcification (VC) is age dependent and a risk factor for cardiovascular and all-cause mortality. VC involves the senescence-induced transdifferentiation of vascular smooth muscle cells (SMCs) toward an osteochondrogenic lineage resulting in arterial wall mineralization. miR-34a increases with age in aortas and induces vascular SMC senescence through the modulation of its target SIRT1 (sirtuin 1). In this study, we aimed to investigate whether miR-34a regulates VC.

***Approach and Results***—We found that miR-34a and Runx2 (Runt-related transcription factor 2) expression correlates in young and old mice. *Mir34a*$^{+/+}$ and *Mir34a*$^{-/-}$ mice were treated with vitamin D, and calcium quantification revealed that *Mir34a* deficiency reduces soft tissue and aorta medial calcification and the upregulation of the VC Sox9 (SRY [sex-determining region Y]-box 9) and Runx2 and the senescence p16 and p21 markers. In this model, miR-34a upregulation was transient and preceded aorta mineralization. *Mir34a*$^{-/-}$ SMCs were less prone to undergo senescence and under osteogenic conditions deposited less calcium compared with *Mir34a*$^{+/+}$ cells. Furthermore, unlike in *Mir34a*$^{+/+}$ SMC, the known VC inhibitors SIRT1 and Axl (AXL receptor tyrosine kinase) were only partially downregulated in calcifying *Mir34a*$^{-/-}$ SMC. Strikingly, constitutive miR-34a overexpression to senescence-like levels in human aortic SMCs increased calcium deposition and enhanced Axl and SIRT1 decrease during calcification. Notably, we also showed that miR-34a directly decreased Axl expression in human aortic SMC, and restoration of its levels partially rescued miR-34a-dependent growth arrest.

***Conclusions***—miR-34a promotes VC via vascular SMC mineralization by inhibiting cell proliferation and inducing senescence through direct Axl and SIRT1 downregulation, respectively. This miRNA could be a good therapeutic target for the treatment of VC.

***Visual Overview***—An online visual overview is available for this article. **(*Arterioscler Thromb Vasc Biol*. 2018;38:2079-2090. DOI: 10.1161/ATVBAHA.118.311298.)**

**Key Words:** aging ■ humans ■ mice ■ senescence ■ vascular calcification



Vascular calcification (VC) is an age-related complication of atherosclerosis, type 2 diabetes mellitus, and chronic kidney disease and is characterized by the maladaptive transdifferentiation of vascular smooth muscle cells (VSMCs) toward an osteochondrogenic lineage, which results in hydroxyapatite deposition and eventually mineralization of the arterial wall.[1,2]

Although VC is a risk factor for cardiovascular and all-cause mortality, a therapy is not yet available, mostly because the pathways responsible for the VSMC osteochondrogenic phenotypic shift are still poorly understood.[3]

It has recently emerged that senescence and the acquisition of an inflammatory senescence-associated secretory phenotype increase the propensity of VSMC to experience the osteoblastic transition.[4,5] Remarkably, senescent VSMCs are characterized by the expression of bone-related genes, such as Runx2 (Runt-related transcription factor 2), alkaline phosphatase, and osteocalcin, and secretion of senescence-associated secretory phenotype molecules, such as IL-6 (interleukin 6), BMP2 (bone morphogenetic protein 2), and OPG (osteoprotegerin), that can induce the senescence and osteoblastic phenotype of neighboring VSMCs and local or circulating stem

Received on: January 9, 2018; final version accepted on: July 2, 2018.

From the Experimental Cardio-Oncology and Cardiovascular Aging Unit (I.Ba., L.M., A.P., D.F., F.Z., A.R.), Vascular Biology and Regenerative Medicine Unit (I.Bu., G.M., G.P.), and Vascular and Endovascular Surgery Unit (C.S.), Centro Cardiologico Monzino Istituto di ricovero e cura a carattere scientifico (IRCCS), Milan, Italy; Department of Heart and Vessels, Laboratory of Cardiovascular Research, University Hospital of Lausanne, Switzerland (G.M.); Chromatin Dynamics Unit, San Raffaele University, Milan, Italy (F.B., M.E.B.); and Department of Cardiology, Ochsner Medical Center, New Orleans, LA (M.C.C.).

**The online-only Data Supplement is available with this article at https://www.ahajournals.org/doi/suppl/10.1161/ATVBAHA.118.311298.**

Correspondence to Angela Raucci, PhD, Experimental Cardio-Oncology and Cardiovascular Aging Unit, Centro Cardiologico Monzino IRCCS, Via Carlo Parea 4, 20138 Milan, Italy. Email aruacci@ccfm.it

**Nonstandard Abbreviations and Acronyms**

| | |
|---|---|
| **Axl** | AXL receptor tyrosine kinase |
| **BMP2** | bone morphogenetic protein 2 |
| **CDK** | cyclin-dependent kinase |
| **COMP** | cartilage oligomeric matrix protein |
| **HASMCs** | human aortic smooth muscle cells |
| **IL-6** | interleukin 6 |
| **OPG** | osteoprotegerin |
| **Runx2** | Runt-related transcription factor 2 |
| **SA-βgal** | senescence-associated β-galactosidase |
| **SIRT1** | sirtuin 1 |
| **SMCs** | smooth muscle cells |
| **Sox9** | sex-determining region Y-box 9 |
| **SRY** | sex-determining region Y |
| **VC** | vascular calcification |
| **VSMCs** | vascular smooth muscle cells |
| **vWF** | von Willebrand factor |

cells.[4–9] Accordingly, during aging, the molecular mechanisms that favor VSMC senescence, like prelamin A accumulation[4] and ZMPSTE24[10] and COMP (cartilage oligomeric matrix protein) [11,12] downregulation, promote VSMC osteogenic differentiation as well.

miRNAs are negative post-transcriptional regulators of gene expression and have potential as therapeutic targets.[13] Although they have been implicated in several cardiovascular biological processes, the role of miRNAs in VC is still largely unexplored.[14] miR-34a was firstly described as a tumor suppressor that can regulate cancer cell proliferation, apoptosis, and senescence.[15] Notably, miR-34a plays an important role during the aging process.[16,17] Indeed, its expression increases in different aged organs and tissues,[6,16,18–20] and its genetic ablation or inhibition in mice has been shown to improve cardiac performance and ventricular remodeling in the aged heart.[16] Notably, miR-34a is a senescence-inducer miRNA[21] and can mediate endothelial and endothelial progenitor cell senescence through the modulation of its target—the longevity-associated gene SIRT1 (sirtuin 1).[18,22] We have recently reported that miR-34a is upregulated in aged mouse aortas, promoting VSMC senescence through the direct downregulation of SIRT1 and the expression of a subset of senescence-associated secretory phenotype factors, including the pro-osteogenic molecules BMP2 and IL-6.[6] Interestingly, Takemura et al[5] have demonstrated that SIRT1 acts as a VC inhibitor by counteracting VSMC senescence and their consequent calcification. Notably, miR-34a can regulate other VSMC calcification inhibitors, for instance, the antiapoptotic receptor tyrosine kinase Axl (AXL receptor tyrosine kinase) has been described as a miR-34a target in solid cancer and able to inhibit VSMC calcium deposition in vitro.[23,24]

Given the association among miR-34a, senescence, and calcification, we hypothesized that the age-dependent upregulation of this miRNA may drive the senescence-induced VSMC osteochondroblastic changes and thereby VC. We found that miR-34a deficiency in vivo reduces soft tissue, including aorta, calcification by preventing the expression of the VC markers Sox9 (SRY [sex-determining region Y]-box 9) and Runx2, as well as of the senescence factors p16 and p21. Expression of miR-34a increases before aorta mineralization. Smooth muscle cell (SMC) isolated from *Mir34a*$^{-/-}$ mice shows reduced senescence and calcification and slightly higher expression of SIRT1 and Axl during the mineralization process induced by hyperphosphatemia. Strikingly, miR-34a–overexressing human aortic SMCs (HASMCs) exhibit increased senescence and calcium deposition along with lower levels of SIRT1 and Axl. We also demonstrated that miR-34a directly targets Axl in HASMC and inhibits their proliferation, at least in part, through Axl downregulation.

This study suggests that miR-34a is a promoter of VC, by inducing VSMC growth arrest and senescence via direct Axl and SIRT1 downregulation, respectively. In the future, a therapeutic strategy targeted against miR-34a might be considered for the treatment or prevention of age-associated VC.

## Materials and Methods

The authors declare that all supporting data are available within the article and its online-only Data Supplement.

### Animal Experiments

Animal work was performed in conformity with the guidelines from Directive 2010/63/EU of the European Parliament on the protection of animals used for scientific purposes and in accordance with experimental protocols approved by the University Committee on Animal Resources at the University of Milan (734–2015). Mice were housed in standard cages on a 12:12-hour light-dark cycle and fed a normal chow diet ad libitum. JAX C57BL/6J mice (*Mir34a*$^{+/+}$, wild type) were purchased from Charles River Laboratories International, Inc. (stock No. 000664; Wilmington, MA). *Mir34a*$^{-/-}$ mouse line was already generated[25] and purchased from The Jackson Laboratory (stock No. 018279; Bar Harbor, ME).

Only male mice were included in this study because there are evidences from the literature showing sex differences as the estrogen hormone protects females from VC.[26–28] Twelve-week-old male *Mir34a*$^{-/-}$ and *Mir34a*$^{+/+}$ were treated with either 500 000 IU·kg$^{-1}$·d$^{-1}$ vitamin D (cholecalciferolor, C1357; Sigma-Aldrich, St. Louis, MO) or a mock solution (1% [v/v] ethanol, 7% [v/v] Kolliphor EL, and 3.75% [wt/vol] dextrose, all from Sigma-Aldrich) administrated subcutaneously for 3 consecutive days and euthanized 7 days after the first injection.[29,30] Animals were anesthetized with an intraperitoneal injection of ketamine:medetomidine cocktail (100:10 mg/kg) and perfused with PBS from the apex of the heart. Blood was collected by cardiac puncture; aortas, hearts, lungs, and kidneys were dissected out and processed for aortic medial thickness and cellular density measurement, calcium content quantification, von Kossa staining, and immunohistochemistry as described in the online-only Data Supplement. A semiquantitative calcification score was also determined.[31] Calcification on arterial cross section at 3 different levels for every mouse was scored using the following system: 0, no calcification; 1, focal calcification spots; 2, partial calcification covering 20% to 80% of the arterial circumference; and 3, circumferential calcification.

For the aging experiments, aortas were isolated from C57BL/6J male young (2.5 months old) and old (21 months old) mice and immediately frozen for RNA and protein extraction or paraffin embedded for Alizarin Red staining as described in the online-only Data Supplement.

### Cell Culture

HASMCs were purchased from Lonza (Basel, Switzerland) and cultured in SmGM-2 complete medium (Lonza). The cell donors were white men of 22, 30, and 43 years of age.

Murine SMCs were isolated as already described.[32] Immunofluorescence analyses confirmed that isolated cells express α-smooth muscle actin while were not positive for the endothelial marker vWF (von Willebrand factor; Figure IIIA and IIIB in the online-only Data Supplement).

Cells were transfected and infected as described in the online-only Data Supplement.

### Calcification Assay

Cells were cultured in osteogenic medium (DMEM supplemented with 15% fetal bovine serum, 5 mmol/L phosphate, 10 mmol/L sodium pyruvate, and 50 µg/mL ascorbic acid) for 3 or 7 days. To quantify the precipitated calcium, cells grown in 12-well plates were incubated overnight with 250 µL of 0.6 N HCl at 4°C, and then, supernatants were collected. To extract protein for normalization, cells were incubated overnight at 4°C with 250 µL of 0.1% SDS-0.1 N NaOH lysis buffer. The precipitated calcium was quantified by colorimetric analysis with the QuantiChrom Calcium Assay Kit (DICA-500; Gentaur, Kampenhout, Belgium), whereas the protein concentration was determined with the Bio-Rad protein assay (Bio-Rad Laboratories, Hercules, CA). Cells undergone calcification were also processed for quantitative reverse transcriptase polymerase chain reaction and Western blot analyses as described in the online-only Data Supplement.

### Statistical Analysis

In vitro experiments were performed at least 3×. Data were analyzed with GraphPad Prism software, version 7 (GraphPad Software, Inc, La Jolla, CA). The Shapiro-Wilk test was used to assess the normality of distribution of investigated parameters. Differences between 2 groups were analyzed with unpaired Student *t* test or Mann-Whitney *U* test for normally or not normally distributed variables, respectively, otherwise stated in the figure legends. Statistical analysis between >2 groups was conducted by 1- or 2-way ANOVA with Bonferroni post hoc test, as reported in the figure legends. A value of $P < 0.05$ was considered statistically significant; values are presented as mean±SE.

## Results

### *Mir34a* Genetic Ablation Reduces Soft Tissue and VC In Vivo

We have previously demonstrated that miR-34a levels increase in the aortas of aged mice along with senescence-associated proteins, such as p16 and p21, and that miR-34a induces VSMC senescence.[6] Old aortas also show signs of calcification when compared with young ones (Figure IA and IB in the online-only Data Supplement).[33,34] Hence, as a prerequisite of our study, we correlated the expression of miR-34a and the VC marker Runx2 in aortas of young (2.5 months old) and old (21 months old) mice. Both miR-34a and Runx2 were upregulated in aortas of aged animals, with a positive association (Figure IC through IE in the online-only Data Supplement). Accordingly, Runx2 protein levels increased in old aortas (Figure IF in the online-only Data Supplement).

To evaluate whether miR-34a could play a role in VC, *Mir34a*$^{+/+}$ and *Mir34a*$^{-/-}$ mice were subcutaneously injected for 3 consecutive days with a toxic dose of vitamin D or a mock solution (control [Ctrl]) and euthanized 7 days after the first injection.[29,30] Although *Mir34a*$^{+/+}$ and *Mir34a*$^{-/-}$ animals showed a slightly different body weight before the treatment (Figure IIA in the online-only Data Supplement), weight loss on vitamin D treatment was significantly lower in *Mir34a*$^{-/-}$ than in *Mir34a*$^{+/+}$ mice, indicating a major discomfort in the latter group (Figure 1A). As expected, calcium levels increased in the sera of vitamin D-treated mice when compared with the corresponding control group; interestingly, serum calcium in vitamin D-treated *Mir34a*$^{-/-}$ animals was lower than those in corresponding *Mir34a*$^{+/+}$ mice (Figure 1B). We quantified calcium deposition in soft tissues, including kidneys, lungs, hearts, and aortas. Whereas calcium deposition was negligible in control mice, it significantly raised in vitamin D-treated mice; notably, the genetic ablation of *Mir34a* reduced calcification in all tested organs (Figure 1C).

To investigate VC, we further characterized aortas of these animals. Aortas of *Mir34a*$^{-/-}$ mice showed a basal higher medial thickness and cellular density than *Mir34a*$^{+/+}$ (Figure IIB through IID in the online-only Data Supplement). Then, we assessed calcium deposition by von Kossa staining on aortic sections. In comparison with *Mir34a*$^{+/+}$ animals, fewer *Mir34a*$^{-/-}$ mice accumulated calcium in the medial arterial layer and to a lesser extent after vitamin D administration (Figure 2A through 2C). We also analyzed by immunohistochemistry the expression pattern of 2 well-known VC makers, Runx2 and Sox9,[2,31] as well as of p16 and p21; we observed that only *Mir34a*$^{+/+}$ mice displayed positive staining in VSMC nearby the calcified regions (Figure 2D).

Altogether, our data demonstrate that *Mir34a* deficiency reduces soft tissue and VC induced by an overdose of vitamin D in vivo. In the aorta, *Mir34a* deficiency prevented senescence and transdifferentiation of VSMC.

### miR-34a Is Upregulated in Aortas That Display Features of Senescence Before Overt Calcification

To gain further insight in the role of miR-34a in VC, we determined its expression in aortas and serum of wild-type mice during the mineralization process induced by vitamin D. In the aorta, calcium deposition was detectable at day 5 and was significantly higher at day 7 after the first injection of vitamin D in comparison with the corresponding mice treated with mock solution (Ctrl; Figure 3A). Notably, an induction of miR-34a by vitamin D was already evident at day 3 but soon decreased to the levels of Ctrl at day 5 (Figure 3B). Interestingly, p21 mRNA was markedly upregulated at days 3 and 5 (Figure 3C). No significant differences in circulating miR-34a levels were detected between vitamin D-treated and Ctrl mice at any time point, although a trend to a decrease in its amount was observed during the progression of calcification (Figure 3D).

These results indicate that in vivo vitamin D treatment induces a transient upregulation of miR-34a that is concomitant with p21 induction and precedes overt aortic calcification.

### *Mir34a* Genetic Ablation Decreases SMC Senescence and Calcium Deposition Ex Vivo

To better investigate the possible role of miR-34a in the SMC osteochondrogenic transition, we isolated SMC from *Mir34a*$^{+/+}$ and *Mir34a*$^{-/-}$ mice (Figure IIIA and IIIB in the online-only Data Supplement). In accordance with our previously published data[6] and aorta cell density data (Figure IIB and IID in the online-only Data Supplement), *Mir34a*$^{-/-}$ cells displayed a higher proliferation rate than *Mir34a*$^{+/+}$ cells (Figure IIIC in the online-only Data Supplement);

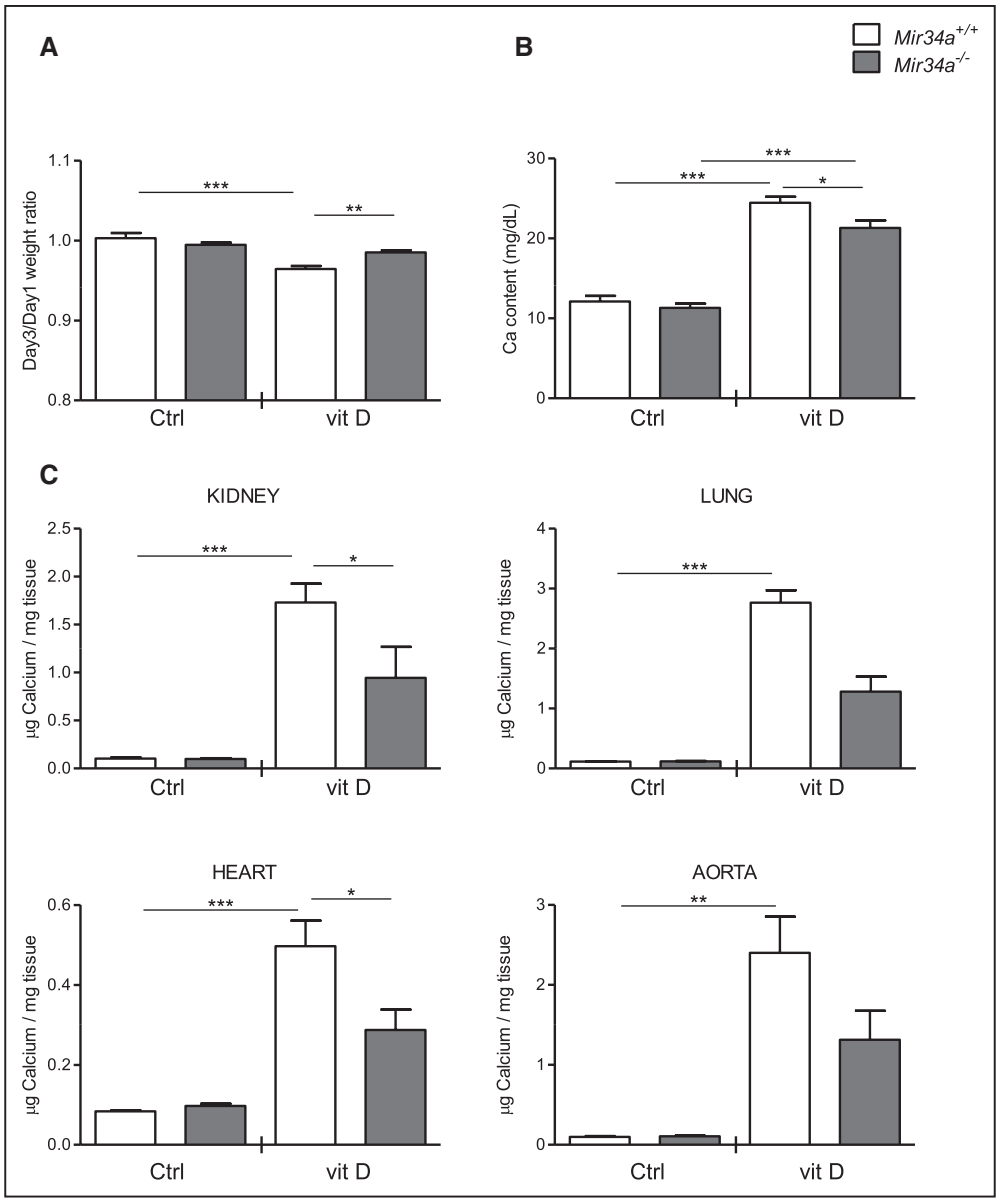


**Figure 1.** *Mir34a* genetic ablation reduces soft tissue calcification. **A**–**C**, Twelve-week-old *Mir34a*$^{-/-}$ and *Mir34a*$^{+/+}$ mice were treated subcutaneously with either vitamin D (vit D) or a mock solution (control [Ctrl]) for 3 consecutive days and euthanized 7 d (day 7) after the first injection. **A**, Mice weight ratio at the third day (day 3) and before the first vit D injection (day 1; n=6, 5, 13, and 8). **B**, Calcium content in the sera at day 7 was quantified by a colorimetric analysis (n=9, 8, 17, and 11). **C**, Calcium content in the indicated organs and tissue was quantified by the colorimetric analysis (n=6, 5, 12–13, and 8). Values are mean±SE. One-way ANOVA with Bonferroni post hoc test. **P*<0.05, ***P*<0.01, ****P*<0.0001.

furthermore, they showed lower SA-βgal (senescence-associated β-galactosidase) activity and p16 expression, when compared with *Mir34a*$^{+/+}$ cells (Figure IIID and IIIE in the online-only Data Supplement). We induced *Mir34a*$^{+/+}$ and *Mir34a*$^{-/-}$ SMC calcification by culturing them for 7 days in an osteogenic medium containing a pathological concentration of inorganic phosphate. In accordance with our in vivo results, *Mir34a*$^{-/-}$ SMCs deposited lower levels of calcium relative to *Mir34a*$^{+/+}$ cells (Figure 4A).

To get deeper insight in the molecular pathways affected by miR-34a that promote SMC calcification, we evaluated the expression of the VC inhibitors Axl and SIRT1.[5,23] We have previously demonstrated that miR-34a directly targets SIRT1 and promotes senescence in HASMC,[6] whereas Axl is known to be targeted by miR-34a in other cell types.[24] Interestingly, during SMC mineralization, Axl mRNA level was higher in *Mir34a*$^{-/-}$ SMCs in respect to *Mir34a*$^{+/+}$ cells at day 3 (Figure 4B), whereas SIRT1 mRNA expression was not significantly increased (Figure 4C). At day 7, both transcripts were not influenced by the absence of *Mir34a* (Figure 4B and 4C). Both SIRT1 and Axl proteins were downregulated in *Mir34a*$^{+/+}$ cells at day 7 when compared with day 3, whereas they were not or less modulated in *Mir34a*$^{-/-}$ SMCs, respectively (Figure 4D through 4F).

These results demonstrate that SMCs lacking miR-34a expression have higher proliferation rate, reduced propensity to undergo senescence and deposit calcium, and show higher expression of the VC inhibitors SIRT1 and Axl.

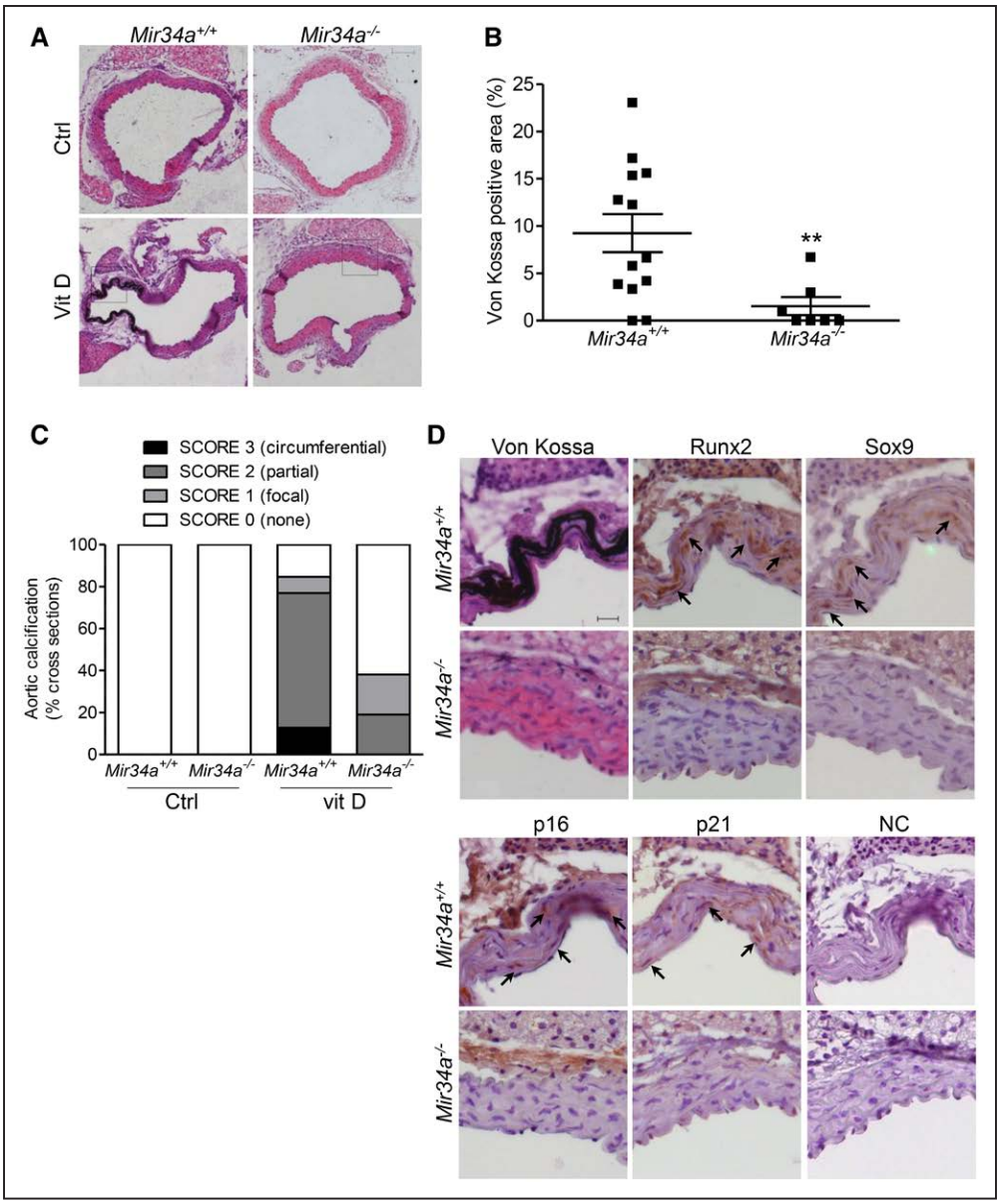


**Figure 2.** *Mir34a* genetic ablation reduces vascular calcification. **A**, Representative images of von Kossa staining (black) on sections from distal thoracic aortas. Nuclei were counterstained with hematoxylin (purple; scale bar=100 μm). **B**, Bars show the percentage of von Kossa-positive area to the total aortic area of vitamin D (Vit D)-treated mice (n=13 and 7). Values are mean±SE. Mann-Whitney *U* test. ***P*<0.01. **C**, Evaluation of vascular calcification by a semiquantitative scoring of von Kossa-stained aortic sections of vit D-treated and (control [Ctrl]) mice. **D**, Enlarged images of the von Kossa-stained sections shown in **A** and adjacent sections stained with antibodies specific for the indicated proteins or nothing (negative control [NC]) of vit D-treated mice (brown, black arrows; scale bar=20 μm). Nuclei were counterstained with hematoxylin (purple). Runx2 indicates Runt-related transcription factor 2; and SA-βgal, senescence-associated β-galactosidase.

## miR-34a Inhibits VSMC Proliferation by Directly Targeting Axl in HASMC

Next, we verified whether miR-34a can specifically modulate Axl in VSMC. We transfected HASMC with a miR-34a mimic or a mimic negative control; miR-34a overexpression downregulates Axl protein levels already at 24 hours post-transfection (Figure 5A). Accordingly, Axl expression was higher in HASMC transfected with a miR-34a inhibitor compared with the scramble (SCR) control (Figure 5B). To prove that miR-34a directly affects Axl expression, we transfected HASMCs with a vector carrying Axl cDNA devoid of the 3′-UTR (untranslated region) containing miR-34a seed sequence[24] or an empty vector, together with a miR-34a mimic or a mimic negative control. Western blot analysis confirmed that the endogenous Axl was severely lowered upon miR-34a overexpression, whereas the exogenous Axl was unaffected by miR-34a ectopic expression (Figure 5C). Because Axl regulates cell proliferation and survival,[35] we determined whether its downregulation mediated by miR-34a could affect HASMC growth. As expected, miR-34a reduced cell number 72 hours after transfection (empty miR-34a versus empty SCR; Figure 5D); Axl ectopic expression alone increased the number of HASMC (Axl SCR versus empty SCR; Figure 5D) and, in combination with miR-34a, partially

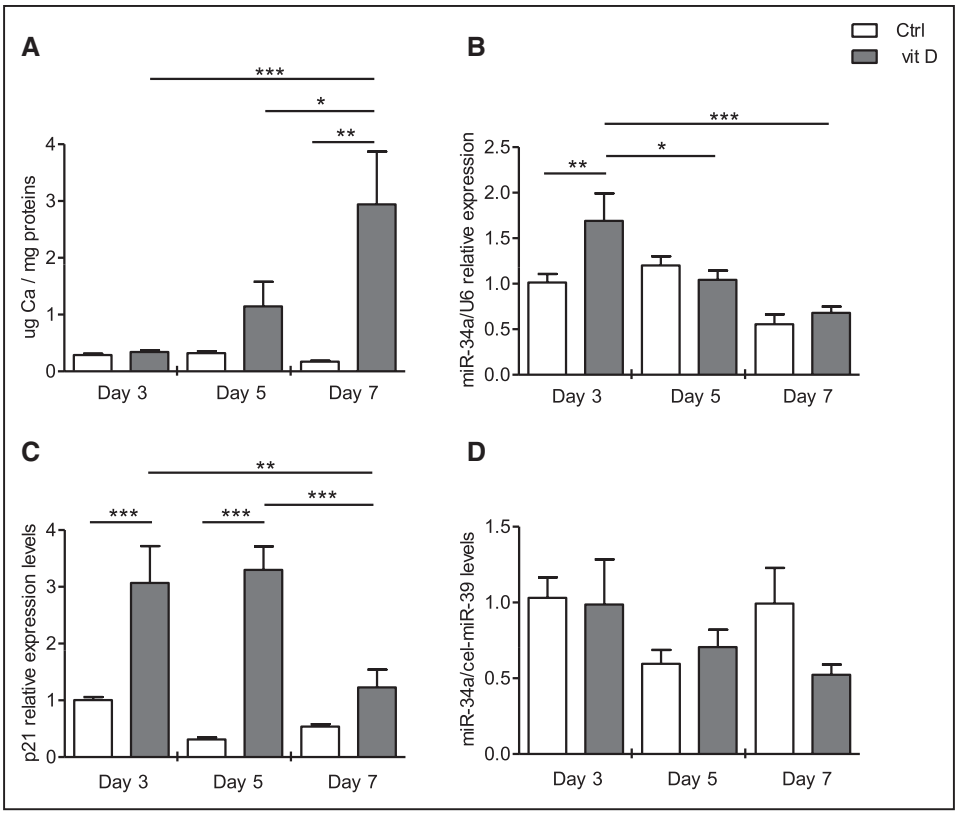


**Figure 3.** miR-34a is upregulated in aortas of vitamin D (vit D)-treated mice that display features of senescence before overt calcification. Twelve-week-old wild-type mice were treated subcutaneously with either vit D or a mock solution (control [Ctrl]) for 3 consecutive days and euthanized 3 (day 3), 5 (day 5), or 7 (day 7) d after the first injection. **A**, Calcium content in the aortas was quantified by colorimetric analysis (n=5, 5, 5, 5, 3, and 5). **B** and **C**, miR-34a and p21 expression in the aortas was analyzed by quantitative reverse transcriptase polymerase chain reaction and normalized to corresponding U6 and Hprt levels, respectively (n=5, 5-3, 5, 5-4, 3, and 5). **D**, miR-34a levels in the sera of mice were determined at the indicated days (n=5, 4, 5, 5, 3, and 5). Values are mean±SE. Two-way ANOVA with Bonferroni post hoc test. *$P$<0.05, **$P$<0.01, ***$P$<0.0001.

reversed miR-34a–mediated inhibition of cell proliferation (Axl miR-34a versus empty miR-34a; Figure 5D).

All together, these data indicate that miR-34a inhibits VSMC proliferation to some extent through the direct modulation of Axl.

## miR-34a–Induced Senescence Enhances HASMC Calcification Through Axl and SIRT1 Downregulation

We previously demonstrated that proliferative/young HASMCs express lower miR-34a levels compared with old/senescent HASMC, and transient miR-34a overexpression in young cells induces senescence.[6] Because old/senescent HASMC calcify more compared with young cells,[5,36] we verified whether miR-34a–induced VSMC senescence enhances VC. First, we set up an in vitro model of proliferative/young HASMC calcification induced by hyperphosphatemia. A significant augmentation of calcium deposition was observed by von Kossa staining and colorimetric analysis (Figure IVA and IVB in the online-only Data Supplement) along with an upregulation of VC markers alkaline phosphatase and Runx2 during the calcification process (Figure IVC through IVE in the online-only Data Supplement).

Then, we confirmed in our experimental conditions that senescent HASMC (passage 15) expressing higher levels of miR-34a mineralize more than young cells (passage 5; Figure 6A). Thus, we used a lentiviral infection to stably express miR-34a in proliferative HASMC to a level comparable with senescent HASMC (Figure VA in the online-only Data Supplement). Indeed, miR-34a-overexpressing HASMCs had greater SA-βgal activity, increased or decreased levels of the growth arrest marker p21 or Axl and SIRT1 mRNA, respectively (Figure VB through VE in the online-only Data Supplement). Strikingly, miR-34a-overexpressing HASMCs evidenced a rise in calcium deposition at day 7 of calcification, which was not seen in scramble control cells (SCR; Figure 6B).

Hence, we assessed Axl and SIRT1 expression during the mineralization process. Axl mRNA levels were lower in miR-34a–overexpressing HASMC at both days 3 and 7 in respect to SCR cells, whereas no major differences were detected for the SIRT1 transcript (Figure 6C and 6D). Western blot analysis revealed that both proteins decreased significantly at day 3 of calcification in miR-34a–overexpressing cells compared with control SCR HASMC (Figure 6E through 6G).

Finally, we determined miR-34a expression in HASMC at different days of culture in the osteogenic medium observing no significant modulation of its levels during the osteochondrogenic transition (Figure VI in the online-only Data Supplement).

Taken together, our findings show that miR-34a upregulation is necessary to induce HASMC growth arrest and

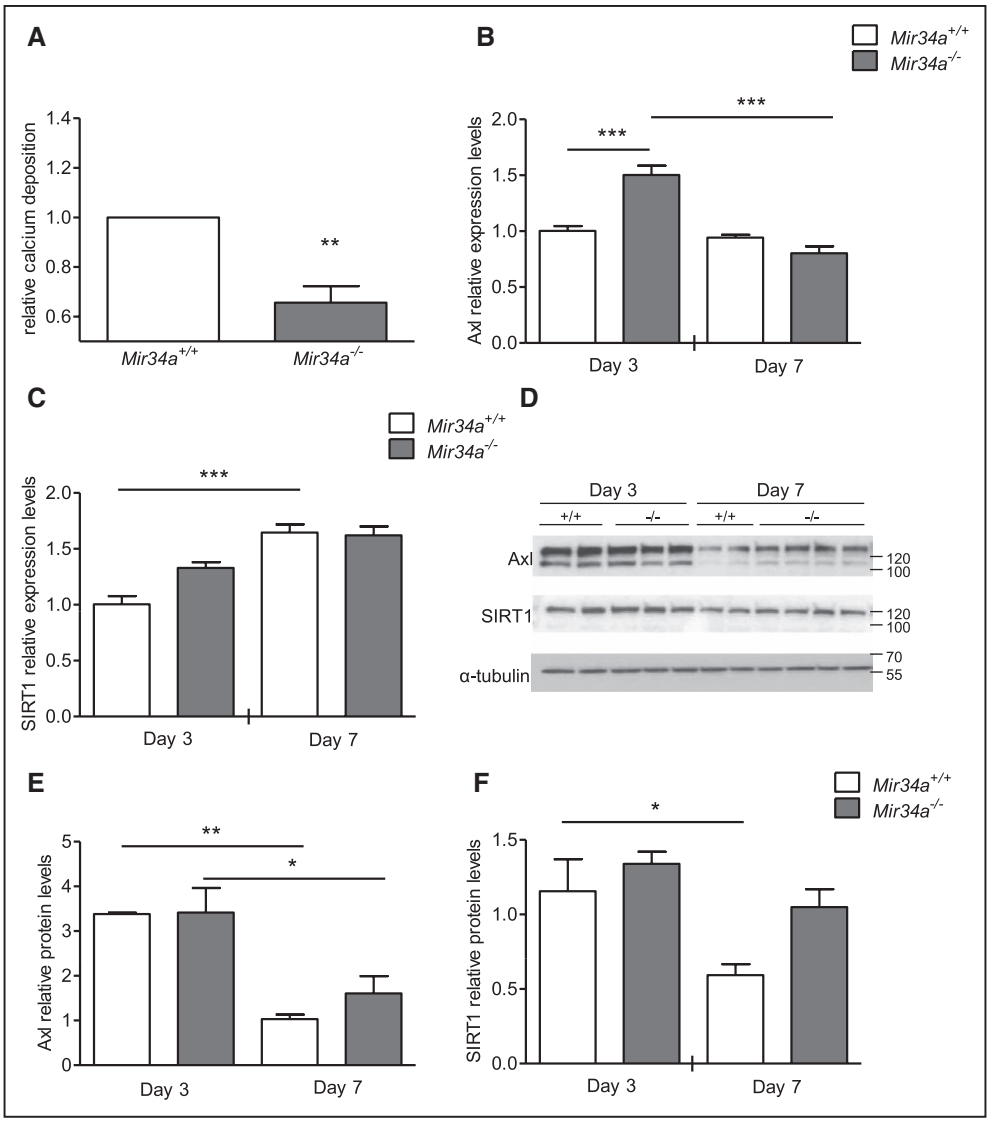


**Figure 4.** *Mir34a* genetic ablation significantly decreases smooth muscle cell (SMC) senescence and calcium deposition in vitro. **A–F**, SMCs were isolated from *Mir34a*$^{-/-}$ and *Mir34a*$^{+/+}$ mice. **A**, Cells were cultured in the osteogenic medium for 7 d, and the amount of precipitated calcium was quantified by colorimetric analysis (n=7). Relative calcium levels of *Mir34a*$^{-/-}$ to corresponding *Mir34a*$^{+/+}$ SMC were shown. Values are mean±SE. $^{**}P<0.01$. Paired *t* test. **B–F**, Cells were cultured in the osteogenic medium for 3 or 7 d (days 3 and 7). **B** and **C**, Axl (AXL receptor tyrosine kinase) and SIRT1 (sirtuin 1) mRNA levels were analyzed by quantitative reverse transcriptase polymerase chain reaction and normalized to corresponding Hprt levels (n=3, 3, 4, and 3). **D–F**, Protein extracts were subjected to Western blot analysis with anti-Axl, anti-SIRT1, or anti–α-tubulin (loading control) antibodies. **E** and **F**, Bars show quantification of normalized densitometric ratios (n=3, 4, 4, and 5). Values are mean±SE. One-way ANOVA with Bonferroni post hoc test. $^{*}P<0.05$, $^{**}P<0.01$, $^{***}P<0.0001$.

senescence to promote calcification through downregulation of its targets Axl and SIRT1.

## Discussion

VC is a pathology that occurs frequently in the elderly population and is associated with atherosclerosis, type 2 diabetes mellitus, and chronic kidney disease, which are diseases displaying features of premature aging.[8,37,38] Although the subjects with VC are high-risk patients, an effective therapy is not yet available because of the poor understanding of the molecular mechanisms underlying this complication.[3]

We recently published that miR-34a is upregulated in aged murine aortas and that an increase of its levels in VSMC induces growth arrest, senescence, and the expression of certain senescence-associated secretory phenotype factors, including the pro-osteogenic molecules BMP2 and IL-6.[6] In the present study, we demonstrated for the first time that the aging-associated miR-34a is a VC promoter.

We confirmed previous data reporting that aortas of aged mice show signs of calcification along with increased expression of VC markers, such as Runx2 (Figure IA, IB, ID, and IF in the online-only Data Supplement).[33,34] Using an established mouse model of soft tissue and aortic medial layer calcification induced by an overdose of vitamin D,[29,30] we demonstrated that *Mir34a* gene deletion prevents VC in vivo. miR-34a deficiency significantly reduced calcium levels in the serum and all tested organs and, with particular regard to aortas, prevented the induction of Runx2 and Sox9 and aortic VSMC osteochondrogenic transdifferentiation (Figures 1 and 2). Expression of p16 and p21 was found only around the calcified regions of

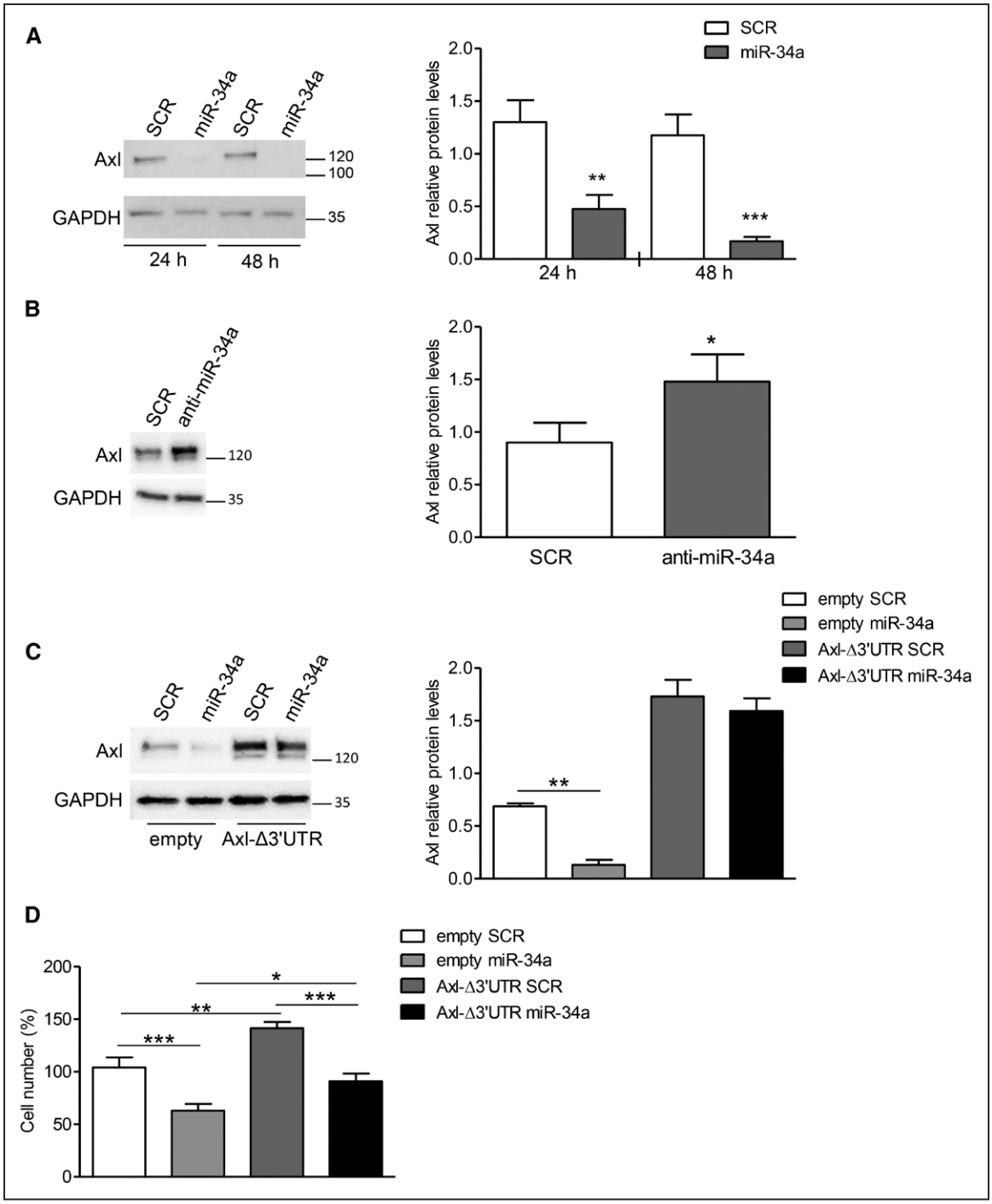


**Figure 5.** Axl (AXL receptor tyrosine kinase) expression is directly modulated by miR-34a in human aortic smooth muscle cells (HASMC). **A**, HASMC were transfected with a miR-34a mimic (miR-34a) or a mimic control (scramble, SCR) and cultured for 24 or 48 h. Protein extracts were analyzed with anti-Axl or anti-GAPDH (loading control) antibody (**left**). Bars show quantification of normalized densitometric ratios (n=4 and 5; **right**). **B**, HASMCs were transfected with a miR-34a hairpin inhibitor (anti-miR-34a) or a hairpin inhibitor negative control (SCR) and cultured for 72 h. Protein extracts were analyzed with anti-Axl or anti-GAPDH (loading control) antibody (**left**). Bars show normalized densitometric ratios (n=4; **right**). **C** and **D**, HASMCs were transfected with miR-34a or SCR along with either a 3′ untranslated region-deleted Axl-expression vector (Axl-Δ3′UTR) or an empty vector (empty). **C**, Twenty-four hours after transfection, protein extracts were analyzed with anti-Axl or anti-GAPDH (loading control) antibody (**left**). Bars show quantification of normalized densitometric ratios (n=3; **right**). **D**, The graph shows the cell number at 72 h after transfection (n=5). Values are mean±SE. Student *t* test or 1-way ANOVA with Bonferroni post hoc test. **P*<0.05, ***P*<0.01, ****P*<0.0001.

aortas of *Mir34a*$^{+/+}$ mice (Figure 2D) that is in line with previously published data showing that these 2 senescence markers are upregulated in calcified rodent aortas, human arteries, and VSMCs.[4,5,39–42] Notably, after vitamin D treatment, miR-34a levels raised in a transient manner before a detectable amount of calcium was deposited in the aorta and along with p21 induction (Figure 3A through 3C) suggesting that in vivo miR-34a upregulation is necessary to promote tissue senescence

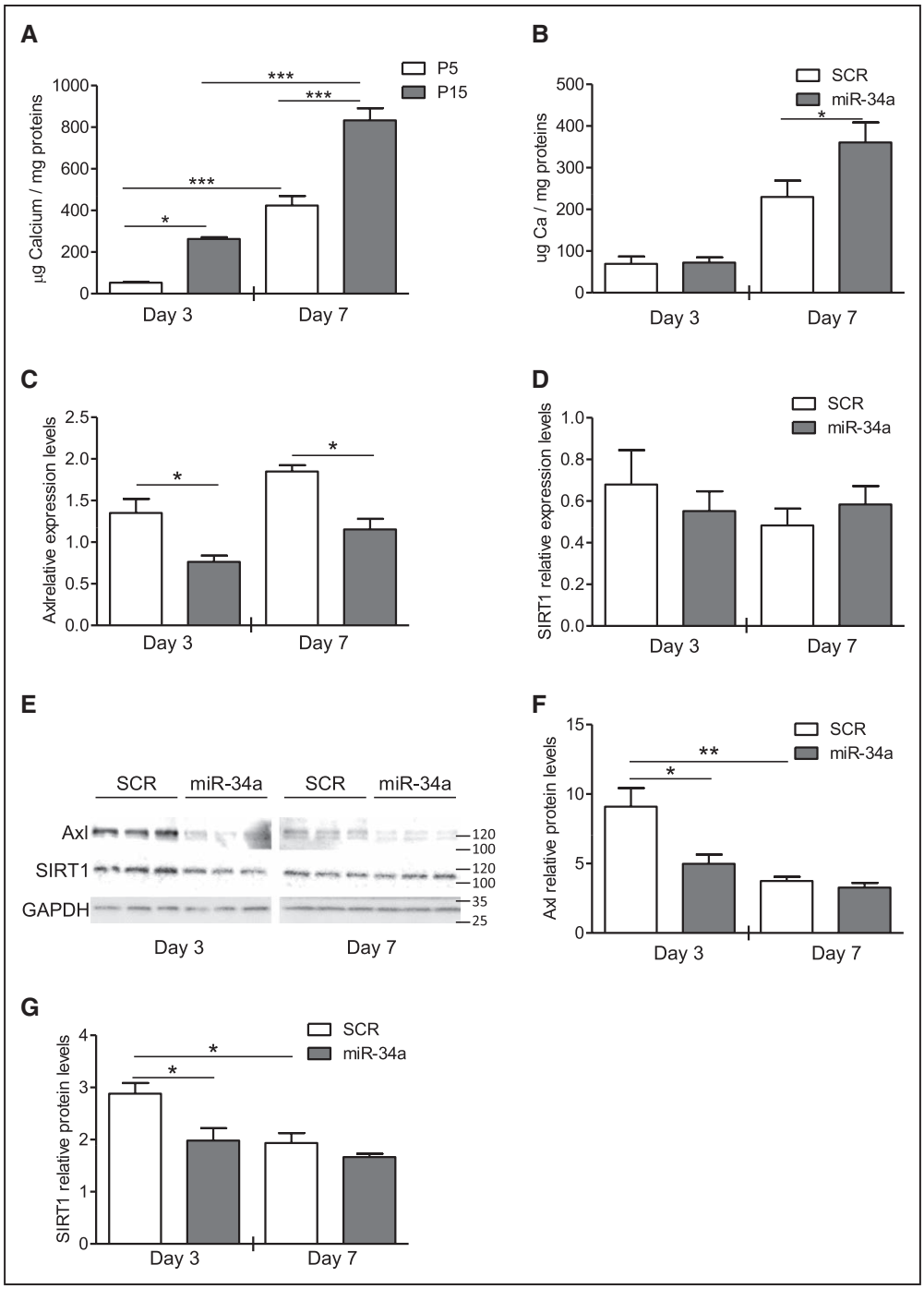


**Figure 6.** miR-34a overexpression increases human aortic smooth muscle cell (HASMC) calcium deposition. **A**, Calcium deposition quantification with the colorimetric analysis at 3 and 7 d of culturing in osteogenic medium of HASMC at a proliferative passage (P5) and at senescence (passage 15 [P15]). **B**–**G**, HASMCs were infected with either pMIRNA1 (SCR) or pMIRH34a (miR-34a) lentivirus at an MOI (multiplicity of infection) of 10 and cultured in growth medium for 48 h. Then, they were cultured in the osteogenic medium for 3 (day 3) or 7 (day 7) d. **B**, The amount of precipitated calcium was quantified by colorimetric analysis (n=7). **C** and **D**, Axl (AXL receptor tyrosine kinase) and SIRT1 (sirtuin 1) mRNA levels were analyzed by quantitative reverse transcriptase polymerase chain reaction and normalized to corresponding GAPDH levels (n=3). **E**, Protein extracts were analyzed with anti-Axl, anti-SIRT1, or anti-GAPDH (loading control) antibody. **F** and **G**, Bars show quantification of normalized densitometric ratios (n=3). Values are mean±SE. One-way ANOVA with Bonferroni post hoc test. **P*<0.05, ***P*<0.01, ****P*<0.0001.

that eventually triggers the onset and progression of calcification. In accordance, it has been shown that the activation of the senescence program by a calcification stimulus precedes and controls VSMC mineralization process,[43] and senescence still occurs when osteogenesis is blocked by silencing specific calcification factors like Runx2.[10]

Our in vitro data support the in vivo findings. Senescent VSMCs that express higher amount of miR-34a are more prone to calcify in response to high phosphate compared with younger cells (Figure 6A)[5,6,36] and miR-34a–induced senescence facilitates calcification mediated by hyperphosphatemia. Indeed, murine *Mir34a*$^{-/-}$ SMCs displayed decreased

senescence features, as revealed by lower SA-βgal staining signal and p16 expression, and reduced calcium deposition when compared with *Mir34a*$^{+/+}$ cells (Figure IIID and IIIE in the online-only Data Supplement; Figure 4A); conversely, constitutive overexpression of miR-34a to senescence-like levels in HASMC enhanced calcification (Figure VA through VC in the online-only Data Supplement; Figure 6B). Furthermore, miR-34a is not modulated during HASMC mineralization (Figure VI in the online-only Data Supplement). Hence, miR-34a being an inducer of VSMC growth arrest and senescence is involved in the early mechanisms indispensable for VSMC osteochondrogenic transdifferentiation.

Interestingly, our in vitro experiments showed milder effects of miR-34a on SMC calcification compared with the in vivo results. The difference may depend on the contribution of other cell types to VC. In fact, it has been shown that pericytes, endothelial cells, fibroblasts, and resident and circulating progenitor cells can differentiate toward an osteochondrogenic lineage as well and thereby participate to the calcification process.[44] Hence, the low propensity to VC of *Mir34a*$^{-/-}$ mice could be explained by the prevention of the osteochondrogenic transition of other cell types in addition to SMC.

Mechanistically, we identified 2 VC inhibitors, SIRT1 and Axl,[5,23] as miR-34a targets during the calcification process. It has been already shown that SMC osteoblastic transdifferentiation is characterized by SIRT1 downregulation, and maintaining of high levels of this protein prevents SMC calcification through senescence inhibition.[5] We have already proven that SIRT1 is a direct miR-34a target in HASMC and that its miR-34a–mediated downregulation enhances senescence in these cells.[6] In this study, we further show that the direct modulation of SIRT1 by miR-34a influences calcification of VSMC. In fact, unlike wild-type murine SMCs, SIRT1 protein levels were not significantly altered in *Mir34a*$^{-/-}$ cells under high phosphate conditions (Figure 4D and 4F), whereas they were significantly reduced at an early stage of calcification in miR-34a–overexpressing HASMCs (Figure 6E and 6G). A similar behavior was found for Axl (Figures 4D, 4E, 6E, and 6F).

Cells must arrest their cell cycle before undergoing senescence.[40] miR-34a inhibits HASMC proliferation by blocking the G1- to S-phase transition along with the upregulation of p21 protein levels before SIRT1 downregulation.[6] Herein, we demonstrated that *Mir34a*$^{-/-}$ aortas display a higher VSMC density and isolated *Mir34a*$^{-/-}$ SMC, an enhanced proliferative rate (Figures IIB through IID and IIIC in the online-only Data Supplement) further corroborating miR-34a as an important regulator of VSMC proliferation. Furthermore, we validated Axl as a miR-34a target in HASMC and found that miR-34a downregulates Axl with a faster kinetic compared with SIRT1 (24 versus 48 hours) and alongside with p21 upregulation and cell cycle arrest (Figure 5A through 5C).[6] Axl signaling has been shown to control several VSMC functions including proliferation,[45] migration,[46] and cell survival[47]; furthermore, Axl is also known to be downregulated during cell mineralization and its overexpression inhibits VSMC calcification via activation of the antiapoptotic PI3K (phosphatidylinositol 4,5-bisphosphate 3-kinase)/AKT (RAC-alpha serine/threonine-protein kinase) pathway.[23] Our findings demonstrate that miR-34a, at least in part, inhibits HASMC proliferation by directly reducing Axl protein levels (Figure 5C and 5D) and that under a procalcification stimulus, miR-34a–dependent Axl decrease favors SMC osteocondrogenic transition (Figures 4D, 4E, 6E, and 6F). The mild effect of Axl modulation on HASMC proliferation is likely because miR-34a is known to influence cell growth by targeting also several regulators of the cell cycle machinery, such as CDKs (cyclin-dependent kinases) and cyclins.[48–51]

At the molecular level, miRNAs bind mRNA targets to mediate RNA degradation or inhibit protein translation.[52] We found that both Axl and Sirt1 mRNAs diminish in HASMC soon after miR-34a overexpression, nevertheless, the effect on Axl mRNA levels is much greater (Figure VD and VE in the online-only Data Supplement) indicating 2 different mechanisms of regulation. It has been demonstrated that miR-34a does not completely degrade SIRT1 transcript but interferes mainly with its translation.[53,54] In line with published evidences, during SMC and HASMC calcification, miR-34a decreases SIRT1 protein expression mainly by interfering with the translation of its transcript (Figures 4C, 4D, 4F, 6D, 6E, and 6G). On the contrary, miR-34a affects Axl protein expression by inducing degradation of the mRNA (Figures 4B, 4D, 4E, 6C, 6E, and 6F).

Taken together, our data suggest that miR-34a may promote VC by influencing proliferation and senescence of VSMC through different pathways; first, it inhibits cell growth partially via Axl downregulation and then enhances senescence by inhibiting SIRT1. Both events ultimately lead to VSMC osteochondrogenic transition (Graphic Abstract). Other miR-34a targets are likely to be involved in the calcification process: for instance, it has been reported that miR-34a can inhibit SMC proliferation via Notch1.[55]

A limitation of the present study is that soft tissue calcification has been induced in young animals. Future works must include aged Mir34a$^{-/-}$ and Mir34a$^{+/+}$ mice.

Altogether, the present study pinpoints miR-34a inhibition as a promising therapeutic approach for the treatment of age-related cardiovascular diseases.

## Acknowledgments

We thank Matteo Bertolotti and Clarissa Ruggeri for their technical help.

## Sources of Funding

This work was supported by the Italian Ministry of Health (Ricerca Corrente 2013–2017 to A. Raucci) and Fondazione Cariplo (Research on Ageing diseases 2015 to M.E. Bianchi and A. Raucci). I. Badi was supported by Fondazione Umberto Veronesi (Postdoctoral Fellowship 2016–2018).

## Disclosures

None.

## References

1. Naik V, Leaf EM, Hu JH, Yang HY, Nguyen NB, Giachelli CM, Speer MY. Sources of cells that contribute to atherosclerotic intimal calcification: an in vivo genetic fate mapping study. *Cardiovasc Res*. 2012;94:545–554. doi: 10.1093/cvr/cvs126
2. Speer MY, Yang HY, Brabb T, Leaf E, Look A, Lin WL, Frutkin A, Dichek D, Giachelli CM. Smooth muscle cells give rise to osteochondrogenic precursors and chondrocytes in calcifying arteries. *Circ Res*. 2009;104:733–741. doi: 10.1161/CIRCRESAHA.108.183053

3. Sage AP, Tintut Y, Demer LL. Regulatory mechanisms in vascular calcification. *Nat Rev Cardiol*. 2010;7:528–536. doi: 10.1038/nrcardio.2010.115
4. Liu Y, Drozdov I, Shroff R, Beltran LE, Shanahan CM. Prelamin A accelerates vascular calcification via activation of the DNA damage response and senescence-associated secretory phenotype in vascular smooth muscle cells. *Circ Res*. 2013;112:e99–e109. doi: 10.1161/CIRCRESAHA.111.300543
5. Takemura A, Iijima K, Ota H, Son BK, Ito Y, Ogawa S, Eto M, Akishita M, Ouchi Y. Sirtuin 1 retards hyperphosphatemia-induced calcification of vascular smooth muscle cells. *Arterioscler Thromb Vasc Biol*. 2011;31:2054–2062. doi: 10.1161/ATVBAHA.110.216739
6. Badi I, Burba I, Ruggeri C, Zeni F, Bertolotti M, Scopece A, Pompilio G, Raucci A. MicroRNA-34a induces vascular smooth muscle cells senescence by SIRT1 downregulation and promotes the expression of age-associated pro-inflammatory secretory factors. *J Gerontol A Biol Sci Med Sci*. 2015;70:1304–1311. doi: 10.1093/gerona/glu180
7. Rodier F, Coppé JP, Patil CK, Hoeijmakers WA, Muñoz DP, Raza SR, Freund A, Campeau E, Davalos AR, Campisi J. Persistent DNA damage signalling triggers senescence-associated inflammatory cytokine secretion. *Nat Cell Biol*. 2009;11:973–979. doi: 10.1038/ncb1909
8. Shanahan CM. Mechanisms of vascular calcification in CKD-evidence for premature ageing? *Nat Rev Nephrol*. 2013;9:661–670. doi: 10.1038/nrneph.2013.176
9. Burton DG, Giles PJ, Sheerin AN, Smith SK, Lawton JJ, Ostler EL, Rhys-Williams W, Kipling D, Faragher RG. Microarray analysis of senescent vascular smooth muscle cells: a link to atherosclerosis and vascular calcification. *Exp Gerontol*. 2009;44:659–665. doi: 10.1016/j.exger.2009.07.004
10. Afonso P, Auclair M, Boccara F, Vantyghem MC, Katlama C, Capeau J, Vigouroux C, Caron-Debarle M. LMNA mutations resulting in lipodystrophy and HIV protease inhibitors trigger vascular smooth muscle cell senescence and calcification: role of ZMPSTE24 downregulation. *Atherosclerosis*. 2016;245:200–211. doi: 10.1016/j.atherosclerosis.2015.12.012
11. Du Y, Wang Y, Wang L, Liu B, Tian Q, Liu CJ, Zhang T, Xu Q, Zhu Y, Ake O, Qi Y, Tang C, Kong W, Wang X. Cartilage oligomeric matrix protein inhibits vascular smooth muscle calcification by interacting with bone morphogenetic protein-2. *Circ Res*. 2011;108:917–928. doi: 10.1161/CIRCRESAHA.110.234328
12. Wang M, Fu Y, Gao C, Jia Y, Huang Y, Liu L, Wang X, Wang W, Kong W. Cartilage oligomeric matrix protein prevents vascular aging and vascular smooth muscle cells senescence. *Biochem Biophys Res Commun*. 2016;478:1006–1013. doi: 10.1016/j.bbrc.2016.08.004
13. van Rooij E, Purcell AL, Levin AA. Developing microRNA therapeutics. *Circ Res*. 2012;110:496–507. doi: 10.1161/CIRCRESAHA.111.247916
14. Goettsch C, Hutcheson JD, Aikawa E. MicroRNA in cardiovascular calcification: focus on targets and extracellular vesicle delivery mechanisms. *Circ Res*. 2013;112:1073–1084. doi: 10.1161/CIRCRESAHA.113.300937
15. Hermeking H. The miR-34 family in cancer and apoptosis. *Cell Death Differ*. 2010;17:193–199. doi: 10.1038/cdd.2009.56
16. Boon RA, Iekushi K, Lechner S, et al. MicroRNA-34a regulates cardiac ageing and function. *Nature*. 2013;495:107–110. doi: 10.1038/nature11919
17. Dimmeler S, Nicotera P. MicroRNAs in age-related diseases. *EMBO Mol Med*. 2013;5:180–190. doi: 10.1002/emmm.201201986
18. Ito T, Yagi S, Yamakuchi M. MicroRNA-34a regulation of endothelial senescence. *Biochem Biophys Res Commun*. 2010;398:735–740. doi: 10.1016/j.bbrc.2010.07.012
19. Li X, Khanna A, Li N, Wang E. Circulatory miR34a as an RNAbased, noninvasive biomarker for brain aging. *Aging (Albany NY)*. 2011;3:985–1002. doi: 10.18632/aging.100371
20. Xu Q, Seeger FH, Castillo J, Iekushi K, Boon RA, Farcas R, Manavski Y, Li YG, Assmus B, Zeiher AM, Dimmeler S. Micro-RNA-34a contributes to the impaired function of bone marrow-derived mononuclear cells from patients with cardiovascular disease. *J Am Coll Cardiol*. 2012;59:2107–2117. doi: 10.1016/j.jacc.2012.02.033
21. Rippo MR, Olivieri F, Monsurrò V, Prattichizzo F, Albertini MC, Procopio AD. MitomiRs in human inflamm-aging: a hypothesis involving miR-181a, miR-34a and miR-146a. *Exp Gerontol*. 2014;56:154–163. doi: 10.1016/j.exger.2014.03.002
22. Zhao T, Li J, Chen AF. MicroRNA-34a induces endothelial progenitor cell senescence and impedes its angiogenesis via suppressing silent information regulator 1. *Am J Physiol Endocrinol Metab*. 2010;299:E110–E116. doi: 10.1152/ajpendo.00192.2010
23. Collett GD, Sage AP, Kirton JP, Alexander MY, Gilmore AP, Canfield AE. Axl/phosphatidylinositol 3-kinase signaling inhibits mineral deposition by vascular smooth muscle cells. *Circ Res*. 2007;100:502–509. doi: 10.1161/01.RES.0000258854.03388.02
24. Mudduluru G, Ceppi P, Kumarswamy R, Scagliotti GV, Papotti M, Allgayer H. Regulation of Axl receptor tyrosine kinase expression by miR-34a and miR-199a/b in solid cancer. *Oncogene*. 2011;30:2888–2899. doi: 10.1038/onc.2011.13
25. Choi YJ, Lin CP, Ho JJ, He X, Okada N, Bu P, Zhong Y, Kim SY, Bennett MJ, Chen C, Ozturk A, Hicks GG, Hannon GJ, He L. miR-34 miRNAs provide a barrier for somatic cell reprogramming. *Nat Cell Biol*. 2011;13:1353–1360. doi: 10.1038/ncb2366
26. Detrano R, Guerci AD, Carr JJ, Bild DE, Burke G, Folsom AR, Liu K, Shea S, Szklo M, Bluemke DA, O'Leary DH, Tracy R, Watson K, Wong ND, Kronmal RA. Coronary calcium as a predictor of coronary events in four racial or ethnic groups. *N Engl J Med*. 2008;358:1336–1345. doi: 10.1056/NEJMoa072100
27. Osako MK, Nakagami H, Koibuchi N, Shimizu H, Nakagami F, Koriyama H, Shimamura M, Miyake T, Rakugi H, Morishita R. Estrogen inhibits vascular calcification via vascular RANKL system: common mechanism of osteoporosis and vascular calcification. *Circ Res*. 2010;107:466–475. doi: 10.1161/CIRCRESAHA.110.216846
28. Peng YQ, Xiong D, Lin X, Cui RR, Xu F, Zhong JY, Zhu T, Wu F, Mao MZ, Liao XB, Yuan LQ. Oestrogen inhibits arterial calcification by promoting autophagy. *Sci Rep*. 2017;7:3549. doi: 10.1038/s41598-017-03801-x
29. Cui RR, Li SJ, Liu LJ, Yi L, Liang QH, Zhu X, Liu GY, Liu Y, Wu SS, Liao XB, Yuan LQ, Mao DA, Liao EY. MicroRNA-204 regulates vascular smooth muscle cell calcification in vitro and in vivo. *Cardiovasc Res*. 2012;96:320–329. doi: 10.1093/cvr/cvs258
30. Han MS, Che X, Cho GH, Park HR, Lim KE, Park NR, Jin JS, Jung YK, Jeong JH, Lee IK, Kato S, Choi JY. Functional cooperation between vitamin D receptor and Runx2 in vitamin D-induced vascular calcification. *PLoS One*. 2013;8:e83584. doi: 10.1371/journal.pone.0083584
31. Neven E, Persy V, Dauwe S, De Schutter T, De Broe ME, D'Haese PC. Chondrocyte rather than osteoblast conversion of vascular cells underlies medial calcification in uremic rats. *Arterioscler Thromb Vasc Biol*. 2010;30:1741–1750. doi: 10.1161/ATVBAHA.110.204834
32. Huber A, Badylak SF. Phenotypic changes in cultured smooth muscle cells: limitation or opportunity for tissue engineering of hollow organs? *J Tissue Eng Regen Med*. 2012;6:505–511. doi: 10.1002/term.451
33. Akiyoshi T, Ota H, Iijima K, Son BK, Kahyo T, Setou M, Ogawa S, Ouchi Y, Akishita M. A novel organ culture model of aorta for vascular calcification. *Atherosclerosis*. 2016;244:51–58. doi: 10.1016/j.atherosclerosis.2015.11.005
34. Roos CM, Hagler M, Zhang B, Oehler EA, Arghami A, Miller JD. Transcriptional and phenotypic changes in aorta and aortic valve with aging and MnSOD deficiency in mice. *Am J Physiol Heart Circ Physiol*. 2013;305:H1428–H1439. doi: 10.1152/ajpheart.00735.2012
35. Axelrod H, Pienta KJ. Axl as a mediator of cellular growth and survival. *Oncotarget*. 2014;5:8818–8852. doi: 10.18632/oncotarget.2422
36. Nakano-Kurimoto R, Ikeda K, Uraoka M, Nakagawa Y, Yutaka K, Koide M, Takahashi T, Matoba S, Yamada H, Okigaki M, Matsubara H. Replicative senescence of vascular smooth muscle cells enhances the calcification through initiating the osteoblastic transition. *Am J Physiol Heart Circ Physiol*. 2009;297:H1673–H1684. doi: 10.1152/ajpheart.00455.2009
37. Kovacic JC, Moreno P, Hachinski V, Nabel EG, Fuster V. Cellular senescence, vascular disease, and aging: part 1 of a 2-part review. *Circulation*. 2011;123:1650–1660. doi: 10.1161/CIRCULATIONAHA.110.007021
38. Kovacic JC, Moreno P, Nabel EG, Hachinski V, Fuster V. Cellular senescence, vascular disease, and aging: part 2 of a 2-part review: clinical vascular disease in the elderly. *Circulation*. 2011;123:1900–1910. doi: 10.1161/CIRCULATIONAHA.110.009118
39. Kuilman T, Michaloglou C, Mooi WJ, Peeper DS. The essence of senescence. *Genes Dev*. 2010;24:2463–2479. doi: 10.1101/gad.1971610
40. Salama R, Sadaie M, Hoare M, Narita M. Cellular senescence and its effector programs. *Genes Dev*. 2014;28:99–114. doi: 10.1101/gad.235184.113
41. Stenvinkel P, Luttropp K, McGuinness D, Witasp A, Qureshi AR, Wernerson A, Nordfors L, Schalling M, Ripsweden J, Wennberg L, Söderberg M, Bárány P, Olauson H, Shiels PG. CDKN2A/p16INK4a expression is associated with vascular progeria in chronic kidney disease. *Aging (Albany NY)*. 2017;9:494–507. doi: 10.18632/aging.101173
42. Yamada S, Tatsumoto N, Tokumoto M, Noguchi H, Ooboshi H, Kitazono T, Tsuruya K. Phosphate binders prevent phosphate-induced cellular senescence of vascular smooth muscle cells and vascular calcification in a modified, adenine-based uremic rat model. *Calcif Tissue Int*. 2015;96:347–358. doi: 10.1007/s00223-014-9929-5
43. Burton DG, Matsubara H, Ikeda K. Pathophysiology of vascular calcification: pivotal role of cellular senescence in vascular smooth muscle cells. *Exp Gerontol*. 2010;45:819–824. doi: 10.1016/j.exger.2010.07.005

44. Bardeesi ASA, Gao J, Zhang K, Yu S, Wei M, Liu P, Huang H. A novel role of cellular interactions in vascular calcification. *J Transl Med*. 2017;15:95. doi: 10.1186/s12967-017-1190-z
45. Nakano T, Kawamoto K, Kishino J, Nomura K, Higashino K, Arita H. Requirement of gamma-carboxyglutamic acid residues for the biological activity of Gas6: contribution of endogenous Gas6 to the proliferation of vascular smooth muscle cells. *Biochem J*. 1997;323(pt 2):387–392.
46. Fridell YW, Villa J Jr, Attar EC, Liu ET. GAS6 induces Axl-mediated chemotaxis of vascular smooth muscle cells. *J Biol Chem*. 1998;273:7123–7126.
47. Melaragno MG, Fridell YW, Berk BC. The Gas6/Axl system: a novel regulator of vascular cell function. *Trends Cardiovasc Med*. 1999;9:250–253.
48. Chen L, Holmstrøm K, Qiu W, Ditzel N, Shi K, Hokland L, Kassem M. MicroRNA-34a inhibits osteoblast differentiation and *in vivo* bone formation of human stromal stem cells. *Stem Cells*. 2014;32:902–912. doi: 10.1002/stem.1615
49. He L, He X, Lim LP, et al. A microRNA component of the p53 tumour suppressor network. *Nature*. 2007;447:1130–1134. doi: 10.1038/nature05939
50. Sun F, Fu H, Liu Q, Tie Y, Zhu J, Xing R, Sun Z, Zheng X. Downregulation of CCND1 and CDK6 by miR-34a induces cell cycle arrest. *FEBS Lett*. 2008;582:1564–1568. doi: 10.1016/j.febslet.2008.03.057
51. Tazawa H, Tsuchiya N, Izumiya M, Nakagama H. Tumor-suppressive mir-34a induces senescence-like growth arrest through modulation of the e2f pathway in human colon cancer cells. *Proc Natl Acad Sci USA*. 2007;104:15472–15477.
52. Olson EN. MicroRNAs as therapeutic targets and biomarkers of cardiovascular disease. *Sci Transl Med*. 2014;6:239ps3. doi: 10.1126/scitranslmed.3009008
53. Lee J, Padhye A, Sharma A, Song G, Miao J, Mo YY, Wang L, Kemper JK. A pathway involving farnesoid X receptor and small heterodimer partner positively regulates hepatic sirtuin 1 levels via microRNA-34a inhibition. *J Biol Chem*. 2010;285:12604–12611. doi: 10.1074/jbc.M109.094524
54. Yamakuchi M, Ferlito M, Lowenstein CJ. Mir-34a repression of sirt1 regulates apoptosis. *Proc Natl Acad Sci USA*. 2008;105:13421–13426.
55. Chen Q, Yang F, Guo M, Wen G, Zhang C, Luong le A, Zhu J, Xiao Q, Zhang L. miRNA-34a reduces neointima formation through inhibiting smooth muscle cell proliferation and migration. *J Mol Cell Cardiol*. 2015;89(pt A):75–86. doi: 10.1016/j.yjmcc.2015.10.017


## Highlights

- miR-34a genetic ablation reduces soft tissue and vascular calcification.
- miR-34a promotes vascular smooth muscle cell calcification by inducing cell growth arrest and senescence.
- miR-34a affects the expression of targets, such as Axl (AXL receptor tyrosine kinase) and SIRT1 (sirtuin 1), that are vascular calcification inhibitors.